

University of Windsor

Scholarship at UWindor

Electronic Theses and Dissertations

Theses, Dissertations, and Major Papers

2005

Electric surface properties of Delrin used for high voltage insulation.

Hadi Tajalli
University of Windsor

Follow this and additional works at: <https://scholar.uwindsor.ca/etd>

Recommended Citation

Tajalli, Hadi, "Electric surface properties of Delrin used for high voltage insulation." (2005). *Electronic Theses and Dissertations*. 1890.
<https://scholar.uwindsor.ca/etd/1890>

This online database contains the full-text of PhD dissertations and Masters' theses of University of Windsor students from 1954 forward. These documents are made available for personal study and research purposes only, in accordance with the Canadian Copyright Act and the Creative Commons license—CC BY-NC-ND (Attribution, Non-Commercial, No Derivative Works). Under this license, works must always be attributed to the copyright holder (original author), cannot be used for any commercial purposes, and may not be altered. Any other use would require the permission of the copyright holder. Students may inquire about withdrawing their dissertation and/or thesis from this database. For additional inquiries, please contact the repository administrator via email (scholarship@uwindsor.ca) or by telephone at 519-253-3000ext. 3208.

Electric Surface Properties of Delrin Used for High Voltage Insulation

by

Hadi Tajalli

A Thesis

Submitted to the Faculty of Graduate Studies and Research
through the Department of Electrical and Computer Engineering
in Partial Fulfillment of the Requirements for
the Degree of Master of Applied Science
at the University of Windsor

Windsor, Ontario, Canada

2005

© 2005 Hadi Tajalli



Library and
Archives Canada

Bibliothèque et
Archives Canada

Published Heritage
Branch

Direction du
Patrimoine de l'édition

395 Wellington Street
Ottawa ON K1A 0N4
Canada

395, rue Wellington
Ottawa ON K1A 0N4
Canada

Your file *Votre référence*

ISBN: 0-494-09810-4

Our file *Notre référence*

ISBN: 0-494-09810-4

NOTICE:

The author has granted a non-exclusive license allowing Library and Archives Canada to reproduce, publish, archive, preserve, conserve, communicate to the public by telecommunication or on the Internet, loan, distribute and sell theses worldwide, for commercial or non-commercial purposes, in microform, paper, electronic and/or any other formats.

The author retains copyright ownership and moral rights in this thesis. Neither the thesis nor substantial extracts from it may be printed or otherwise reproduced without the author's permission.

AVIS:

L'auteur a accordé une licence non exclusive permettant à la Bibliothèque et Archives Canada de reproduire, publier, archiver, sauvegarder, conserver, transmettre au public par télécommunication ou par l'Internet, prêter, distribuer et vendre des thèses partout dans le monde, à des fins commerciales ou autres, sur support microforme, papier, électronique et/ou autres formats.

L'auteur conserve la propriété du droit d'auteur et des droits moraux qui protègent cette thèse. Ni la thèse ni des extraits substantiels de celle-ci ne doivent être imprimés ou autrement reproduits sans son autorisation.

In compliance with the Canadian Privacy Act some supporting forms may have been removed from this thesis.

Conformément à la loi canadienne sur la protection de la vie privée, quelques formulaires secondaires ont été enlevés de cette thèse.

While these forms may be included in the document page count, their removal does not represent any loss of content from the thesis.

Bien que ces formulaires aient inclus dans la pagination, il n'y aura aucun contenu manquant.


Canada

Abstract

In this study surface properties of Delrin have been investigated. Delrin is a homopolymer of acetal resin. To study the degradation and the effect of the environment on the surface of this material, samples of Delrin were immersed in saline water with salinities of 0.005-100 mS/cm at 0, 23, 60 and 98 °C. Specimens were also placed in air at these four temperatures. The contact angle of a 4 µl sessile droplet of distilled water on the surface of Delrin as a measure of the surface wettability or the hydrophobicity has been measured in this study. Increasing the parameters of temperature, salinity (up to certain level), and the length of time of immersion decreased the contact angle until it reached saturation.

The dc and ac breakdown, water absorption and surface roughness of Delrin were also measured and were found to have correlations with the hydrophobicity of Delrin. After the reduction of hydrophobicity had reached saturation, the specimens were removed from the saline solutions.

The effects of volume of the droplet of distilled water and the time to measure the contact angle after placing the droplet on the surface were also studied. The contact angle decreased after exposure to the RF discharge but subsequently recovered.

Scanning electro microscopy (SEM) and Fourier transform infrared spectroscopy (FTIR) were performed to detect the oxidation of the surface.

The surface free energy per unit area of the virgin and aged samples of Delrin was determined. The diffusion coefficients of the saline solution having different levels of salinity at different temperatures were also determined. The weight increases of Delrin, and Acetron, a copolymer of acetal resin, under the above stress conditions were studied.

The temperature and the conductivity of the solution in which the specimens were previously immersed had effects on the recovery of the contact angle. Higher temperature and mid salinity solutions of 1-10 mS/cm resulted in longer times to recovery of the contact angle. The contact angle and corresponding surface energies recovered to their initial value after 4800 h, but the recovery rate was slower in mid-salinity solutions and high temperatures than for the other salinities and temperatures.

Dedication

To those I love and cherish and who have supported me throughout this endeavor, especially my mother Batool, my sister Parvin and her family, and my beloved wife Daphne and our little Joojoo

Acknowledgments

First of all I give thanks to God for letting me prepare this research and helping me in every step of my life.

My supervisor, Dr. R. Hackam, has been tremendously supportive throughout this work and I am greatly appreciative of his encouragements and wise guidance.

I would like to thank my department reader, Professor P. H. Alexander and my external reader, Dr. M.K.S. Madugula and my defense chair, Dr. C. Chen; their advice was invaluable.

I also would like to thank Dr. Kazu Iida for his generous help during my research work.

I would like to take this opportunity to thank the former head of the ECE Department Dr. S. Erfani and the present head of the Department, Dr. Sid-Ahmed for being so cooperative during my study period in the University of Windsor.

I am grateful to Ms. Shelby Marchand and Ms. Andria Turner, Mr. Don Tersigni and Mr. Frank Cicchello of the Electrical and Computer Engineering Department for their kind help and support.

Great appreciation is expressed to Mr. John Robinson of the Department of Mechanical, Automotive and Materials Engineering for carrying out the scanning electron microscopy (SEM), of Delrin. I am very grateful to my fellow student Behdad Elahipanah for his assistance and I wish him the best in his own graduate studies.

Lastly, I wish to thank my mother Batool and my wife Daphne, their loving support and assistance was invaluable in completing this thesis.

Table of Contents

Abstract	iii
Dedication	v
Acknowledgments	vi
List of Figures	xi
List of Abbreviations and Symbols	xviii

CHAPTER

1. Introduction

1.1 General	1
1.2 Polymer Insulators	3
1.3 PolyOxyMethylen: Delrin, Homopolymer and Acetron, Copolymer	4
1.4 Research Objectives	9
1.5 Research Planning	10

2. Experimental Method

2.1 Introduction	12
2.2 Delrin and Acetron Specimens	12
2.3 Conductivity and Temperature of Saline Solution	13
2.4 Aging Process	14
2.5 Recovery Process	15
2.6 Goniometer	15
2.7 RF Discharge	16

3. Measurement and Diagnostic Techniques

3.1 Contact Angle	18
3.2 Surface Roughness	24
3.2.1 Average Surface Roughness (ASR)	25
3.2.2 Maximum Surface Roughness (MSR)	25
3.3 Scanning Electron Microscopy (SEM)	26
3.4 Infrared Spectroscopy (IR)	28

4. Surface Properties of Delrin

4.1 Introduction	31
4.2 Experimental Procedure	33
4.3 Effect of Water, Salinity and Temperature on the Contact Angle	34
4.4 Percentage Increase in the Weight of Delrin and Acetron	43
4.5 Effect of Aging on the Color Delrin	48
4.6 Effect of RF Discharge on the Contact Angle of Delrin	52
4.7 Scanning Electron Microscopy (SEM)	54
4.8 Surface Tension Measurements	60
4.8.1 Mean Harmonic Method	62
4.8.2 Surface Tension of Delrin	63
4.9 Diffusion of Water in Delrin	71
4.9.1 Introduction	71
4.9.2 Diffusion Coefficient	72

4.9.3 Experimental Method	74
4.9.4 Activation Energy	81
4.10 Attenuated Total Reflectance FTIR Spectroscopy	85
4.10.1 Introduction	85
4.10.2 ATR of Delrin and Acetron	86
4.11. Surface Roughness of Delrin	93

5. Effect of Water Salinity, Temperature and Immersion Time of Immersion on dc/ac Flashover Voltage of Delrin

5.1 Solid Insulators and Breakdown Phenomena	95
5.1.1 Introduction	95
5.1.2 Intrinsic Breakdown	95
5.1.3 Thermal Breakdown	96
5.1.4 Discharge Breakdown	97
5.1.5 Free Volume Breakdown	97
5.1.6 Electromechanical Breakdown	97
5.1.7 Flashover Voltage	98
5.2 Flashover of Delrin under Stress of Water Salinity and Temperature	100
5.2.1 Introduction	100
5.2.2 Experimental Procedure	100
5.2.3 Results and Discussion	101
5.2.3.1 The dc Flashover Voltage of Delrin	101
5.2.3.2 The ac Flashover Voltage of Delrin	112

6. Recovery of Hydrophobicity in Delrin

6.1 Introduction	119
6.2 Experimental Method	119
6.3. Recovery of Contact Angle	120
6.4 Reduction in Weight during Recovery	126
6.5 Recovery of the Contact Angle after Exposure to RF Discharge	127
6.6 Recovery of the Surface Free Energies	131

7. Conclusion & Suggestions

7.1 Conclusion	136
7.1.1 Loss of Hydrophobicity	136
7.1.2 Effect of Water Salinity, Temperature and Duration of Immersion on dc/ac Flashover Voltage	136
7.1.3 Recovery of Hydrophobicity	137
7.2 Suggestions for Future Research	137

<u>References</u>	140
-------------------	-----

<u>Appendix A</u>	146
-------------------	-----

<u>Appendix B</u>	148
-------------------	-----

<u>Vita Auctoris</u>	153
----------------------	-----

List of Figures

- 2.1 Arrangement to apply RF discharge to Delrin specimen.
- 3.1. Dependence of the contact angle of water on time after placing the droplet on the specimen of Delrin. Conductivity of water, 0.005 mS/cm. Volume of droplet 4-5 μ l.
- 3.2 Dependence of the contact angle of droplet of water on Delrin on volume of droplet; Conductivity of water, 0.005 mS/cm.
- 4.1 Time variation of the contact angle of Delrin after immersion in different solutions at 0 ± 1 °C. Initial value of the contact angle before immersion was 82°.
- 4.2 Time variation of the contact angle of Delrin after immersion in different solutions at 23 ± 3 °C. Initial Value of the contact angle before immersion was 82°.
- 4.3 Time variation of the contact angle of Delrin after immersion in different solutions at 60 ± 2 °C. Initial value of the contact angle before immersion was 82°.
- 4.4 Time variation of the contact angle of Delrin after immersion in different solutions at 98 ± 2 °C. Initial value of the contact angle before immersion was 82°.
- 4.5 Variation of the contact angle of Delrin as a function of conductivity of the saline solutions after immersion of specimens for 2160 h at different temperatures. Initial value of the contact angle before immersion was 82°.
- 4.6 Dependence of the contact angle of Delrin on the temperature of the saline solution .Time of immersion was 2160 h.

- 4.7 Weight increase percentage of Delrin vs. time of immersion at 0, 23, 60 and 98 °C in 10 mS/cm saline solution.
- 4.8 Weight increase percentage of Acetron vs. time of immersion at 0, 23, 60 and 98 °C in 10 mS/cm saline solution.
- 4.9a Deterioration of Delrin after immersion in 10 mS/cm and drying at 98 °C for a long time. The sample was taken from a 10 year old material and also it went through few cycling of immersion and drying.
- 4.9b The sample of Delrin in Fig. 4.9a and on the left, a sample of Acetron were in the same condition. Acetron is more resistant against chemical reaction.
- 4.10 Delrin after 4600 h immersion in different salinity solutions at different temperatures. In 10 mS/cm saline solution at 98 °C the change in the color was the most significant.
- 4.11 Acetron after 768 h immersion in different salinity solutions at different temperatures. The change of color at 98 °C in 0.005, 1, 10 and 100 mS/cm saline solutions was almost consistent.
- 4.12 Recovery of contact angle of Delrin after application of RF discharges for durations of 10, 15 and 20 minutes.
- 4.13 Scanning Electron Microscopy of virgin specimen of Delrin.
- 4.14 Scanning Electron Microscopy of Delrin immersed in distilled water for 4600 h at 98 °C.
- 4.15 Scanning Electron Microscopy of Delrin immersed in 1 mS/cm saline solution for 4600 h at 98 °C.

- 4.16 Scanning Electron Microscopy of Delrin immersed in 10 mS/cm saline solution for 4600 h at 98 °C.
- 4.17 Scanning Electron Microscopy of Delrin immersed in 100 mS/cm saline solution for 4600 h at 98 °C.
- 4.18 Surface energy variation of Delrin with time of immersion in 10 mS/cm saline solution at 0 °C. γ_{SD} : Dispersion component; γ_{SH} : Polar component; γ_S : Surface energy of solid.
- 4.19 Surface energy variation of Delrin vs. time of immersion in 10 mS/cm saline solution at 23 °C. There is an increase in γ_{SH} , the polar component. γ_{SD} : dispersion component; γ_S : Surface energy of solid.
- 4.20 Surface energy variation of Delrin with time of immersion in 10 mS/cm saline solution at 60 °C. γ_{SD} : Dispersion component; γ_{SH} : Polar component; γ_S : Surface energy of solid.
- 4.21 Surface energy variation of Delrin with time of immersion in 10 mS/cm saline solution at 98 °C. γ_{SD} : Dispersion component; γ_{SH} : Polar component; γ_S : Surface energy of solid.
- 4.22 Calculated surface energy densities W_{SL} , γ_S , γ_{SH} , γ_{SD} , (mJ/Cm^2) and measured contact angle of methyl iodine θ_M , (degree) vs. contact angle of water θ_W (degree). Delrin immersed in 10 mS/cm saline solution at 98 °C as described in Fig.4.2.

- 4.23 Variation of $M(t)/M_{\infty}(\%)$ of Delrin as a function of square root of time in hours for different conductivities of saline solutions at 60 °C.
- 4.24 Variation of $M(t)$ of Delrin as a function of time in hours for different conductivities of saline solutions at 60 °C.
- 4.25 Variation of $M(t)/M_{\infty}(\%)$ of Delrin as a function of square root of time in hours for different conductivities of saline solution at 98 °C.
- 4.26 Variation of $M(t)$ of Delrin as a function of time in hours for different conductivities of saline solutions at 98 °C.
- 4.27 Variation of $\ln D$ of Delrin as a function of $1/T$ for different conductivities of saline solutions.
- 4.28 Variation of E_d , activation energy of diffusion of saline solution in Delrin, as a function of conductivity of saline solution.
- 4.29 ATR spectrum of virgin sample of Delrin.
- 4.30 ATR spectrum of aged sample of Delrin in 0.005 mS/cm at 98 °C.
- 4.31 ATR spectrum of aged sample of Delrin in 10 mS/cm at 98 °C.
- 4.32 ATR spectrum of virgin ample of Acetron.
- 4.33 ATR spectrum of Acetron aged in 0.005 mS/cm at 98 °C for 768 h.
- 4.34 ATR spectrum of Acetron aged in 10 mS/cm at 98 °C for 768 h.
- 4.35 Variation of average surface roughness (ASR) of Delrin after immersion in saline solutions of different conductivities for 2160 h at different temperatures.
- 5.1 Arrangement to measure the dc flashover voltage.

- 5.2 The dc flashover voltage of Delrin versus the number of shots at 23 ± 3 °C before immersion in a saline solution.
- 5.3 The dc flashover voltage of Delrin versus time of immersion in distilled water at 0, 23, 60 and 98 °C. Voltage measured at 23 °C.
- 5.4 The dc flashover voltage of Delrin versus time of immersion in saline solution of 1 mS/cm at 0, 23, 60 and 98 °C. Voltage measured at 23 °C.
- 5.5 The dc flashover voltage of Delrin versus time of immersion in saline solution of 10 mS/cm at 0, 23, 60 and 98 °C. Voltage measured at 23 °C.
- 5.6 The dc flashover voltage of Delrin versus time of immersion in saline solution of 100 mS/cm at 0, 23, 60 and 98 °C. Voltage measured at 23 °C.
- 5.7 The dc flashover voltage of Delrin versus time of immersion in different saline solution at 60 °C. Voltage measured at 23 °C.
- 5.8 The dc flashover voltage of Delrin versus temperature of saline solution of 10mS/cm. Voltage measured at 23 °C.
- 5.9 The dc flashover voltage of Delrin versus contact angle in 10 mS/cm saline solution at 98 °C. Voltage measured at 23 °C.
- 5.10 Arrangement to measure the ac flashover voltage.
- 5.11 The ac flashover voltage of Delrin versus number of shots at 23 ± 3 °C before immersion in a saline solution.
- 5.12 The ac flashover voltage of Delrin versus time of immersion in distilled water at 0, 23, 60 and 98 °C. Voltage measured at 23 °C.
- 5.13 The ac flashover voltage of Delrin versus time of immersion in saline solution of 1 mS/cm at 0, 23, 60 and 98 °C. Voltage measured at 23 °C.

- 5.14 The ac flashover voltage of Delrin versus time of immersion in saline solution of 10 mS/cm at 0, 23, 60 and 98 °C. Voltage measured at 23 °C.
- 5.15 The ac flashover voltage of Delrin versus time of immersion in saline solution of 100 mS/cm at 0, 23, 60 and 98 °C. Voltage measured at 23 °C.
- 6.1 Recovery of the contact angle on Delrin in air at 23 ± 3 °C after immersion in different saline solution for 4600 h at 0 ± 1 °C.
- 6.2 Recovery of the contact angle on Delrin in air at 23 ± 3 °C after immersion in different saline solution for 4600 h at 23 ± 3 °C.
- 6.3 Recovery of the contact angle on Delrin in air at 23 ± 3 °C after immersion in different saline solution for 4600 h at 60 ± 2 °C.
- 6.4 Recovery of the contact angle on Delrin in air at 23 ± 3 °C after immersion in different saline solution for 4600 hours at 98 ± 2 °C.
- 6.5 Contact angle on Delrin after 720 h recovery in air at 23 ± 3 °C as a function of conductivity level of saline solutions at different temperatures.
- 6.6 Reduction in weight (%) of Delrin after recovery in air at 23 ± 3 °C for 4800 h as a function of the conductivity level of saline solutions at different temperatures.
- 6.7 Recovery of contact angle of Delrin after applying RF discharge for durations of 10, 15 and 20 minutes.
- 6.8 Surface free energy, $\gamma_s(\text{J/m}^2)$ and its Polar component, $\gamma_{SH}(\text{J/m}^2)$ and Dispersion component, $\gamma_{SD}(\text{J/m}^2)$ during recovery in air at 22 ± 3 °C after aging in 10 mS/cm saline solution at 0 ± 1 °C.

- 6.9 Surface free energy, $\gamma_s(\text{J/m}^2)$ and its Polar component, $\gamma_{\text{SH}}(\text{J/m}^2)$ and Dispersion component, $\gamma_{\text{SD}}(\text{J/m}^2)$ during recovery in air at 22 ± 3 °C after aging in 10 mS/cm saline solution at 22 ± 3 °C.
- 6.10 Surface free energy, $\gamma_s(\text{J/m}^2)$ and its Polar component, $\gamma_{\text{SH}}(\text{J/m}^2)$ and Dispersion component, $\gamma_{\text{SD}}(\text{J/m}^2)$ during recovery in air at 22 ± 3 °C after aging in 10 mS/cm saline solution at 60 ± 2 °C
- 6.11 Surface free energy, $\gamma_s(\text{J/m}^2)$ and its Polar component, $\gamma_{\text{SH}}(\text{J/m}^2)$ and Dispersion component, $\gamma_{\text{SD}}(\text{J/m}^2)$ during recovery in air at 22 ± 3 °C after aging in 10 mS/cm saline solution at 98 ± 2 °C.

List of Abbreviations and Symbols:

ASR	Average surface roughness (μm)
ATR	Attenuated total reflectance spectroscopy
C	Concentration (g/cm^3)
Cal	Calorie
D	Diffusion Coefficient (m^2/s)
E_a	Activation Energy (J/mole or kCal/mole)
EPDM	Ethylene-propylene-diene-monomer
F	Time rate of transfer of matter per unit area ($\text{g}/\text{s}\cdot\text{m}^2$)
FTIR	Fourier transform infrared spectroscopy
HTV-SIR	High temperature vulcanized silicon rubber
IR	Infrared spectroscopy
L	Length, thickness (m)
MSR	Maximum surface roughness (μm)
POM	Polyoxymethylene
PTFE	Polytetraflouroethylene
R	Universal gas constant ($8.314 \text{ kJ}/\text{kmol K}$)
RF	Radio frequency
t	Time (second or hour as specified)
T	Absolute temperature (K)

Chapter 1

1. Introduction

1.1 General

High voltage insulators are essential elements of any power distribution system. Long term performance reliability is a major demand of the power industry. Insulators are used to support and insulate current carrying conductors at various voltage levels in electrical equipment for outdoor and indoor applications. Underground cables and overhead transmission lines are both critically dependent on reliable insulating materials. However, due to the short distances between conductors within underground cables, the performance of insulating materials becomes even more critical than for overhead transmission lines. Constant global development demands reliable electrical power distribution, and improved inexpensive insulating materials. Urban development has added to the importance of improving existing insulation materials and developing new ones, with the hope of eliminating major power system failures.

There are two main qualities of an insulating material that are of concern to the insulation designer. First is the mechanical strength of the insulation material which holds the conductor, and the second is its electrical properties and ability to withstand high voltage electrical stress. The external surface of an insulator is the first element which is exposed to aging and degradation. The environmental effects of pollution and ultra violet (UV) radiation are the most common causes of surface degradation of insulators. Contaminants

such as carbon or metal oxides, soluble salts and water make a thin conductive film and cause a flow of leakage current on the surface of the insulator. This layer of contamination acts as a variable resistor which in most cases is non-linear and unstable in the presence of an electrical field. The resulting leakage current will lead to a rise in heat and electrical discharge. This in turn results in erosion and tracking of insulators, and finally, these can intensify further to completely bypass the insulator and cause a flashover. This may cause an outage of the power system which can result in extra material and repair costs plus loss of revenue for electrical power suppliers. Therefore, the prevention of leakage current is a major factor which dictates and constrains the design considerations of outdoor insulators [1].

Traditionally, glass and porcelain have been used to make outdoor insulators and these materials are still in use around the world. They are very stable and exhibit high mechanical strength, performing satisfactorily in environments that are hot, dry and have high UV radiation. A major disadvantage of glass and porcelain is that they are brittle and prone to vandalism. Furthermore, because of their high surface energy, these insulators are more easily wetted in humid conditions. In other words, they possess a low contact angle [2]. In the presence of contamination and moisture, leakage current develops on the surface and this may result in a flashover of the insulator. In recent decades, the use of inorganic insulators has become less common and been replaced by polymeric insulators. This is because the polymeric insulators have better hydrophobic properties, better resistance to vandalism, and are of lighter weight and more economical than glass and porcelain.

The subjects of this study, DuPont Delrin® Acetal polyoxymethylene (POM) resins, are highly versatile engineering polymers that bridge the gap between metals and ordinary plastics. Delrin has been used in variety of applications in which mechanical and thermal stability and a high dielectric constant was needed. Delrin has been incorporated as an insulating component in high voltage cable connectors which are under the mechanical stress of moving conductors. Due to its high degree of crystalline Delrin display good impact resistance and outstanding surface hardness. Roller bearings, gears, reels, counters, control cams, valves and pump parts are some other typical applications of this polymer. The standard grades of Delrin are also approved by United States Food and Drug Administration (FDA) and United States Department of Agriculture (USDA) and due to their excellent resistance to moisture and hydrocarbons; they have a variety of applications in the food and biomedical industry [5].

1.2 Polymer Insulators

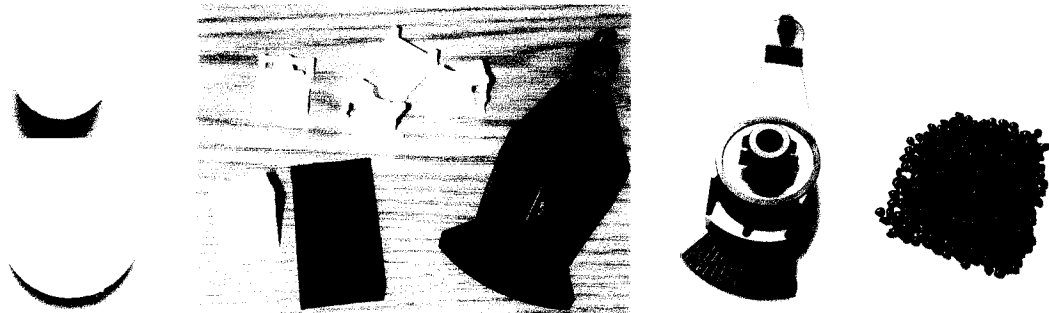
For over forty years polymeric insulators have been used increasingly in both outdoor and indoor applications and due to their superior performance their popularity continues to grow. They possess excellent hydrophobic characteristics which prevent the formation of a continuous film of water on the insulator surface. They also recover from a temporary loss of hydrophobicity significantly well. However, over extended period of time, these materials are subject to degradation and deterioration [3]. This results in loss of surface resistance, increased leakage current, dry band arcing, tracking and erosion of the insulator surface.

Various attempts have been made to improve the performance of polymeric insulators in polluted environments. A commonly used approach is to increase the leakage path by the use of an additional unit in order to reduce the electrical stress across the insulator surface. Another technique is to use Room temperature vulcanizing (RTV) coating to cover the porcelain insulator. These efforts have resulted in limited success.

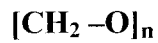
Silicone rubber (SIR), ethylene-propylene-diene-monomer (EPDM), alloy of SIR and EPDM, polytetrafluoroethylene (PTFE), and nylon etc. are the polymers most commonly used in outdoor insulators. Some studies have shown that polymeric insulators perform well in tropical environment. Although algae could grow on polymer (SIR) surface, their influence on insulator performance is negligible [4].

1.3 PolyOxyMethylen: Delrin, Homopolymer and Acetron, Copolymer:

Delrin was introduced by DuPont in 1966. It is considered the most metal-like plastic, that is to say it is a plastic with the strength of metal, and has contributed significantly to many engineering applications [5].



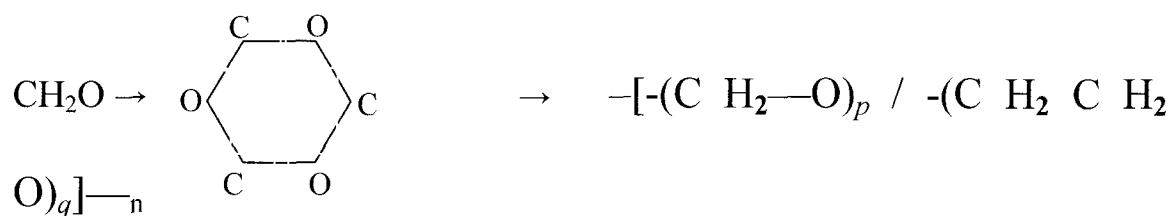
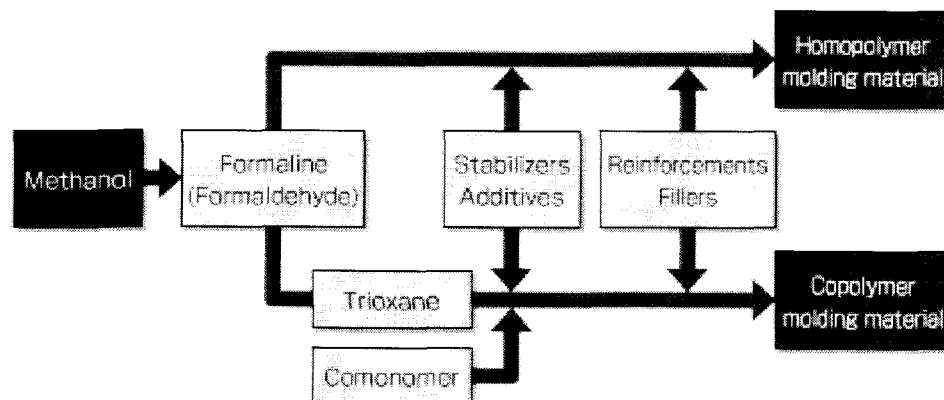
Delrin is an Acetal resin made from the polymerization of formaldehyde. It has been known by other names such as Polyformaldehyde, PolyOxyMethylen etc.



Delrin® is DuPont's registered trade mark for this crystalline plastic. This acetal resin is the homopolymer resulting from the polymerization of formaldehyde (CH₂O). The copolymer of this resin is known as Acetron®. Acetron is a trade mark of DSM Engineering Plastic Products which became Quadrant Plastic Products. The copolymer is also known with different names such as Celcon® and Ultraform®. Celcon is a trade mark of Ticona- Division of the Hoechst Group and Ultraform is a trade mark of BASF Corporation.

Formalin (formaldehyde) is made from methanol, and through polymerization it may be processed in two forms which results in homopolymer and copolymer. In the copolymer process, formaldehyde turns to trioxane (C₃H₆O₃), and then this trioxane, with the help of stabilizers, additives, reinforcement fillers and comonomer of polyoxymethylene, will form the copolymer. In the other form, the above additives and fillers turn formaldehyde directly to homopolymer.

These chemical processes can be illustrated as follows:



(Formaldehyde) → (Trioxane) → (Copolymer, Acetron)



Table 1.1 gives some useful technical properties of Delrin and Acetron [6].

The main challenge to the commercialization of these materials is the different modes of degradation that have to be overcome. Some of these modes are: unzipping from the chain ends, oxidation followed by depolymerization, acidic attack on the acetal chain, and thermal degradation. In order to combat these difficulties, commercial acetal has

additives that resist these types of degradation [7]. Appendix B includes a list prepared by DuPont Plastic of the different grades of Delrin and their ideal applications.

The most commonly used method for processing Delrin is injection molding. Other processing methods include extrusion, stamping and machining.

Table 1.1: Technical properties of Delrin, homopolymer and Acetron, copolymer

Property	Units	Delrin Homopolymer	Acetron Copolymer
Specific Gravity	g/cm ³	1.39-1.44	1.38-1.42
Tensile Strength	psi	10.0	8.6
Tensile Modulus	psi	400.0	380.0
Izod Impact	ft-lb/in	2.3	1.5
Dielectric Constant	-	3.7	3.8
Dielectric Strength	kV/mm	19.7	17
Melting Point	°F	342-363	320-342
Heat Deflection Temperature @ 66 psi	°F	336	315
Heat Deflection Temperature @ 264 psi	°F	257	220
Water Absorption Immersion 24hrs @ 23 °C	%	0.25	0.2
Water Absorption, Immersion Equilibrium	%	0.9	0.9
Relative Chemical Resistance	-	Good	Better for high pH solutions

1.4 Research Objectives:

1. To determine the hydrophobic behavior of Delrin homopolymer after immersion in a saline solution at different temperatures and different conductivity levels over an extended period of time.
2. To study the effect of radio frequency (RF) discharges on the loss and recovery of the hydrophobicity of Delrin.
3. To study the change in the surface roughness of Delrin during aging and recovery.
4. To study the change in the weight of Delrin and Acetron during aging in different salinity of water and temperatures.
5. To determine the coefficient of diffusion of saline water into Delrin and Acetron for different conductivity levels at different temperatures.
6. To determine the surface free energy (and its components) of Delrin at different stages of aging.
7. To study the recovery of hydrophobicity of Delrin at room temperature after aging at different temperatures in saline solutions of different conductivity levels.
8. To study the effects of high temperatures on the hydrophobic behavior of Delrin.
9. To understand the mechanism of loss and recovery of hydrophobicity of Delrin insulation under the stress of heat and salinity.
10. To study the effects of temperature, salinity and the duration of exposure to water on the ac and dc flashover voltages

1.5 Research Planning

In the laboratory environment there are various aging methods to accelerate the life period of insulation materials under different service conditions. This study has employed the immersion in saline solution and in air both at different temperatures. This results in three major causes of degradation: heat, water and salt. The length of immersion is another parameter involved in this study. Delrin specimens were immersed in saline solution of different conductivities at different temperatures over periods of 3000-5000 h. After removal from the saline solutions, the recovery of aged samples of Delrin at room temperature was studied.

Throughout this study, the contact angle was measured as the major indication of the surface hydrophobic characteristic of Delrin. Different researchers have used all three possible ways of measuring the contact angle: static, receding and advancing [8-11]. Through Young's equation static contact angle is more efficiently related to the surface free energy of the insulating material [12-15]. Although it seems a simple method, it is a very effective indicator of the hydrophobic behavior of a surface [9, 16-18]. Therefore, in this study this method was used to calculate the surface free energy of Delrin as a measure of the hydrophobicity of the surface. Alongside the measurements of the contact angle, measurements of ac and dc flashover voltages were also employed to study the surface degradation of polymeric insulators. During exposure to a saline solution, the surface of a polymeric insulating material acquires gradual changes, which affect its ability to withstand voltage. In this case the electric current flows readily across the surface. As the applied voltage is increased the current also increases until flashover takes

place across the surface [4]. In this study the effect of the immersion of Delrin in a saline solution at different temperatures and for different durations on the surface flashover voltage is examined.

Surface roughness is another parameter that can be measured to study the surface degradation level. Measuring the surface roughness is used in this work to understand better the effect of salinity, wetness and heat on the surface of Delrin.

Chapter 2

2. Experimental Method

2.1 Introduction:

The loss and subsequent recovery of the hydrophobicity of Delrin were carried out experimentally to study the aging characteristics of Delrin. Samples of Delrin were subjected to different tests and combined aging stresses of salinity, moisture and heat for extended period of time. These tests approximate the accelerated service life of the insulator in a laboratory environment. The recovery process shows the behavior of the insulator after temporary exposure to contamination and stress.

Because of its excellent mechanical strength, Delrin can be used in many outdoor and indoor high voltage insulation applications. Different additives and fillers which can improve the performance of Delrin as an insulating material for various applications have been recommended [5].

2.2 Delrin and Acetron specimens:

Specimens of Delrin were cut from 19 ± 0.1 mm rod to a length of 9.3 ± 0.3 mm, and for Acetron were cut from 28 ± 0.2 mm rod to a length of 2.5 ± 0.4 mm. The density of the material were 1.43 gr/cm^3 for Delrin and 1.45 gr/cm^3 for Acetron. The initial contact angle of a 4-5 μl distilled water droplet of $5 \pm 1 \text{ }\mu\text{S/cm}$ conductivity on the surface of Delrin was $67.5 \pm 2.5^\circ$. The low contact angle was due to the presence of dust and contamination on the surface of the virgin specimens. This had also been reported in

polyethylene and PTFE [19, 20]. The specimens were washed in a diluted acetic acid solution (5%) in an ultrasonic vibrator for two minutes and then followed by washing in distilled water [8, 9, 19-22]. The mild acetic acid does not react with Delrin or with Acetron and removes the contaminants from the surface of the polymer [19, 20]. The specimens were dried naturally at 23 ± 3 °C for 2-3 days and then the contact angle was measured. It had increased to 82.5 ± 2.5 °C.

The average surface roughness (ASR) of virgin Delrin was measured and was 1.4 ± 0.4 μm . To ensure reproducibility, two specimens were used at each temperature and conductivity in every reading [8, 9, 19, 20]. The specimens were subjected to combination of heat, moisture and salinity.

2.3 Conductivity and Temperature of Saline Solution:

The saline solutions were prepared by adding sodium chloride (NaCl, table salt) to distilled water at room temperature. The conductivity of each solution was measured by *Horiba ES-12* digital conductivity meter. Four conductivity levels of 0.005 ± 0.001 , 1 ± 0.01 , 10 ± 0.1 and 100 ± 1 mS/cm were prepared. The first solution was distilled water and the conductivity of the last solution was determined by the amount of salt in unit volume of distilled water from the conductivity graph which it was 80 gr/liter. The 100 mS/cm saline solution was saturated and salt deposits were visible at the bottom of the container. One set of the specimens were also aged in air at all temperatures. The temperature of air and saline solutions were 0 ± 1 , 23 ± 3 , 60 ± 2 and 98 ± 2 °C.

2.4 Aging Process:

The aging method was the same as had been used in [19, 20]. The set of Delrin and Acetron samples designated for the study of the weight variation and diffusion coefficient were weighed using a high precision ($d = 0.0001$ g) scientific balance Sartorius Ag Gottingen-Model BP 110S.

The Average surface roughness (ASR) was measured before immersion in a saline solution using a precision (± 0.05 μm) surface roughness detector type Surfrest 212 Mitutoyo. The same measurements were repeated for the specimens aged in air at all the temperatures. Two specimens of Delrin were used at fixed conductivity level and temperature for each aging period of time. Clean glass containers were used to house the saline solutions and the specimens. The conductivity and temperature of the saline solutions were monitored intermittently to maintain steady conditions.

The virgin Delrin and Acetron specimens were immersed in different saline solutions with a conductivity of 5 $\mu\text{S}/\text{cm}$, 1, 10 and 100 mS/cm and kept under thermal stress at temperatures of 0 ± 1 , 23 ± 3 , 60 ± 2 and 98 ± 2 $^{\circ}\text{C}$ for different durations. The aged specimens were taken out of the oven or the refrigerator after a set interval of time and allowed to reach room temperature (23 ± 3 $^{\circ}\text{C}$) naturally before measuring the weight or the contact angle. The specimen was first washed in distilled water for 2 minutes and then dried using a blow dryer at room temperature. Then the weight and the contact angle of specimens were measured and then the surface roughness and subsequently the dc and ac

flashover voltages were measured. The above measurements continued during the aging process until saturation was reached in the value of the contact angle.

2.5 Recovery Process:

The recovery started immediately after completion (saturation) of the loss of hydrophobicity. After about 4600 h of immersion in saline solutions at different temperatures, saturated values of the contact angles were reached. Therefore, the aged specimens were removed from the saline solutions and kept in clean and dry glass containers in air at room temperature of 23 ± 3 °C and relative humidity of $55\pm 15\%$ for up to 4800 h. The weight, the surface roughness and the contact angle of the aged specimens were recorded and used as the initial value. During the recovery, the change in the contact angle, weight and the average surface roughness (ASR) were measured intermittently. The changes in the above parameters were opposite to those observed during aging. However, the recovery process was very slow compared to that of aging.

2.6 Goniometer:

The contact angle was measured after placing the specimen on the stable horizontal surface of the goniometer as given in [21]. This was a simple setup comprising of two stands, one of which held a horizontal platform and the other one held a vertical syringe. A one ml syringe was used to control the size of the water droplet within 4-5 μl in order to maintain uniformity throughout the experiment. A table lamp (40 W) was used to illuminate the droplet surroundings and help achieve a clear visual through the eye piece of the goniometer. The contact angle was read within 30 s after placing the droplet of

water on the specimen in order to eliminate the effect of evaporation and absorption of water on the surface of the specimen.

2.7 RF Discharge

Radio Frequency (RF) discharges were applied to virgin specimens of Delrin at 23 ± 2 °C for durations of 10, 15 and 20 minutes using a high frequency (HF) generator. The frequency of the discharge was monitored and measured using an oscilloscope to be approximately 250 kHz. The current flowing on the specimen surface was measured to be 50 ± 30 mA. The contact angles of the virgin specimens were measured before and after their exposure to the RF discharge. HF tester manufactured by Edwards High Vacuum Ltd was used for this experiment. Fig. 2.1 shows the schematic diagram of the RF discharge measurement.

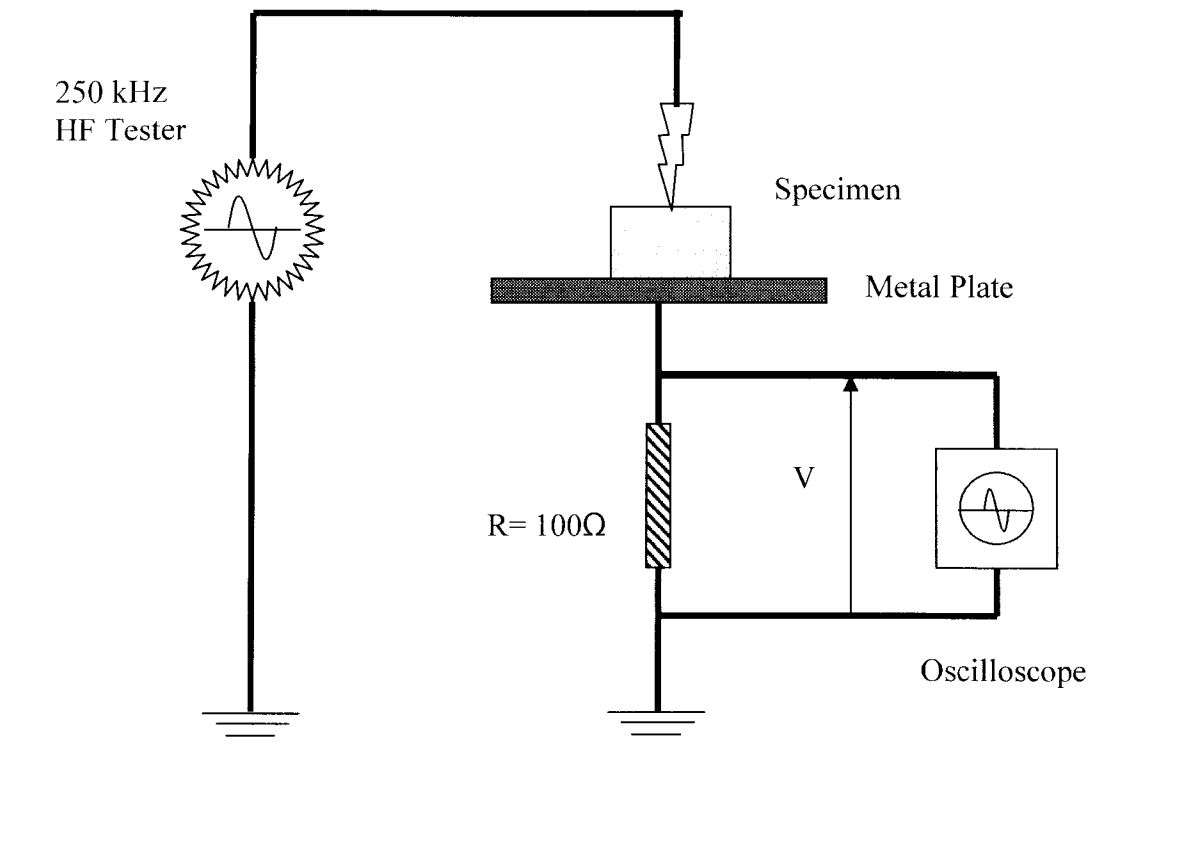


Fig. 2.1 Arrangement to apply RF discharge to Delrin specimen.

Chapter 3

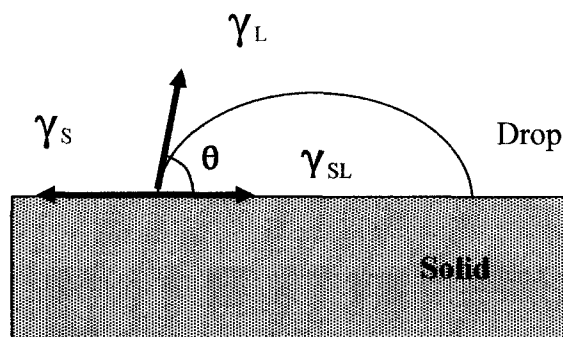
3. Measurement and Diagnostic Techniques

3.1 Contact Angle

The contact angle is the angle formed by a liquid at the three phase boundary where a liquid, gas and solid intersect. The contact angle of a liquid droplet on a solid surface is the angle between the tangent to the droplet at the three phase junction and the horizontal surface [12, 13]. The contact angle is called the static contact angle if the system is at rest. If the system is dynamic then the measured contact angle called the dynamic contact angle. The dynamic contact angle, based on whether in advancing or receding of forming the droplet, is called advancing or receding contact angle. In some literature, authors have also used advancing and/or receding contact angle to measure the surface hydrophobicity of the solid surfaces [11, 23]. The contact angle is a measure of the ability of the solid surface (hydrophobicity) to reject the formation of a continuous film of water. The higher the value of the contact angle, the more hydrophobic the solid surface is said to be. The contact angle depends on the surface tension (surface free energy) of the liquid and that of the solid surface on which the contact angle is measured. Young's equation describes the relationship among the contact angle, the surface tension of the liquid and the surface tension of the solid [12-14].

Young's Equation:

$$\gamma_S = \gamma_{SL} + \gamma_L \cos\theta \quad (3.1)$$



Where γ_S , is surface Tension of the solid, J/m^2

γ_L , Surface tension of liquid, J/m^2

γ_{SL} , Surface tension of Solid/liquid interface, J/m^2

And θ is the Contact angle of the solid surface.

For constant values of γ_L and γ_{SL} the higher the value of γ_S , the lower the value of the contact angle θ . This means that high energy solid surfaces have smaller contact angles and are therefore easily wetted. Surfaces are classified into two categories: high energy and low energy surfaces [12]. Materials with high surface energies consist of metals, metal oxides and inorganic compounds such as glass, silica, sapphire, porcelain and diamond. They are usually hard, obstinate and dense. Their surface free energy is in the range of 200-5000 mJ/m^2 . Water vapor absorbs quickly onto any high energy surface even if relative humidity is low as 0.6 % [12]. On the contrary water beads up on low energy surfaces. The low surface energy materials are organic compounds such as polymers. They are usually soft, have low melting points and light in weight.

The contact angle of a liquid depends on the temperature of the liquid. Near the boiling temperature, the contact angle approaches zero [12]. All measurements of the contact angle in the present work were taken at 23 ± 3 °C. The overall change in the contact angle due to the change in the ambient temperature within the range of 23 ± 3 °C is negligible [12]. The contact angle is independent of the conductivity of the droplet liquid [21].

Distilled water of conductivity of $5\pm 1 \mu\text{S}/\text{cm}$ was used throughout the course of this research.

The contact angle of a liquid droplet depends on the time lapse between placing the sessile droplet on the surface and taking the measurements. After 15 minutes the droplet of 4-5 μl becomes very flat due to evaporation and absorption of water on the surface of Delrin and it becomes difficult to take correct reading on the goniometer. The variation of the contact angle with time after placing a droplet of water on the Delrin is shown in Fig. 3.1.

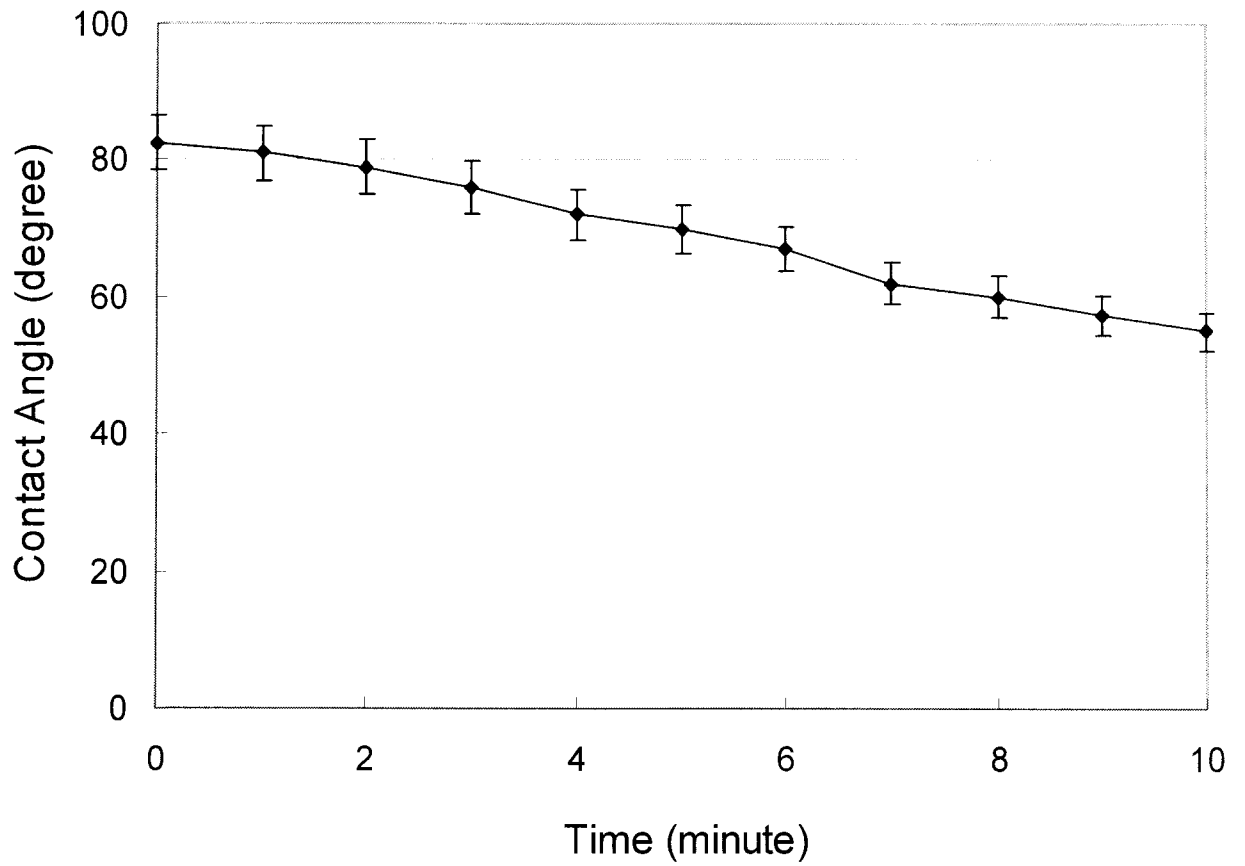


Fig. 3.1: Dependence of the contact angle of water on time after placing the droplet on the specimen of Delrin. Conductivity of water, 0.005 mS/cm. Volume of droplet 4-5 μ l.

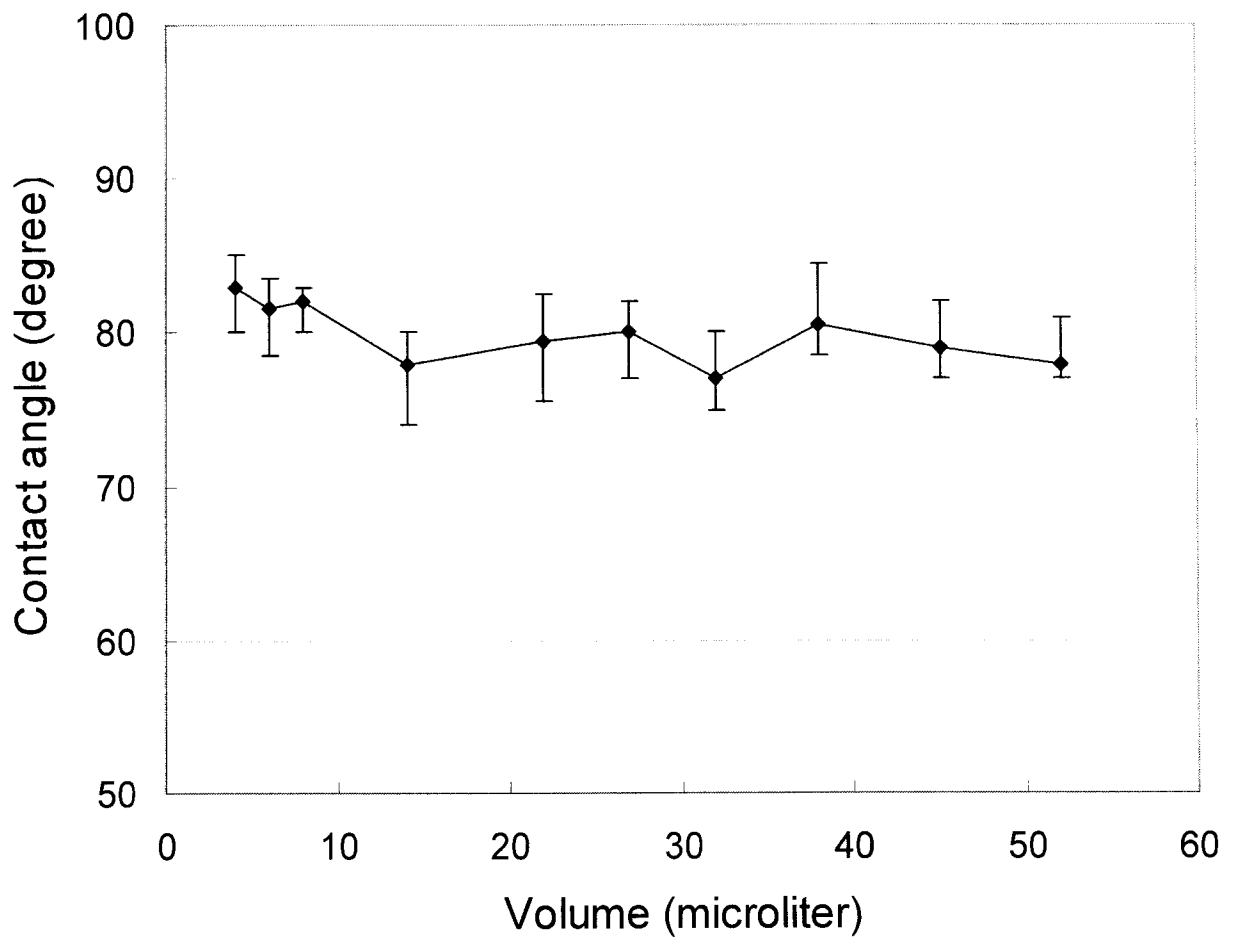


Fig. 3.2: Dependence of the contact angle of droplet of water on Delrin on volume of droplet; Conductivity of water, 0.005 mS/cm

To maintain consistency throughout the study, the contact angle measurements were read within 30 s of placing the sessile droplet of water on the horizontal surface of the samples.

The contact angle was reported to be independent of the size of the water droplet up to 30 μl [8, 19, 20]. This limit was extended up to 40 μl in the present work as shown in Fig. 3.2. It can be seen that the contact angle remains constant at $82\pm 0.5^\circ$ over the range of 1 to 40 μl . However, the size of droplet used throughout this research was approximately 4-5 μl in order to have a consistent result throughout the experiments.

There are several methods to measure the contact angle of a solid surface such as: Drop-bubble Method (Direct Observation –Tangent Method), Reflected Light Method, Interference Microscopy Method and Determination of the contact angle from Drop Dimensions [12].

Drop-Bubble Method (also called sessile drop method or Tangent Method or Direct Observation Method): In this method, a sessile drop placed on the surface of the solid and the contact angle is taken by measuring the angle subtended between the tangents to the drop profile at the point of contact with the solid surface underneath the drop. This measurement can be done on the actual drop or on a projected image or a photograph of the drop profile. Accuracy of the contact angle measured in this work is $\pm 1-2^\circ$. The range of the contact angles measured in this method is $10-160^\circ$ and uncertainty below and above this range is due to difficulty of locating the tri-phase junction point. Despite its

simplicity and low cost, it is a very reliable technique for measuring the contact angle [8, 12, 19-21] in the above range.

Reflected Light Method: in this method a reflected beam from the surface of the drop of liquid is used. This beam is emitted by a microscope and it is at right angle to the drop surface. The limitations of this method are that the contact angle should be less than 90° and all reflections must be eliminated from the drop surface in order to take the reading.

The Interference Microscopy Method: This method overcomes the limitations of both the Tangent Method and the Reflected Light Method. In this method, a monochromatic light (5461-Å green mercury line) is reflected with a beam splitter onto the reflecting substrate to form interference bands parallel to the drop edge. The contact angle is calculated from the spacing of the interference bands, the reflecting index of the liquid and the wavelength of the light [12].

Drop Dimension Method: In this method, the contact angle is calculated using trigonometric relationship of the drop geometry [12]. Contact angle measuring instruments based on these principals are commercially available and have been used by some authors [24].

3.2 Surface Roughness

The contact angle depends on the surface roughness of the solid. Good [13] has established a mathematical relationship between the contact angle and the surface

roughness which implies that if the contact angle is less than 90° , it is decreased by surface roughness, whilst if the contact angle is greater than 90° , it is increased by surface roughness [25]. This effect has been observed during the contact angle measurement of Delrin in this work. Therefore surface wettability depends on surface roughness. The contact angle hysteresis increases with surface roughness [12-14, 25]. An increase in the leakage current with the increase in the surface roughness has been reported by Deng [21]. Hence, a study of the change in the surface roughness of polymeric insulator as a function of aging time is important. In this work, the surface roughness has been studied in two ways:

- 1-Measuring surface roughness using surface detector (Surftest 212 Mitutoyo, Japan)
- 2-Scanning Electron Microscopy (SEM)

3.2.1 Average Surface Roughness (ASR)

Average Surface Roughness by definition is the mean value of the surface roughness profile over a certain distance called the sampling length.

3.2.2 Maximum Surface Roughness (MSR)

Maximum Surface Roughness is defined as the arithmetic mean value measured between the highest peak and the lowest valley.

Hydrophobicity or wettability of a solid surface depends on ASR and not on MSR. Hence, ASR is more important than MSR by observation in this research work. Deng [22] has measured the average surface roughness of the salt fog aged RTV silicon rubber coatings to study their hydrophobic behavior. Therefore, ASR has been measured in the

present research to measure the changes in the surface roughness of Delrin specimens. The sampling length was adjusted to be 8 mm longitudinally along the specimen rod. Surface roughness was measured 12-16 times on the same specimen at different locations and then an average of these values was calculated in order to get a value of ASR. A fixture was designed and built to hold the specimen and surface detector in a stable position for consistent reading on the surface of each specimen.

The SEM studies have been conducted using JEOL JSM-5800 LV Scanning Electron Microscope. The surface roughness evaluation with SEM was carried out after washing the specimens in distilled water (0.005 mS/cm) to remove excess salt deposited on the surface of specimens that were allowed to recover in air for 4000 h.

3.3 Scanning Electron Microscopy (SEM)

SEM has been used [19-21, 26] to examine the aging effects on the insulator surfaces and compare the results with those determined using the surface roughness detector. In this study SEM was used to study both the surface roughness and to determine the composition of the material on the surface.

Electron microscopy is an efficient method to obtain microphotographs of a solid surface. It can also be used to detect the composition of the surface of the material under examination. In many aspects, electron optics is the same as light optics except for two main differences:

1. Light is an electromagnetic radiation with wavelength λ and electrons are subatomic particles. However, we may apply both types of descriptions to light and electrons. Thus visible light can be considered as consisting of photons of wavelength 400-700 nm whereas electrons are radiation of wavelength between 0.001 and 0.01 nm. The advantage of shorter wavelength of electrons is that electrons are easily absorbed by many materials than is light. Hence, we must have vacuum of the order of 10^{-4} Torr (1 Torr =133.3 Pa) or better in order to have depth of penetration of few μm . To have a better resolution a very thin layer of gold has been deposited on the surface of solid which also increases the depth of penetration.

2. Another major difference between light and electrons is the charge of electrons. Therefore, electromagnetic fields can be used as lenses for deflection of electron beams and it is possible to scan a beam of electrons in and out. This has led to the invention of scanning electron microscopy abbreviated as SEM [27].

In principle, an electron beam is focused on to the scanned specimen with the help of condenser lenses and across it by deflector coils. The incident electrons (called primary electrons) produce characteristic radiation as a result of their interaction with the electrons of different elements present in the sample (called secondary electrons). Occasionally the incident beam may remove K, L or M shell electrons thus leaving the atom in an excited or ionized state. The equilibrium or the steady state of the atoms in the specimen has been disturbed. Therefore, the system tries to normalize and atoms return to the steady state by transfer of n outer electron into the vacant position in the inner shell.

The return of an electron to a lower energy shell causes the emission of a photon of X-Ray radiation. The quantum number of electrons in the atom describes that electrons are in discrete energy levels. The emitted X-Ray photon holds a discrete energy equal to the difference between the initial and final energy states of the atom. The wavelength and energy of the characteristic radiation are specific for atoms of an atomic number. The presence of the characteristic X-Ray line indicates the presence of a particular element in the specimen. Detection of characteristic energies is helpful to obtain the composition of the specimen under test. The acquired spectrum is a plot of the count rate of X-Rays as a function of energy. This is done with the help of an attachment called an energy dispersive X-Ray attachment (EDAX or EDS). The count rate is an indication of the quantity of a particular element present in the test specimen [26]. The secondary electrons are converted into a current by the detector and hence the magnified image of the specimen. This current is then amplified and used to control the brightness of the cathode ray tube [27]. This is a second application of the Scanning Electron Microscope.

3.4 Infrared Spectroscopy (IR)

In this work, Fourier Transform Infrared Spectroscopy (FTIR) has been used to study the chemical changes in the surface of Delrin due to the stresses of heat and salinity over a long period of time. In many literatures references [17, 28-30] oxidation of polymeric surface due to aging has been reported. Accordingly, carbonyl and carboxylate groups (in the range $1550-1735\text{ cm}^{-1}$) are formed by the reaction of oxygen with the methyl polymer chain. These compounds are hydrophilic and absorb water resulting in an increase of the surface free energy and a reduction in the contact angle of the polymer.

Infrared Spectroscopy (IR) is a diagnostic tool to find out the chemical composition of a compound by measuring one of its physical properties [31]. Usually the physical property of matter to absorb, transmit or reflect infrared radiation is used in this technique. The instrument is called infrared spectrophotometer.

In principle, absorption of infrared light of appropriate energy level excites the atoms of the specimens under test and the absorbed energy is converted into vibrational and rotational energies of the covalent bonds of the functional groups to which those atoms belong. A beam of infrared light emerging from a cell through a sample is focused and passed through the monochromator. The monochromator focuses the beam onto a collimator and passes it through a dispersing element. The dispersing element deviate the rays by different amounts depending on its wavelength. This is how the light of different frequencies is distinguished to give information about the functional groups present in the sample that is placed in the cell [32]. This technique is commonly used in analytical chemistry. It is useful for both quality wise and quantity wise analysis of materials [33-39]. Its use is limited to detection of chemical functional groups in a particular substance. It cannot be used in a single element substance [21, 31] and it is a non-destructive test. The sample tested for this analysis, can be reused elsewhere. The instrument can be used in the transmission or absorbance mode. The transmittance or absorbance percentage is measured as a function of wave length of the infrared light in the range 2.5×10^{-4} - 5×10^{-3} cm (corresponding to wave number 4000 - 200 cm^{-1}).

FTIR is an improved method of infrared spectroscopy. It reduces the signal to noise ratio of the instrument and gives added response of intensity of chemical functional groups by accumulating the response of each group in the vicinity by using multiple scan method. The quality of the spectrum improves with increasing number of scans [32]. In this work computerized FTIR set up Bomem-100 was used. It uses Win-Bomem B-grams software. Eight scans were carried out in each case.

Usually the specimen under test for transmission should be transparent to furnish sharp peaks of spectrum. However, ATR (Attenuated Total Reflection) attachment should be used where good transmission can not be attained through the specimen due to opaqueness of the material. In this case the radiation penetrates a few microns into the sample and then it is reflected back into the optical element [33].

Samples of Delrin (homopolymer) and Acetron (copolymer) after aging in different condition of stress were subjected to ATR FTIR due to the thickness of the samples was not practical for this work.

Chapter 4

4. Surface properties of Delrin

4.1 Introduction:

Delrin has outstanding mechanical and electrical properties which make it appealing for use as a high voltage insulator. Electrical insulation systems demand high stability against degradation due to the effects of salinity and oxidation in the presence of moisture. Delrin can be used at high temperatures up to 300 °F and has low water absorption, less than 0.9% [5]. This chapter reports on study of the loss of the hydrophobicity of Delrin in the presence of moisture, different salinities and temperatures. As a property of the surface of a solid, hydrophobicity is the ability of a solid to resist the formation of a continuous film of water. The loss of hydrophobicity is due to degradation of the material in wet and polluted conditions. In this research Delrin specimens were immersed in saline solutions where the conductivity was varied from 4 $\mu\text{S}/\text{cm}$ (distilled water) to 100 mS/cm (saturated saline solution). The temperature of the solutions were 0 ± 1 , 23 ± 3 , 60 ± 2 and 98 ± 2 °C. The loss of hydrophobicity was measured by determining the contact angle of a droplet of distilled water on the Delrin surface. It was observed that the decrease in the contact angle depended on the combined stress of salinity, temperature and duration of immersion. The influence of Radio Frequency (RF) discharge on the loss of hydrophobicity was studied. The increase in the weight and the surface roughness and their correlation with hydrophobicity of the specimens were also reported. Increase in the weight of Delrin was measured using a high precision balancing instrument, and the diffusion coefficients of the saline solution into the Delrin specimen were calculated at different temperatures and salinities.

The surface free energy and its components were calculated for 0.005, 1, 10 and 100 mS/cm saline solutions at 98°C and it was observed that the surface free energy increased with increased water salinity up to a certain limit, and for salinity as high as 100 mS/cm it did not increase as much as mid-salinity solutions. In order to determine the surface free energy components of Delrin, the static contact angle, θ measured using two different liquids, water and methyl iodine with known surface energy components. To study the effect of temperature, Delrin was immersed in 10mS/cm which caused the worst case of degradation at different temperatures and the surface free energy was calculated. It was observed that the surface free energy increased with increased temperature and the duration of immersion [20, 40].

Hydrophobicity is the ability of the surface to repel the formation of a thin film of water. The aging process normally starts from the surface of the insulating material, in the form of degradation due to oxidation. This degradation causes a loss of hydrophobicity on the surface of polymers, which is accelerated with the increasing stresses of high temperature and salinity. Water can readily cover the surface and infuse into the bulk, after the loss of hydrophobicity [20].

This chapter covers the effects of various elements such as water, salinity, heat and RF discharge on the contact angle of a water droplet on the surface of the Delrin specimen. The effects of these stresses on the weight, coefficient of diffusion, surface free energy and surface roughness of Delrin are also discussed.

4.2 Experimental Procedure

Cylindrical rods of Delrin with diameter of 19 mm and length of 9.3 ± 0.3 mm were prepared and immersed in saline solutions, at various temperatures and for extended durations. Four conductivities of the saline solutions of 0.005, 1, 10 and 100 mS/cm were used. The required conductivity was obtained by adding sodium chloride (NaCl, table salt) to distilled water, which had a conductivity of 0.005 mS/cm. Containers of saline solutions and Delrin specimens were kept at 0 ± 1 , 23 ± 3 , 60 ± 2 and 98 ± 2 °C for durations of up to 2160 h for studying the contact angle and up to 4600 h for weight increase and consequently the recovery of the contact angle and the loss of absorbed water. The Delrin specimens were also left in air at these temperatures. The specimens were intermittently removed from the saline solution for the measurement of the contact angle θ . The contact angle between the tangent of a droplet of distilled water on the surface of Delrin and the horizontal surface was measured with a goniometer to an accuracy of $\pm 0.5^\circ$ [19, 20]. The volume of the droplet of water was about 5 μ l. Previously, the contact angle was found to be independent of the volume of the droplet up to 50 μ l [19, 20].

The contact angle θ at the triple junction of air, water and Delrin, was initially measured and it was 62° . Samples were washed in a diluted acetic acid (5% vinegar) and distilled water with the aid of an ultrasonic vibrator and dried at room temperature. The contact angle was then measured and found to be 82° . This increase in the value of the contact angle after cleaning is in agreement with previous studies of different polymers as well [19, 20, 40].

The contact angle was determined at 23 ± 3 °C and relative humidity of $55 \pm 15\%$. After specimens were removed from the saline solutions at 0, 23, 60 and 98 °C, and were allowed to cool down or warm up, they were washed in distilled water for 1-2 minutes and then excess water was allowed to dry. After this preparation, the specimens were ready for measurement of the contact angle, surface roughness and dc and ac breakdown. The same procedure was applied before measuring the weight of Delrin specimens. Typically it took 15-20 minutes for the specimens to cool down, and be washed and dried before commencing the measurements of θ . The contact angle was determined within 30 s after placing the droplet of water on the specimen. To maintain the reproducibility of the results, two specimens were employed for each condition. The reported values of θ are the averages of 6-12 readings for each condition.

4.3 Effect of Water, Salinity and Temperature on the Contact Angle

Figs. 4.1 to 4.10 show the variation of the contact angle of Delrin for different conductivity levels at different temperatures with respect to the time of immersion. The conductivities of solutions were 0.005, 1, 10 and 100 mS/cm and the temperatures were 0 ± 1 , 23 ± 3 , 60 ± 2 and 98 ± 2 °C. The time of immersion was extended up to 2160 h. The contact angle was also measured on specimens placed in air over the temperature range of 0- 98 °C. After immersion in the saline solutions the contact angle decreased rapidly with increasing time. The reduction in the contact angle was relatively larger for the mid-salinity levels and higher temperatures. However, the contact angle decreased slowly for all conductivity levels at 0 ± 1 °C (Fig. 4.1) as compared to the high temperatures (Figs. 4.3 and 4.4). The contact angle of the specimens immersed in the

saline solutions at 23 ± 3 °C continued to decrease to 65° and 59° for mid-salinities of 1 and 10 mS/cm, respectively, and for very low and high salinities reached to a saturated level over the immersion period, 71° for 0.005 mS/cm and 75° for 100 mS/cm.

At high temperatures the contact angle for mid-salinities decreased drastically over the period of immersion. The contact angle in 1 and 10mS/cm solution at 60 °C dropped to 63° and 35° respectively, Fig 4.3. The θ in 0.005 and 100 mS/cm was saturated to 70° and 67° respectively.

Fig.4.4 shows results during immersion in 100 mS/cm at 98 °C. At first the contact angle decreased quickly but after 72 h it decreased slowly and reached 46° at the end of the immersion period. The contact angle for low and mid-salinities decreased drastically over the period of immersion. The contact angle in 0.005, 1 and 10 mS/cm solution at 98 °C decreased to 37° , 22° and 17.4° respectively. Accurate measurements for contact angles below 25° were difficult to obtain due to the loss of hydrophobicity of the surface.

Fig. 4.5 shows the variation of the contact angle as a function of the conductivity of the saline solution after immersion of Delrin specimens for 2160 h at different temperatures. It will be observed that increasing the water salinity up to certain limit increases the loss of hydrophobicity of Delrin. Saturated saline solution has a limited effect on decreasing the contact angle. Saline solution of 10 mS/cm has caused the most degradation of the surface of Delrin.

Fig. 4.6 shows the decrease of the contact angle as a function of temperature for different salinities. The contact angle decreased continuously with the increase of temperature in each saline solution.

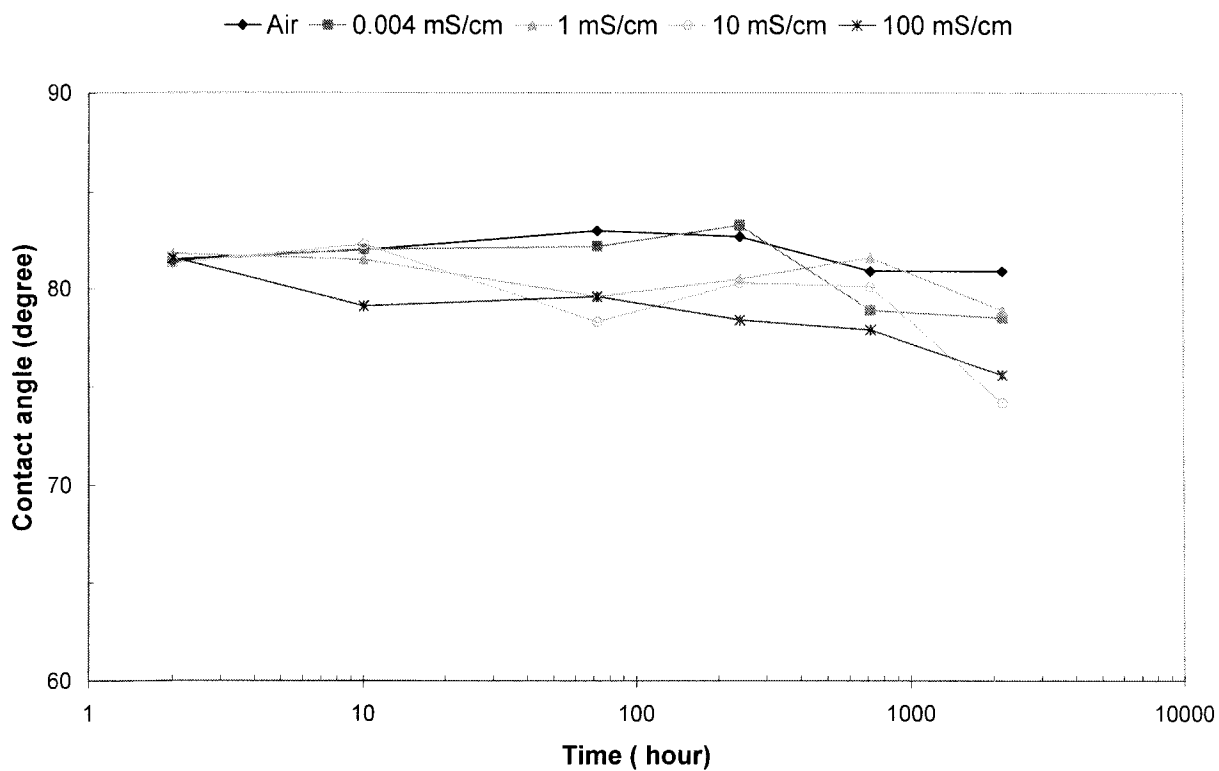


Fig. 4.1: Time variation of the contact angle of Delrin after immersion in different saline solutions at 0 ± 1 °C. Initial value of the contact angle before immersion was 82° .

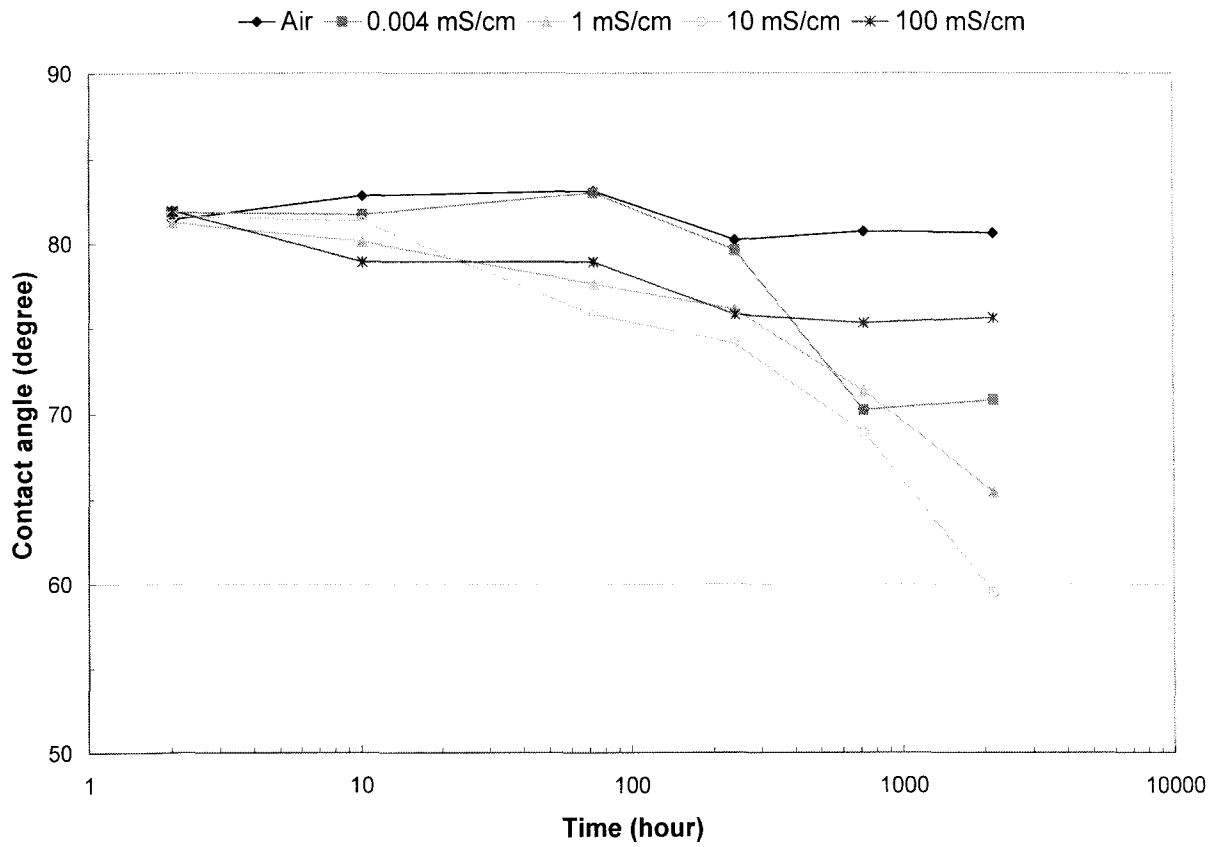


Fig. 4.2: Time variation of the contact angle of Delrin after immersion in different saline solutions at 23 ± 3 °C. Initial value of the contact angle before immersion was 82° .

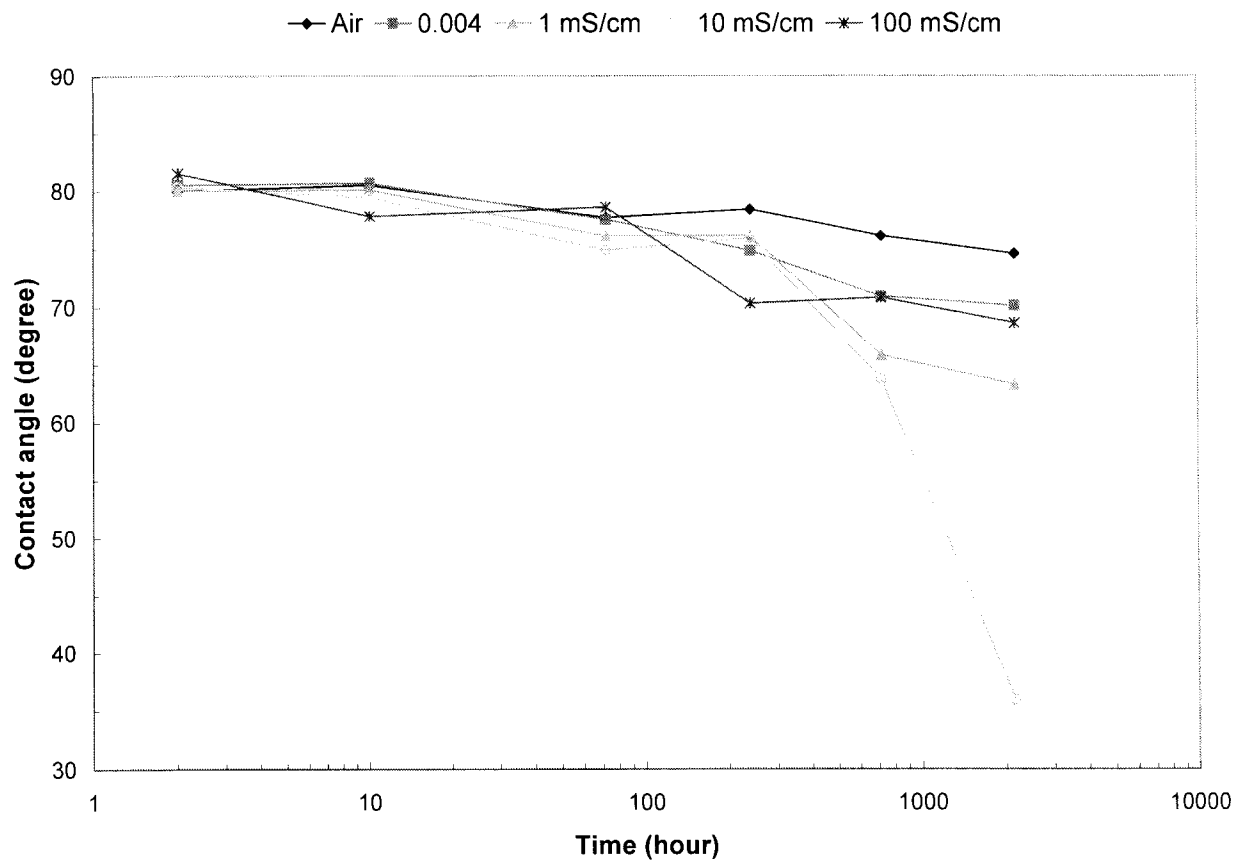


Fig. 4.3: Time variation of the contact angle of Delrin after immersion in different saline solutions at 60 ± 2 °C. Initial value of the contact angle before immersion was 82° .

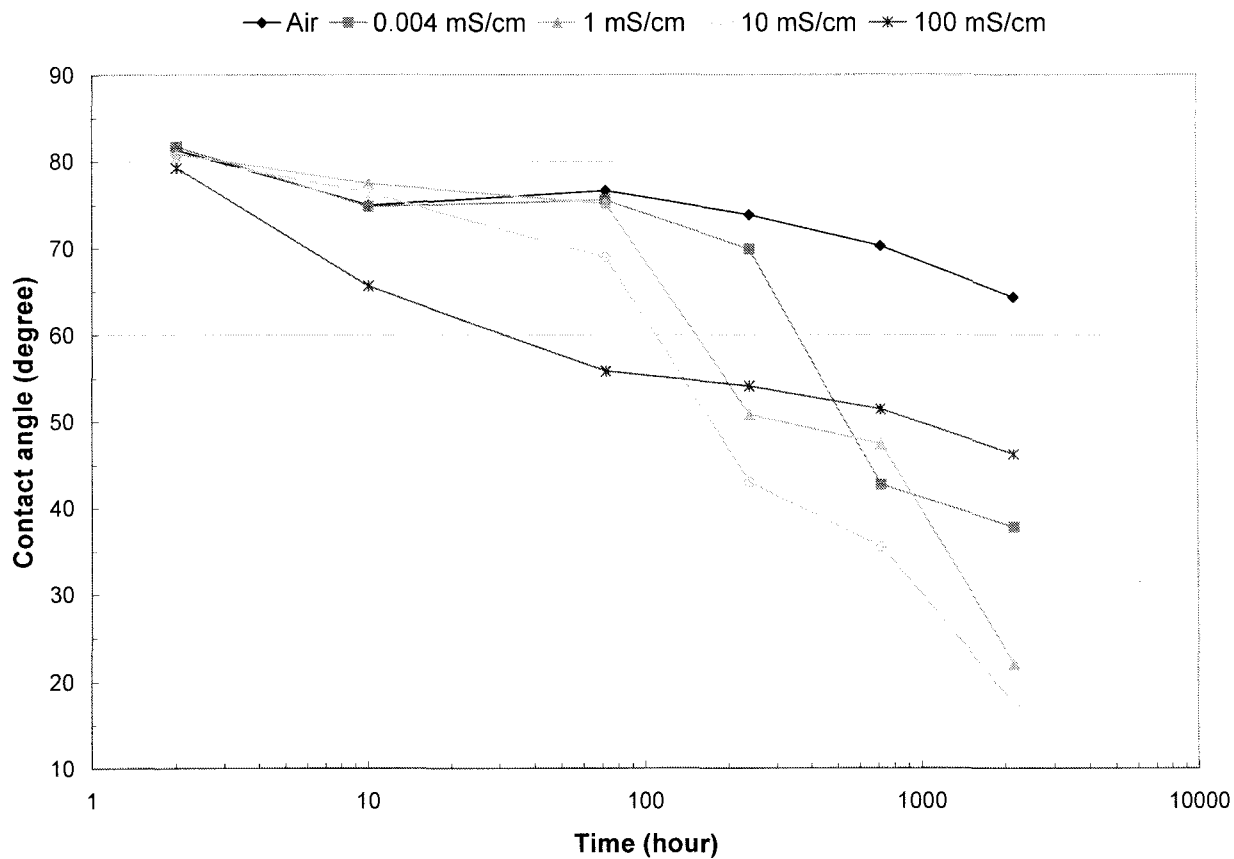


Fig. 4.4: Time variation of the contact angle of Delrin after immersion in different saline solutions at 98 ± 2 °C. Initial value of the contact angle before immersion was 82° .

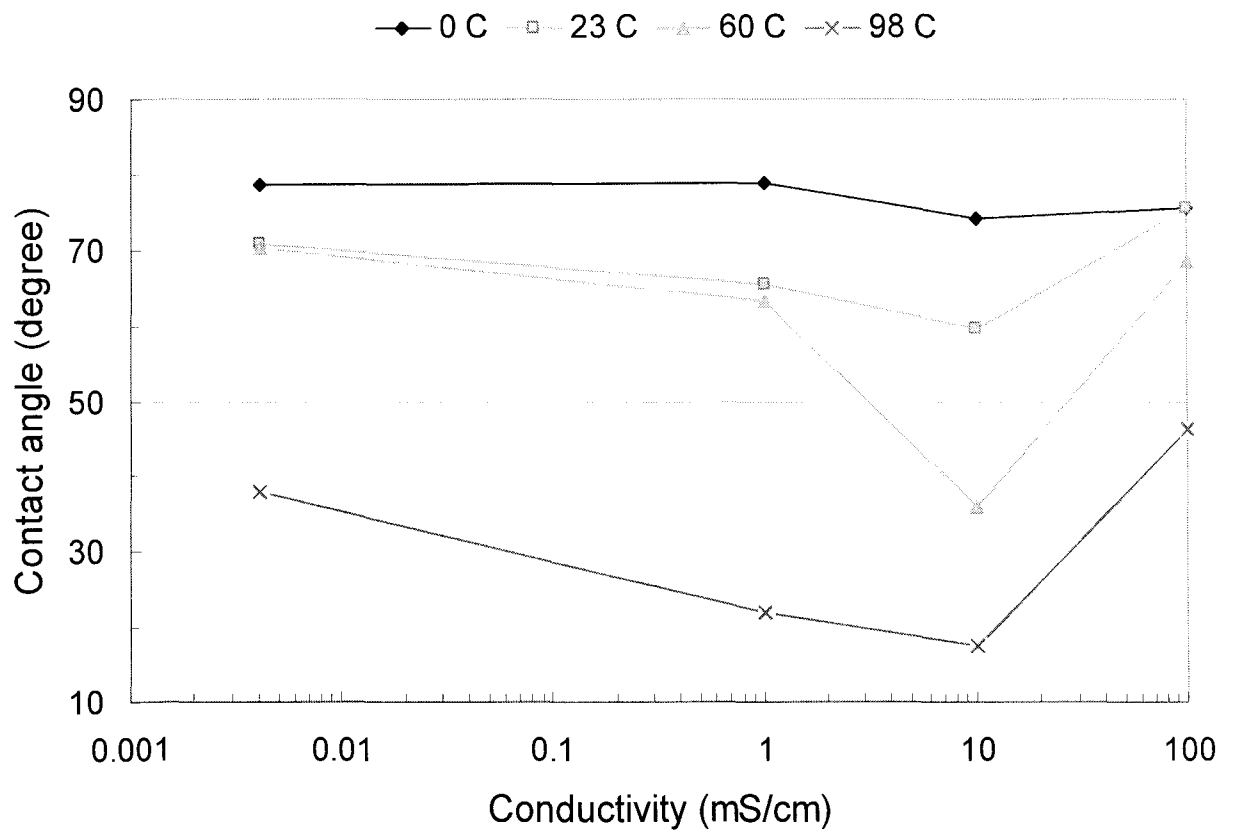


Fig. 4.5: Variation of the contact angle of Delrin as a function of conductivity of the saline solutions after immersion of specimens for 2160 h at different temperatures. Initial value of the contact angle before immersion was 82°.

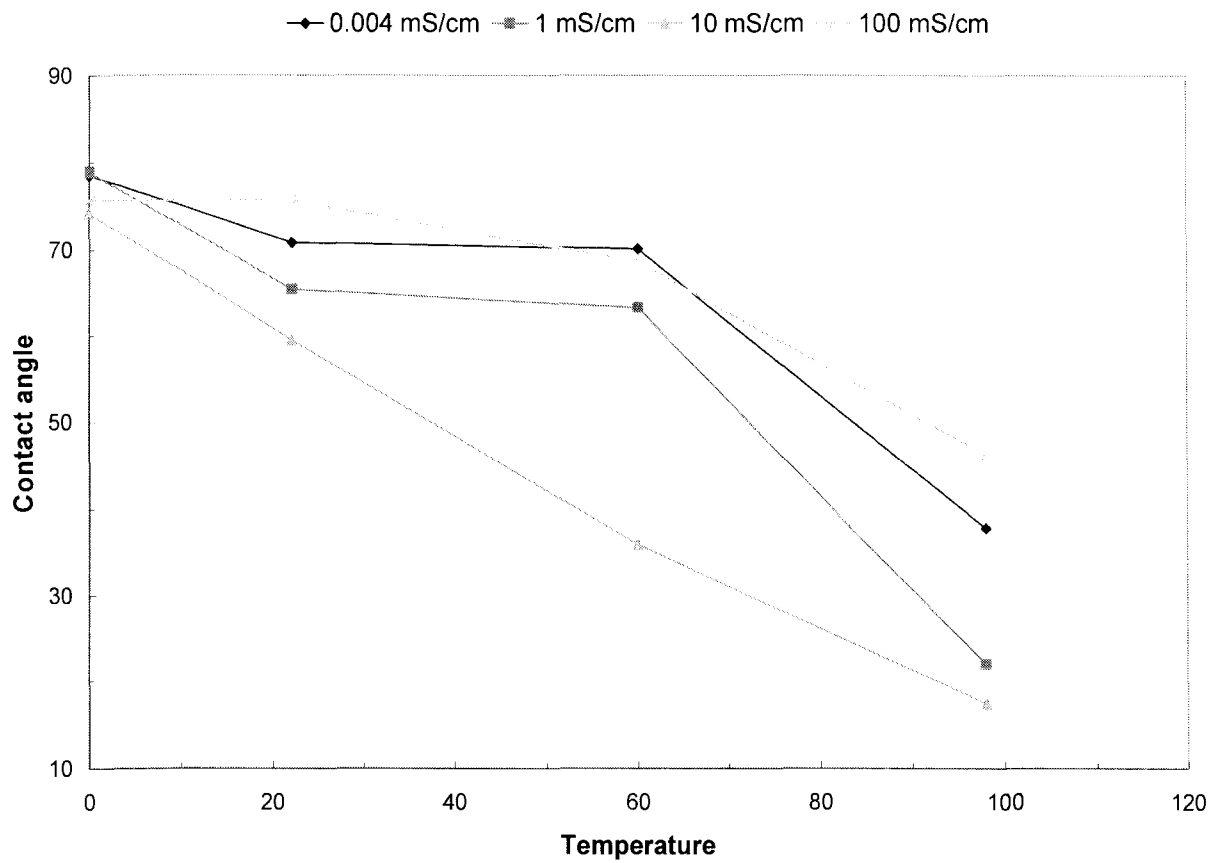


Fig. 4.6: Dependence of the contact angle of Delrin on the temperature of the saline solution. Time of immersion was 2160 h.

4.4 Percentage Increase in the weight of Delrin and Acetron

Figs. 4.7 and 4.8 show the percentage increase in the weight of the Delrin and Acetron specimens and the time of immersion for up to 4600 h for Delrin and 2180 hours for Acetron. Figs. 4.7 and 4.8 show that the weight of Delrin and Acetron at a fixed conductivity of saline solution becomes heavier with increasing temperature. The weight increase percentage of Delrin at 0, 23 and 60 °C continuously increased and saturated at 0.2, 0.5 and 0.8%, respectively. For Acetron at the above temperatures the weight increase percentage reaches to 0.45, 0.66 and 0.87%, respectively. Water uptake of Delrin and Acetron both had a sharp increase at 98 °C and the percentage increase saturated above 1.6%, but as immersion continues the weight starts to decrease. The increase percentage of Delrin dropped to 1.2% and for Acetron the percentage dropped to 0.76%. This behavior of polyoxymethylene opens up the possibility of a chemical reaction between the polymer and the saline solution which can be investigated by further research.

Fig. 4.9.a and 4.9.b show a Delrin and an Acetron sample immersed in 10 mS/cm for a long period of time and dried in the chamber at 98 °C and higher several times. The Delrin sample was cut from a 10 year old rod for a side experiment. The bulk of the Delrin sample deteriorated and only a shell remained.

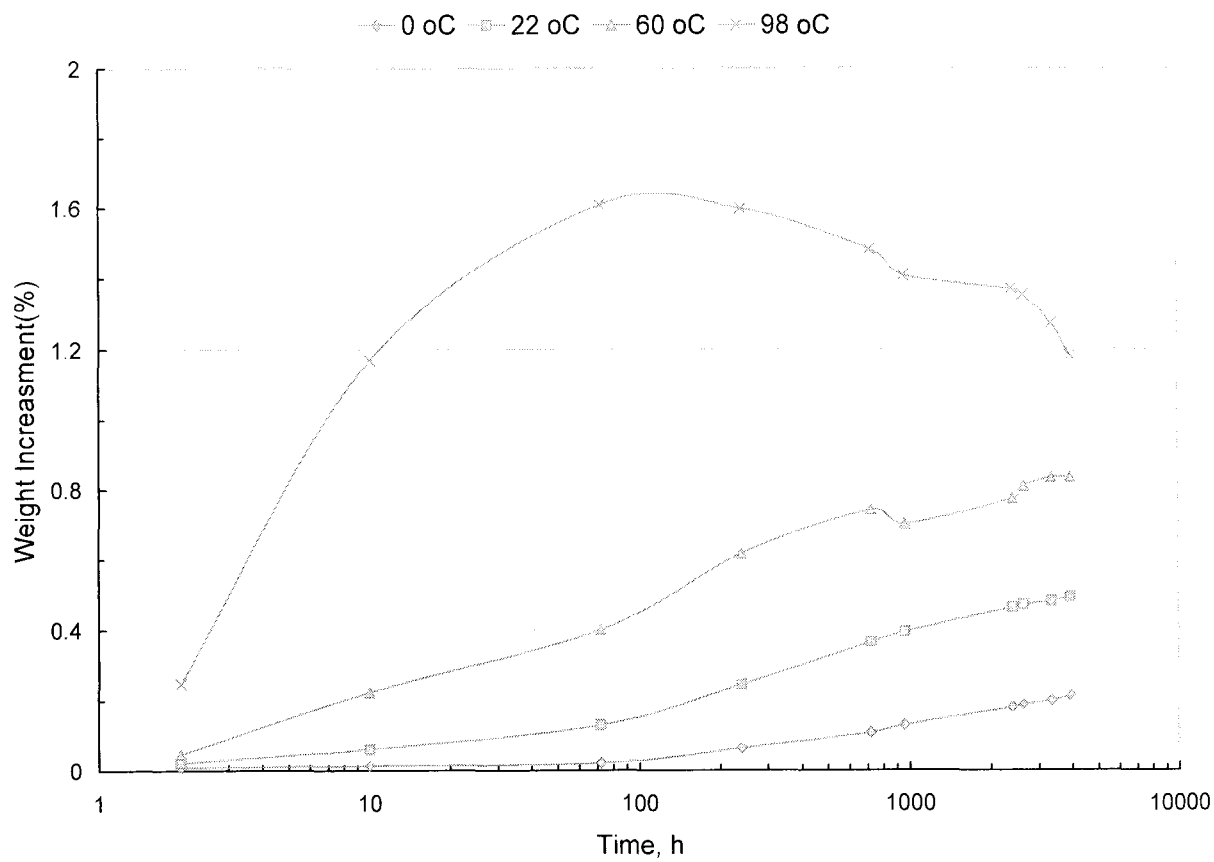


Fig. 4.7: Weight increase percentage of Delrin vs. time of immersion at 0, 23, 60 and 98 °C in 10 mS/cm saline solution.

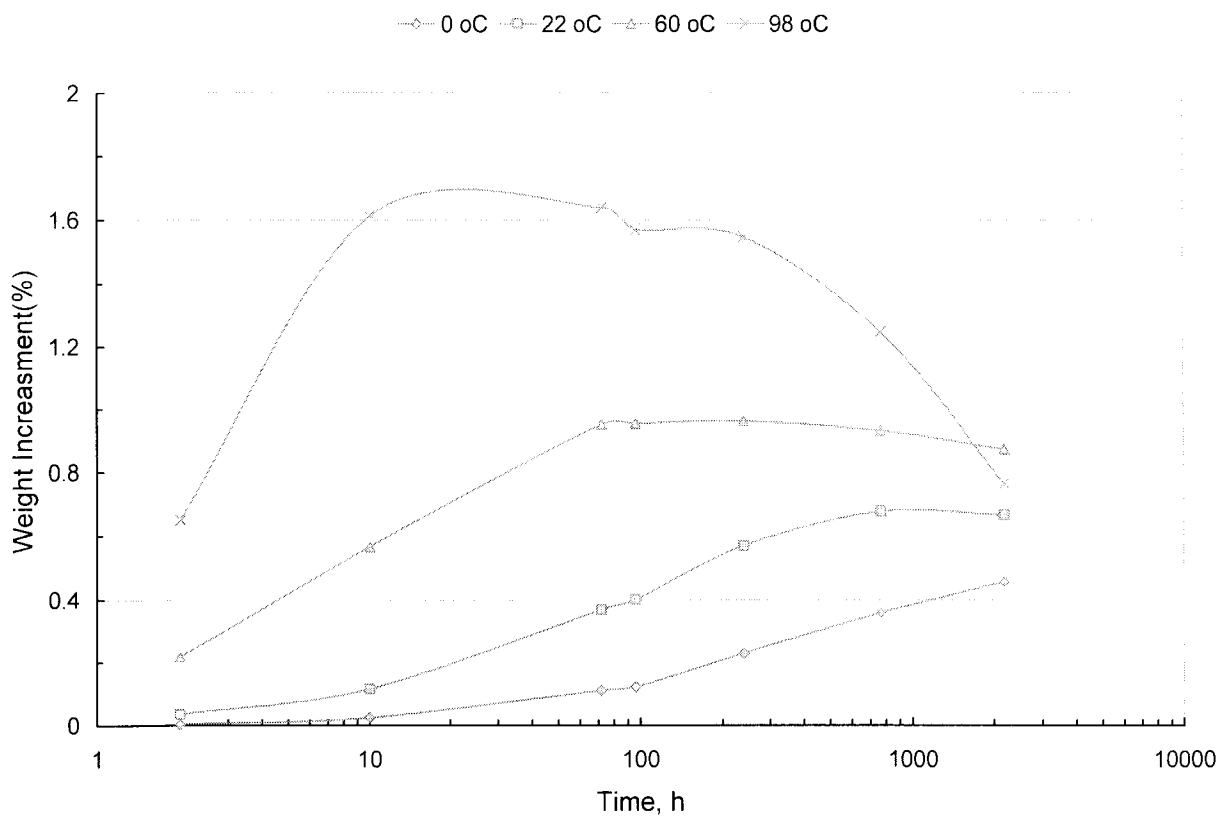


Fig. 4.8: Weight increase percentage of Acetron vs. time of immersion at 0, 23, 60 and 98 °C in 10 mS/cm saline solution.



Fig. 4.9a: Deterioration of Delrin after immersion in 10 mS/cm and drying at 98 °C for an extended period. The sample was taken from a 10 year old material and also it went through several cycles of immersion and drying as a side experiment.



Fig. 4.9b: The sample of Delrin in Fig. 4.9a and on the left, a sample of Acetron were in the same condition. Acetron is more resistant against chemical reaction.

4.5 Effect of aging on the color of Delrin

Most Polymers do not absorb light in the visible range (380-760 nm) and are therefore naturally colorless. Pigments are incorporated to give them color. The only exceptions are some thermosets, elastomers, polyurethanes, epoxies and resins. Loss of transparency of the polymer materials arises from light scattering processes within the material which distort and attenuate the transmitted light. Some polymers consist of alternating single and double covalent bonds or aromatic rings that act as chromophores and absorb light at the frequencies corresponding to the excitation energies of the bonding electron. Such substances appear brownish when they are seen with the help of transmitted or reflected light [19, 40].

Virgin Delrin is white. Fig. 4.10 shows a set of Delrin specimens after immersion in 0.005, 1, 10 and 100 mS/cm saline solutions at 0, 23, 60 and 98 °C for 4600 h. The color of Delrin did not change at low temperatures but at 98 °C the color turned brownish and with the increase of salinity up to certain limit of 10 mS/cm the discoloration is more significant. Fig. 4.11 shows a set of Acetron specimens under the same stress conditions as the Delrin samples, except that the time of immersion was only 768 h. The change in color of Acetron was the same pattern as of Delrin.

It is important to mention here that this change in color may or may not be necessarily due to a chemical change in the polymer material, because it could be due to weathering and environmental effects [41], or the presence of alternate single or double covalent bonds of carbon as mentioned above [40]. The chemical change in the polymer (such as

oxidation) must be confirmed independently by other analytical techniques such as infrared spectroscopy (IR).

Delrin after 4600 hrs immersion in different salinity and temperatures

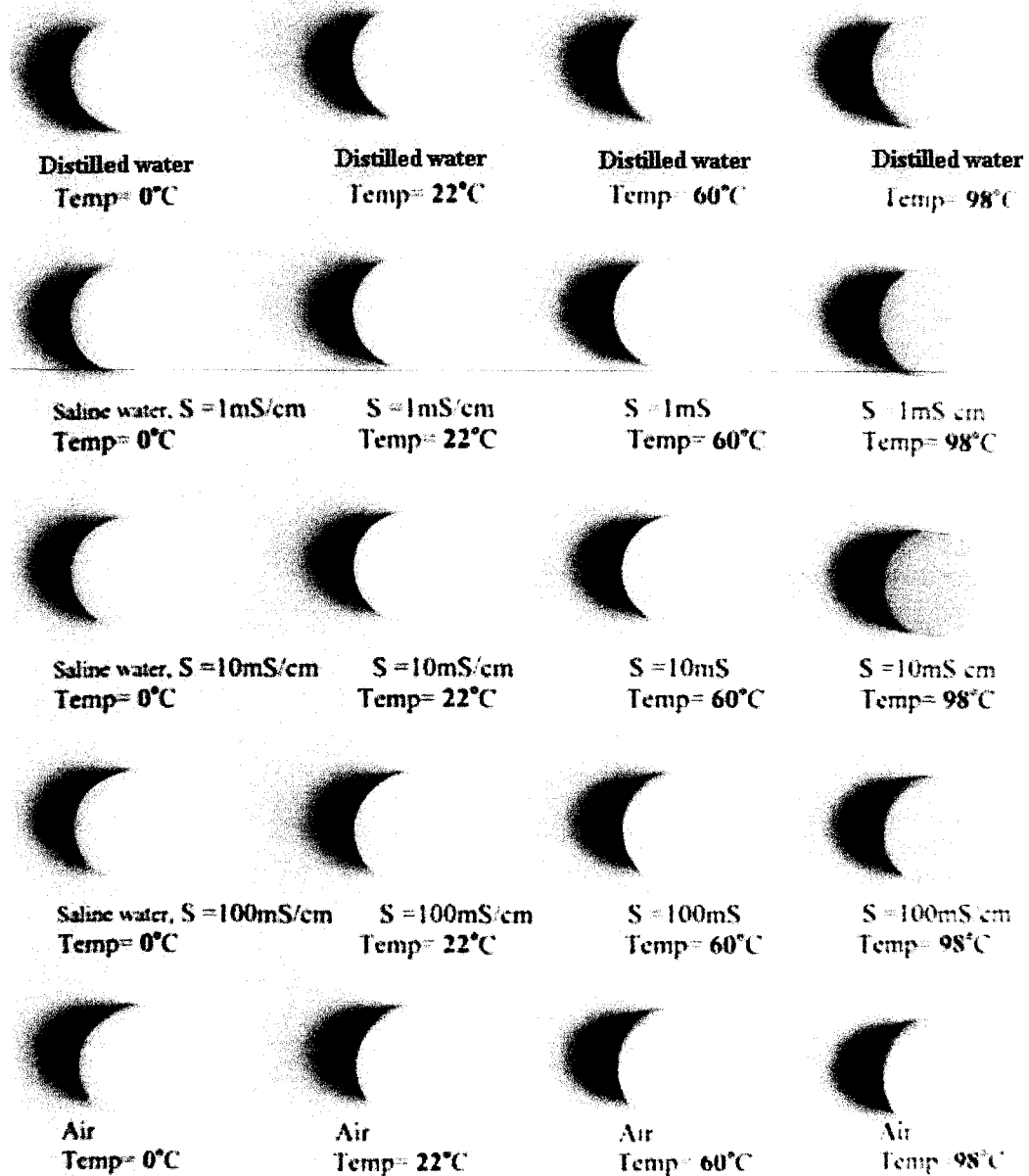


Fig. 4.10: Delrin after 4600 h immersion in different salinity solutions at different temperatures. In 10 mS/cm saline solution at 98 °C, the change in the color was the most significant.

Acetron after 32 days immersion in different salinity and temperatures

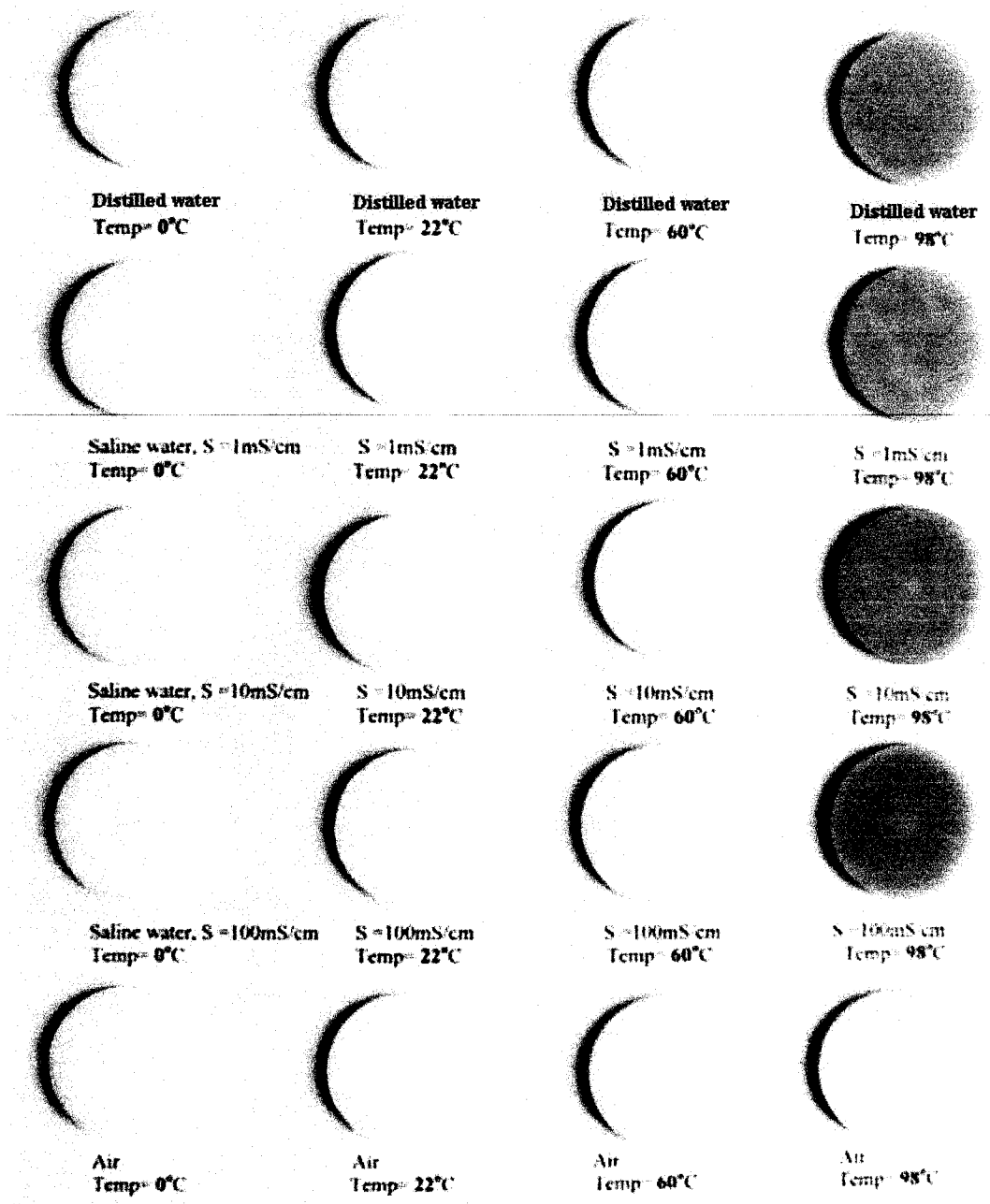


Fig. 4.11: Acetron after 768 h immersion in different salinity solutions at different temperatures. The changes of color at 98 °C in 0.005, 1, 10 and 100 mS/cm saline solutions were almost consistent.

4.6 Effect of RF Discharge on the Contact Angle of Delrin

Dry band electrical stress on the surface of a polymer insulator causes tracking and erosion of the surface which in turn affects the surface hydrophobicity. The complete loss of hydrophobicity of silicon rubber (SR) subjected to RF discharge has been reported by Gorur. In his experiment, RF discharges were subjected to SR by a Tesla coil for a few minutes [18]. Partial loss of hydrophobicity on HDPE and PTFE after subjection to RF discharge have also been reported [19,20].

Fig. 4.7 shows the recovery of the contact angle in air after subjecting the Delrin specimens to RF discharge for durations of 10, 15 and 20 minutes. The contact angle decreased from 82° to 74°, 72° and 69° respectively. The reduction in the contact angle was larger with longer durations of the RF discharge. The recovery time of Delrin was much shorter than the reported recovery time of EPDM and PTFE subjected to same durations of RF discharge [19, 20]. The contact angle θ recovered to its initial value after 120 h.

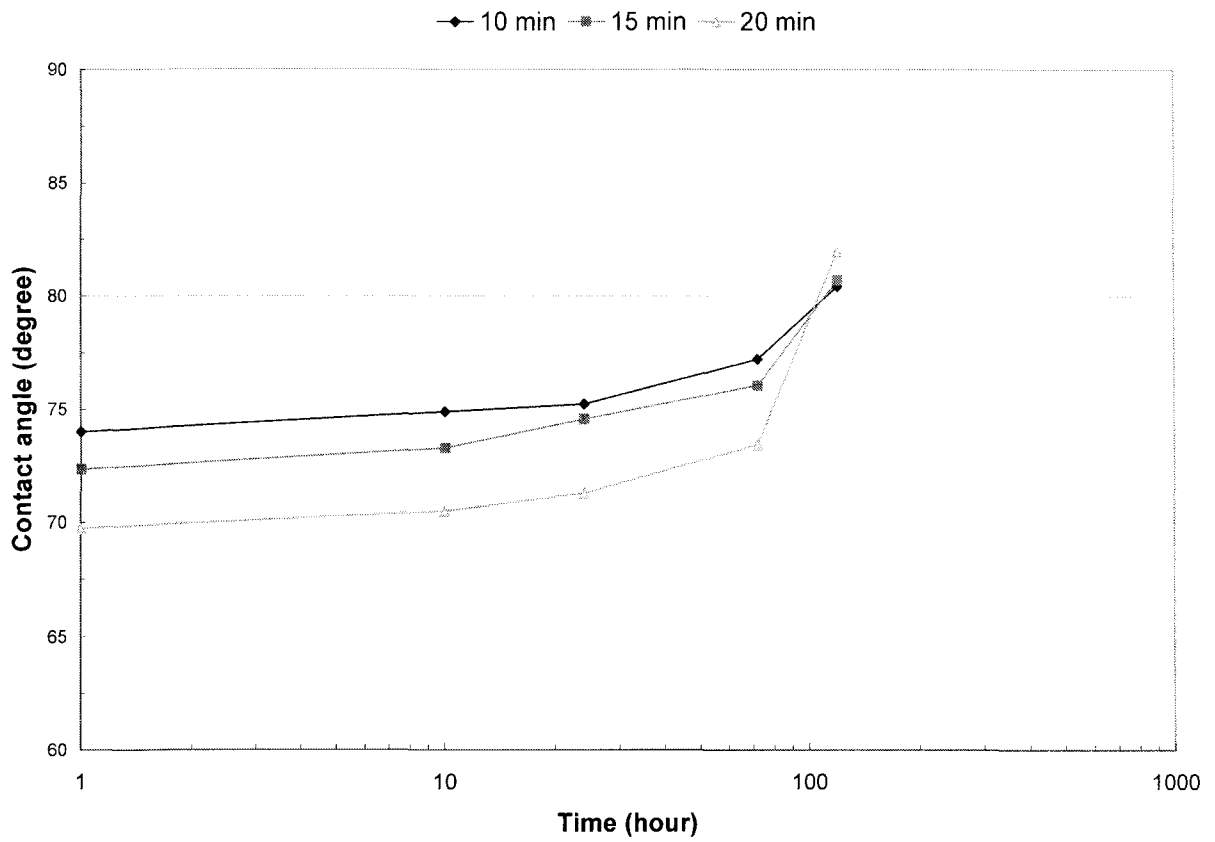


Fig. 4.12: Recovery of the contact angle of Delrin after the application of RF discharges for durations of 10, 15 and 20 minutes.

4.7 Scanning Electron Microscopy (SEM)

Scanning Electron Microscopy (SEM) is a powerful tool to inspect the surface structure of the samples visually on a microscopic scale. SEM was carried out in order to have an independent confirmation of the results of surface roughness measurements, taken by the surface detector, Surftest 212, and to investigate into other surface changes of the Delrin samples. Delrin samples aged in various saline solutions at different temperatures were removed from stress conditions, cooled down and then washed in 0.005 mS/cm distilled water with the help of an ultrasonic vibrator for approximately 1-2 minutes to remove the salt deposits and any other debris on the surface of the specimens.

Fig. 4.13 shows a SEM microphotograph of a virgin Delrin specimen. The magnification is 500. Fig. 4.13 shows that the Delrin surface is clear and free of debris.

Figs. 4.14 to 4.17 show the SEM of Delrin aged in 0.005, 1, 10 and 100 mS/cm saline solution at 98 °C. As can be observed, Delrin did not acquire debris while aging in distilled water. Aging in 1, 10 and 100 mS/cm saline solutions caused Delrin to acquire some salt deposits. The sample aged in 10 mS/cm is covered with white salt deposits. The density of salt deposits on the 1 mS/cm sample was less than the 10 mS/cm sample. The sample aged in 100 mS/cm had less density of salt deposits but a larger local concentration.

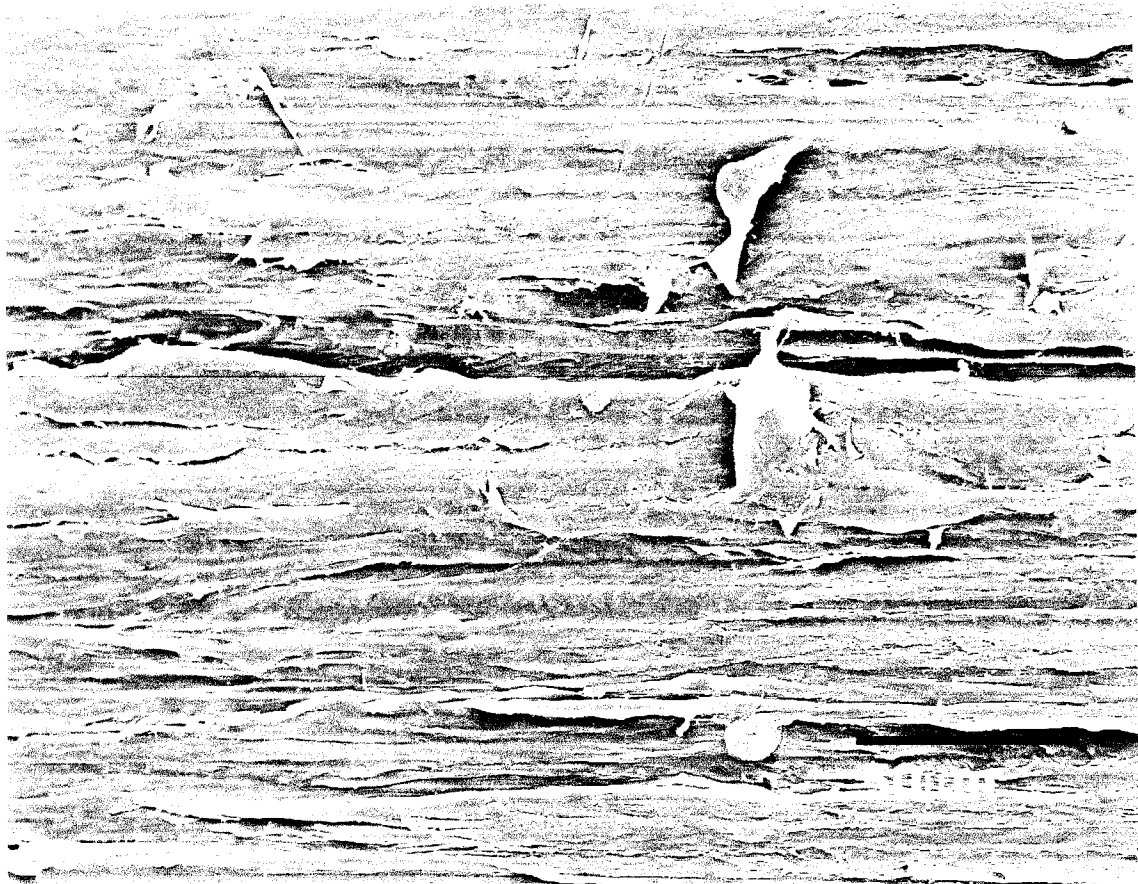


Fig. 4.13: Scanning Electron Microscopy of a virgin specimen of Delrin.
Magnification, 500.

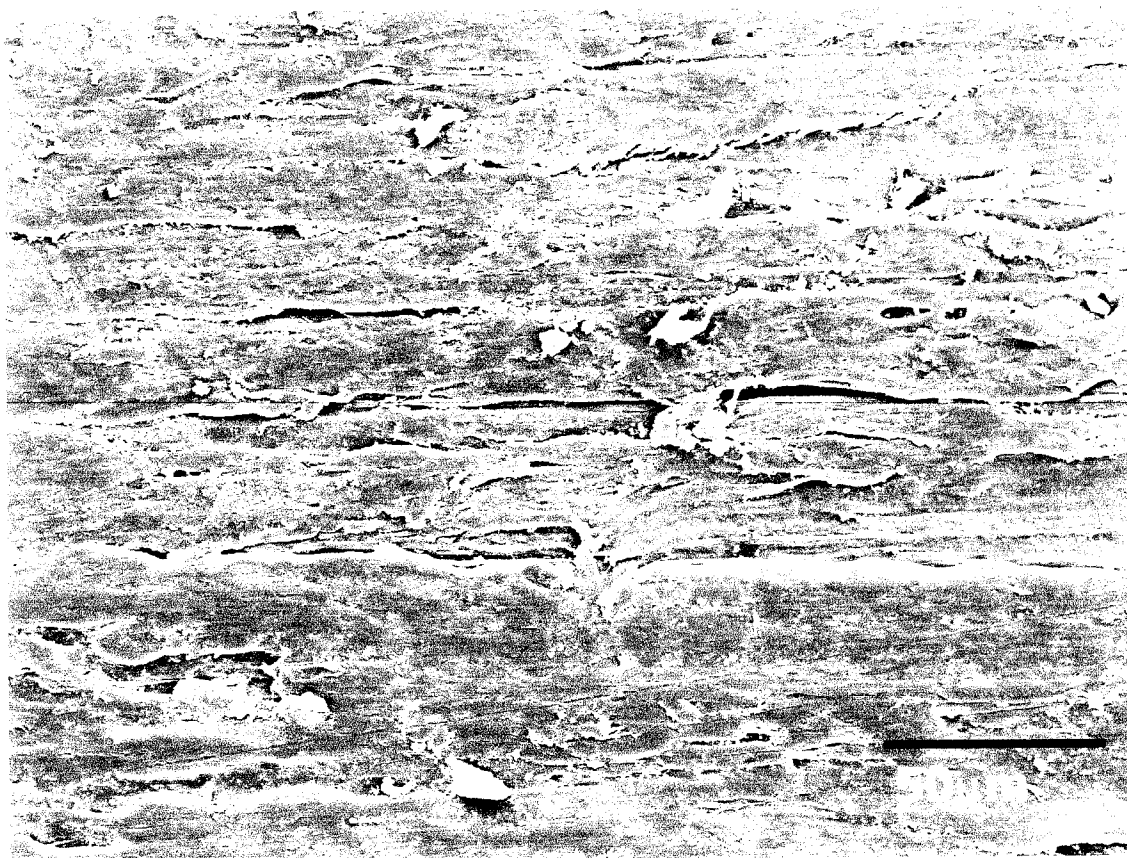


Fig. 4.14: Scanning Electron Microscopy of Delrin immersed in distilled water for 4600 h at 98 °C. Magnification, 500.

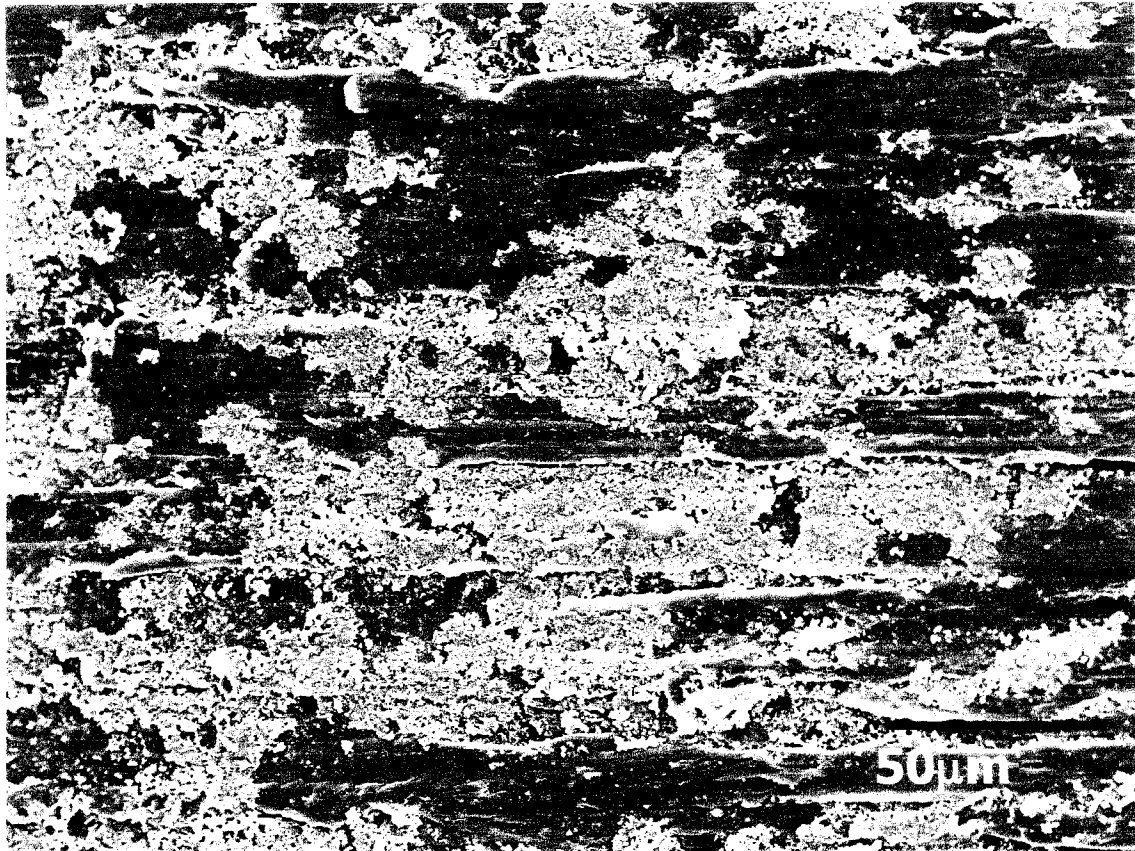


Fig. 4.15: Scanning Electron Microscopy of Delrin immersed in 1 mS/cm saline solution for 4600 h at 98 °C. Magnification, 500.



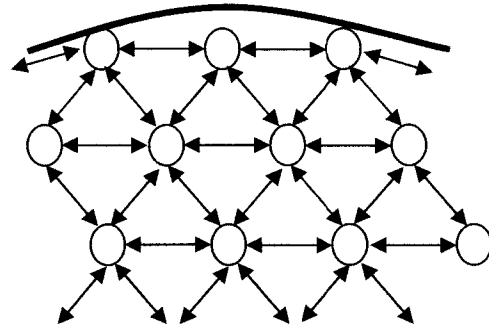
Fig. 4.16: Scanning Electron Microscopy of Delrin immersed in 10 mS/cm saline solution for 4200 h at 98 °C. Magnification, 500.



Fig. 4.17: Scanning Electron Microscopy of Delrin immersed in 100 mS/cm saline solution for 4200 h at 98 °C. Magnification, 500.

4.8 Surface Tension Measurements

Surface Tension, γ , is created when molecules inside the liquid, which are under equal attraction forces in all directions, interact with the molecules at the surface of the liquid, which are only affected by the attraction forces toward the inside. This causes liquid to form a drop when it is placed on a solid surface. The other intermolecular attraction forces are the surface tension of solid and surface tension of solid/liquid.

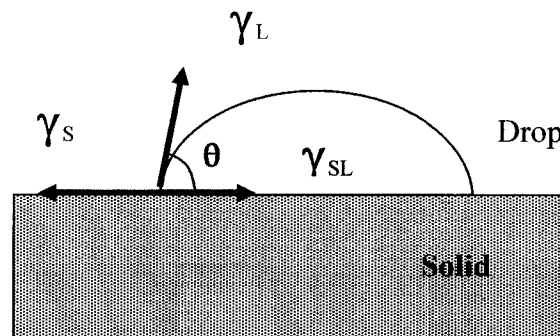


Section 3.1 explains the definition and role of the surface free energy per unit area (surface tension) on the wettability of a solid surface.

Young's equation describes the relationship between the contact angle and the surface free energies.

Young's Equation:

$$\gamma_s = \gamma_{SL} + \gamma_L \cos\theta$$



Where γ_s , is surface Tension of the solid, J/m^2

γ_L , Surface tension of liquid, J/m²

γ_{SL} , Surface tension of Solid/liquid interface, J/m²

And θ is the contact angle of the solid surface.

The shape of the drop is controlled by the three interfacial tensions as shown in the above diagram. According to the equation (4.1), for constant values of γ_L and γ_{SL} the higher the value of the γ_S , the lower the value of the contact angle θ . The material becomes hydrophilic when θ is low.

Surface tension or surface energy is composed of a dispersion (non-polar) component, due to the London dispersive force, and a polar non-dispersive component, due to the polar forces.

Therefore the surface tension of solid, γ_S , can be presented in the following way:

$$\gamma_S = \gamma_{SD} + \gamma_{SH} \quad (4.2)$$

Where the suffix SD denotes the **dispersion** component of surface tension of the solid and SH denotes the **polar** component of surface tension of the solid.

γ_{SD} and γ_{SH} are the surface free energies per unit area of the solid due to the dispersion forces and the hydrogen bonding forces. For Delrin γ_{SD} and γ_{SH} contribute to the hydrophobicity and hydrophilicity of the solid surface, respectively.

For a liquid, equation (4.1) can be written as follows:

$$\gamma_L = \gamma_{LD} + \gamma_{LH} \quad (4.3)$$

Where the suffix LD denotes the dispersion component of surface tension of the liquid and the suffix LH denotes the polar component of surface tension of the liquid.

The surface tension of a solid polymer cannot be measured directly. Many indirect methods have been developed to determine the surface tension of solid polymers. These include the polymer melt method, the liquid homolog method, the equation of state method and the mean harmonic method, all of which give consistent and reliable results [19, 20]. For this study the mean harmonic method has been used.

4.8.1 Mean Harmonic method

This method requires measurement of the contact angle of two liquids of known surface tension and their hydrogen bonding and dispersion force components, γ_{LH} and γ_{LD} respectively. According to [2, 42]:

$$\gamma_{SD} = \gamma_S + \gamma_L - \left(\frac{4\gamma_{SD} \cdot \gamma_{LD}}{\gamma_{SD} + \gamma_{LD}} \right) - \left(\frac{4\gamma_{SH} \cdot \gamma_{LH}}{\gamma_{SH} + \gamma_{LH}} \right) \quad (4.4)$$

Substituting the value of γ_{SL} from equation (4.1) into equation (4.3):

$$\gamma_L \cdot (1 + \cos \theta) = \left(\frac{4\gamma_{SD} \cdot \gamma_{LD}}{\gamma_{SD} + \gamma_{LD}} \right) + \left(\frac{4\gamma_{SH} \cdot \gamma_{LH}}{\gamma_{SH} + \gamma_{LH}} \right) \quad (4.5)$$

In equation (4.5) γ_{SD} and γ_S are unknowns, and if we write that for water and methylene iodide and solve them simultaneously for γ_{SD} and γ_{SH} , then γ_S according to equation (4.2) which is sum of γ_{SD} and γ_{SH} can be calculated.

To solve the two equations, a computer program using MATLAB has been written (Appendix A). By using this program, surface free energies of any solid material could be calculated.

The Dupre equation relates the energy of adhesion on the surface W_{SL} (J/m^2) to the surface free energy γ_S , the surface free energy of water γ_L , and the interfacial energy of water and solid γ_{SL} [42, 43]:

$$\gamma_{SL} = \gamma_S + \gamma_L - W_{SL} \quad (4.6)$$

From equations (4.1) and (4.5),

$$W_{SL} = \gamma_L \cdot (1 + \cos\theta) \quad (4.7)$$

4.8.2 Surface Tension of Delrin

The loss of hydrophobicity of Delrin during immersion in a saline solution is due to the interaction between the water and the surface which results in a higher surface tension on Delrin. During the aging in the saline solution, γ_{SH} increases with increasing time of immersion. This causes an increase in the surface tension γ_S , because of absorption of the

saline water and its adhesion on the surface of Delrin. This results in a decrease in the contact angle. γ_{SD} and γ_{SH} can be determined by using the mean harmonic method as described previously. This is accomplished by measuring the static contact angle θ using two different liquids, water and methyl iodine with known surface energy components as follows [42]:

$$\begin{aligned} \gamma_{L(\text{water})} &= 72.8 \times 10^{-3} \text{ J/m}^2 & \gamma_{L(\text{methylene iodide})} &= 50.8 \times 10^{-3} \text{ J/m}^2 \\ \gamma_{LD(\text{water})} &= 22.1 \times 10^{-3} \text{ J/m}^2 & \gamma_{LD(\text{methylene iodide})} &= 44.1 \times 10^{-3} \text{ J/m}^2 \\ \gamma_{LH(\text{water})} &= 50.7 \times 10^{-3} \text{ J/m}^2 & \gamma_{LH(\text{methylene iodide})} &= 6.7 \times 10^{-3} \text{ J/m}^2 \end{aligned}$$

Fig. 4.18 shows the surface energy variation of Delrin with time of immersion in 10 mS/cm saline solution at 0 °C. Since the contact angle of Delrin was steady during immersion, there are no significant variations in the surface energy and its components.

Fig. 4.19 shows the variation of surface energy and its components vs. the time of immersion in 10 mS/cm saline solution at room temperature, 23 °C. There is an increase in the polar component of surface energy with increasing time of immersion. This trend is more significant in the higher temperatures. Figs. 4.20 and 4.21 show the variation of surface energy and its components with the time of immersion in 10 mS/cm saline solution at 60 and 98 °C, respectively. The surface free energy of Delrin will increase with the time of immersion, and this increase will be higher in high temperature environments.

Fig. 4.22 shows the variation of the energy adhesion of Delrin and water, W_{SL} , the surface energy, γ_s , the polar component of surface energy, γ_{SH} , the dispersion component of surface energy, γ_{SD} and the contact angle of methyl iodine θ_M , vs. the contact angle of water, θ_w during immersion in saline solution of 10 mS/cm at 98 °C. As the contact angle of water reduced, the energy of adhesion increased. This complies with the same observation of Tokoro on nylon and HTV silicone rubber [42, 43].

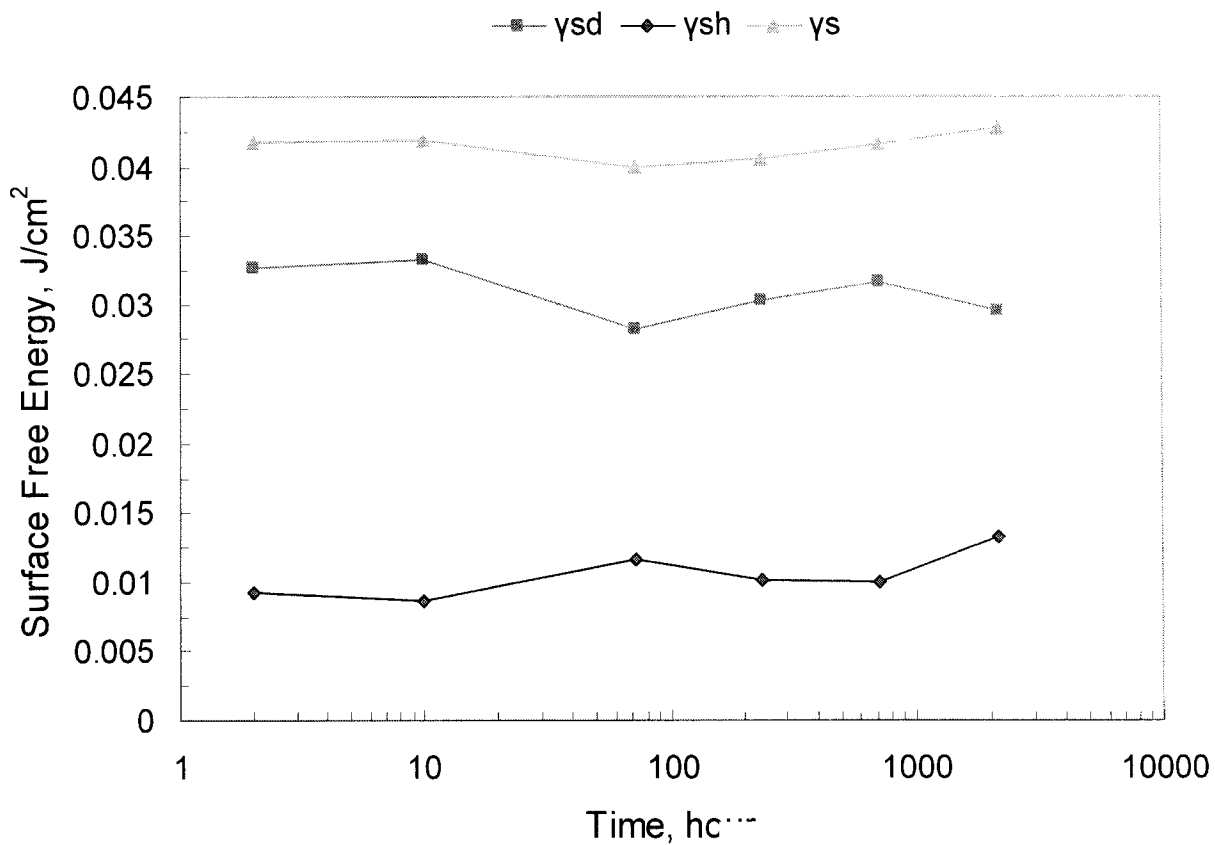


Fig. 4.18: Surface energy variation of Delrin with time of immersion in 10 mS/cm saline solution at 0 °C. γ_{SD} : Dispersion component; γ_{SH} : Polar component; γ_S : Surface energy of solid.

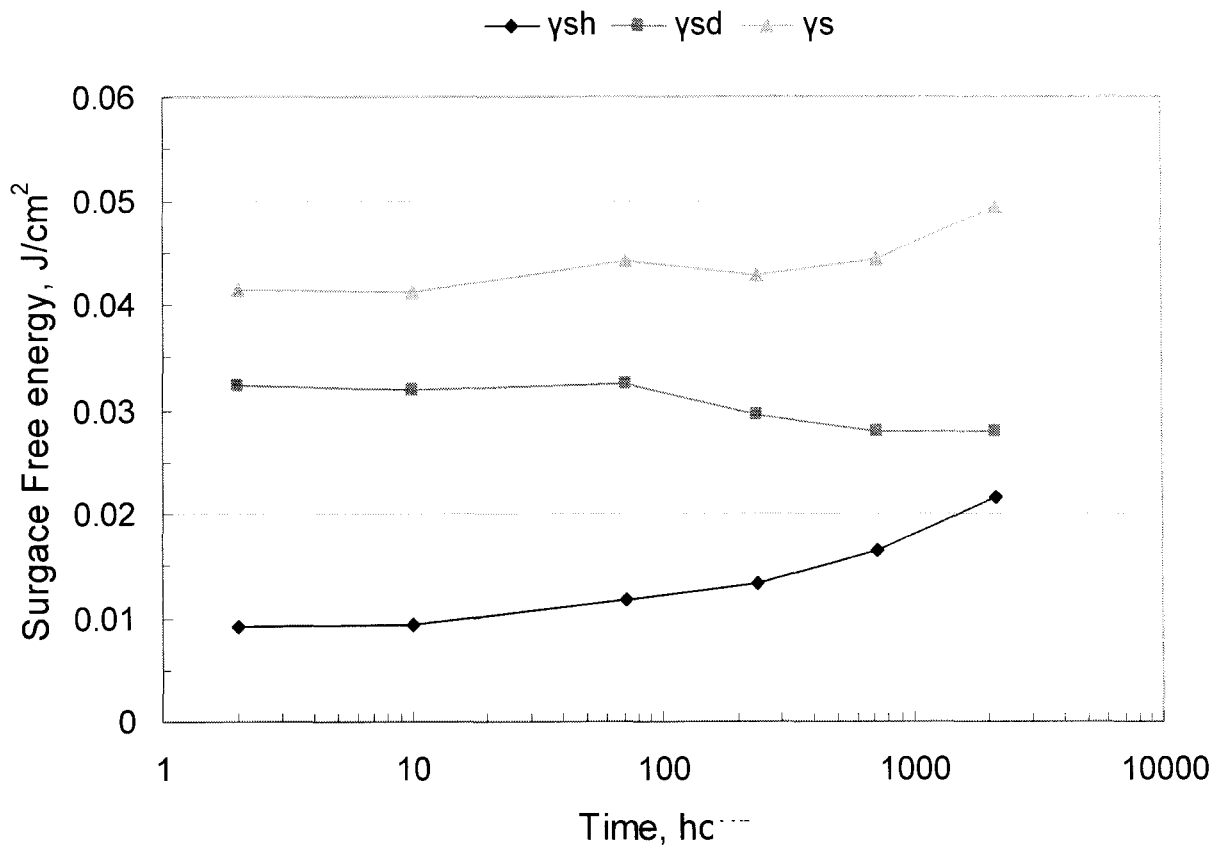


Fig. 4.19: Surface energy variation of Delrin with time of immersion in 10 mS/cm saline solution at 23 °C. There is an increase in polar component.

γ_{SD} : Dispersion component; γ_{SH} : Polar component; γ_S : Surface energy of solid.

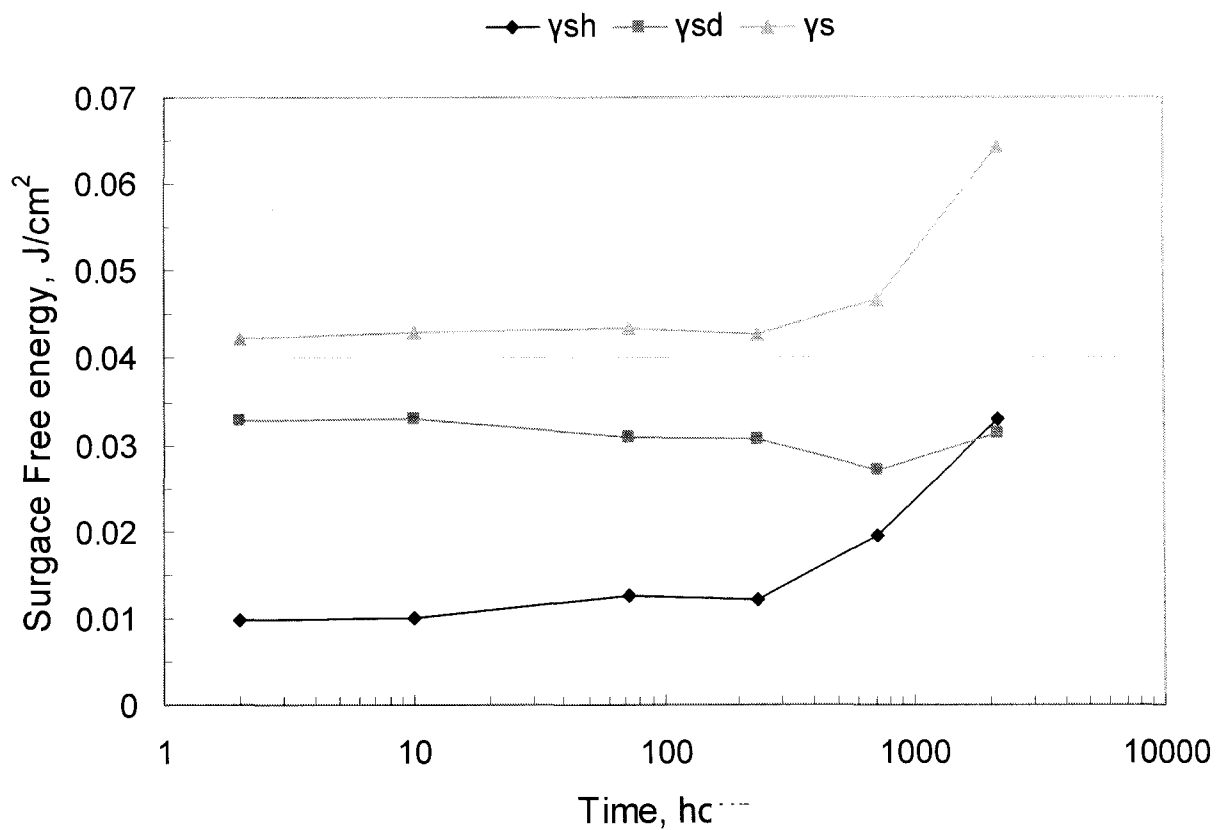


Fig. 4.20: Surface energy variation of Delrin with time of immersion in 10 mS/cm saline solution at 60 °C. γ_{SD} : Dispersion component; γ_{SH} : Polar component; γ_S : Surface energy of solid.

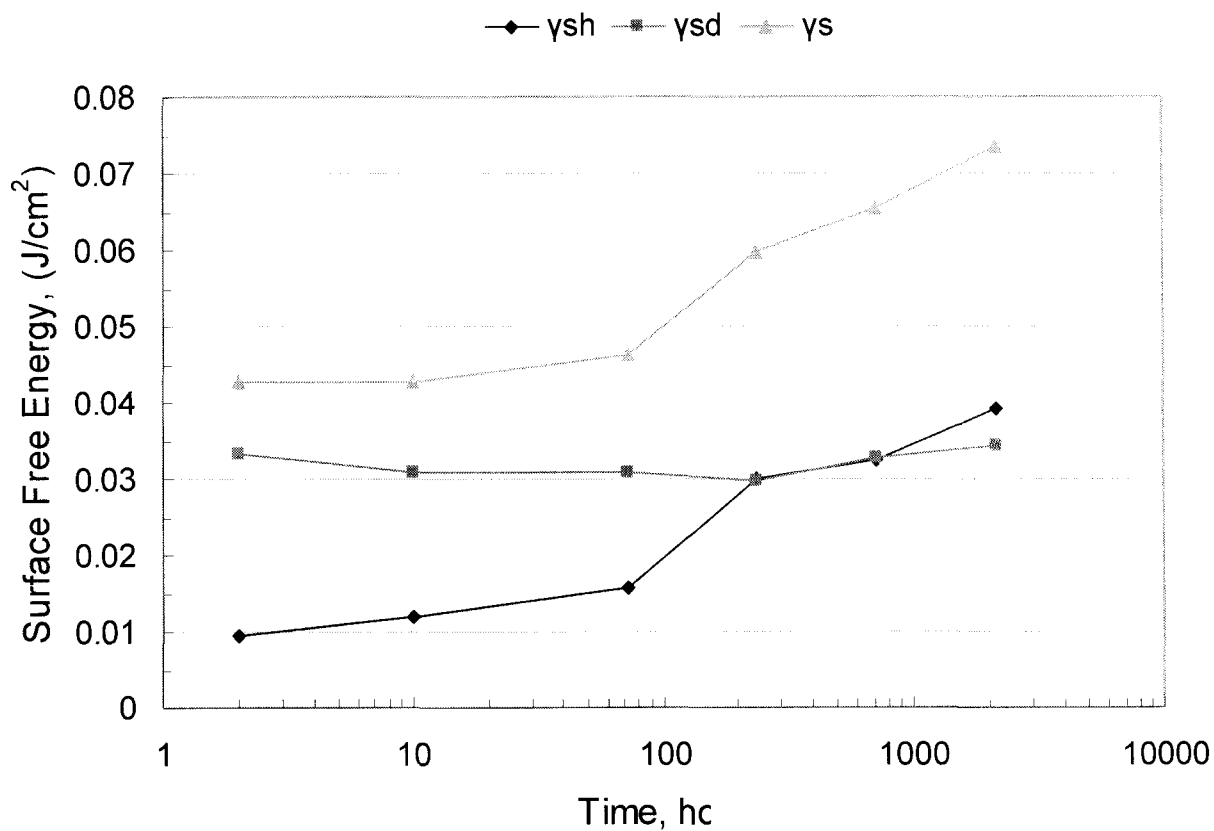


Fig. 4.21: Surface energy variation of Delrin with the time of immersion in 10 mS/cm saline solution at 98 °C. γ_{SD} : Dispersion component; γ_{SH} : Polar component; γ_S : Surface energy of solid.

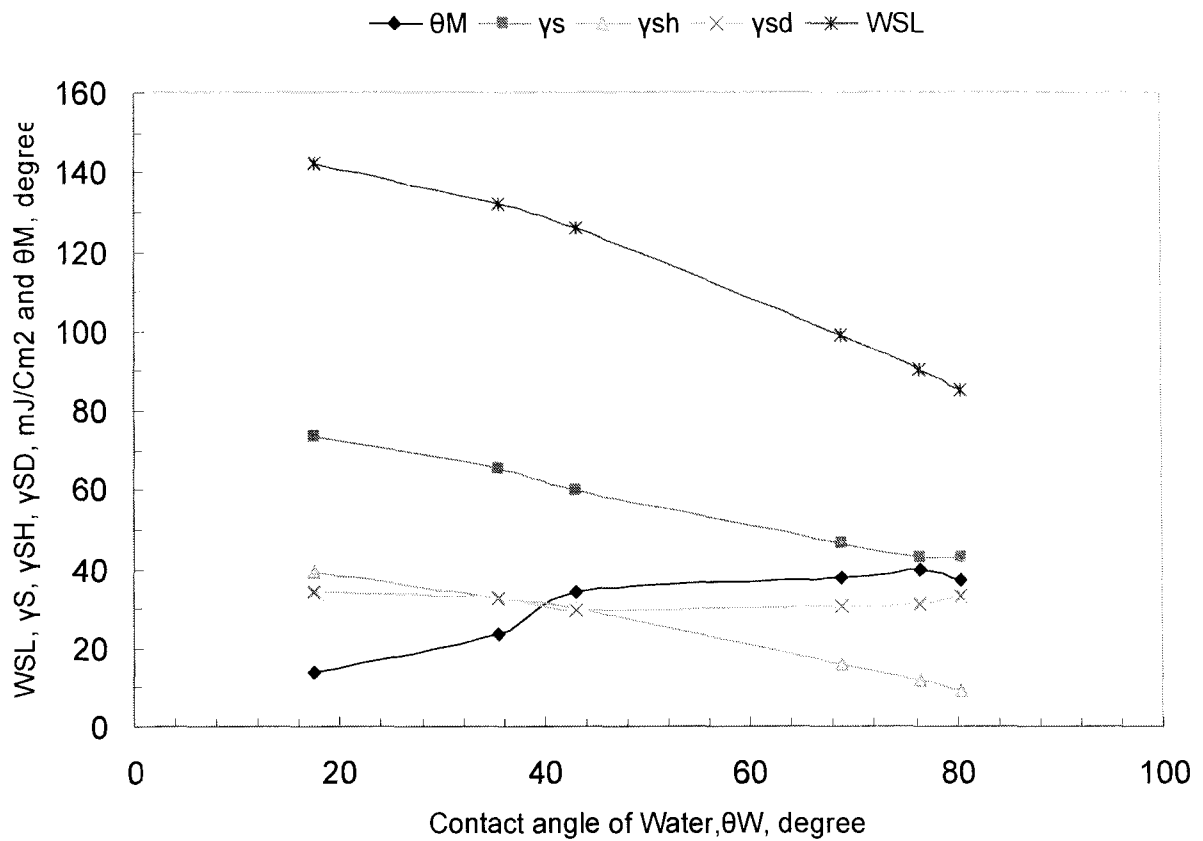


Fig. 4.22: Calculated surface energy components γ_S , γ_{SH} , γ_{SD} , (mJ/Cm²), adhesion energy W_{SL} (mJ/Cm²) and measured the contact angle of methyl iodine θ_M , (degree) vs. the contact angle of water θ_W (degree). Delrin immersed in 10 mS/cm saline solution at 98 °C as described in Fig.4.2.

4.9 Diffusion of water in Delrin and Acetron

4.9.1 Introduction

Polyoxymethylene (POM) absorbs water as it has been observed in section 4.4 and was reported by the manufacturer's design guide [5]. The uptake of water in Delrin and Acetron reaches a saturation level with increasing time of immersion. The amount of water absorbed by Delrin and Acetron is dependent on the temperature of the saline solution. The higher the temperature, the quicker and the more is the absorption. The time it takes to saturate the POM is also impacted by temperature, with higher temperatures resulting in shorter saturation time. These characteristics can also be observed in the study of the absorption properties of polyethylene [19, 44].

Water absorption in Polymeric Insulation is very important when it is seen from the point of view of the possible change in its surface properties. Water trees contain water and they grow in the presence of water, therefore a better understanding of the process of diffusion of water in Delrin or Acetron is valuable. The quantitative measurement of the rate of the diffusion process can be obtained from the knowledge of the diffusion coefficient. In order to achieve that, the diffusion coefficient of water into Delrin was determined experimentally for different saline solutions at different temperatures. This helps us to better understand the decrease in the contact angle of water droplet on the surface of Delrin in different saline solutions at different temperatures.

4.9.2 Diffusion Coefficient

The nature of the diffusion is a process by which matter is transported from one part of a system to another as a result of random motion of molecules. The flow of matter is controlled mainly by the difference in the concentration of the diffusing substances. Diffusion of an isotropic substance is based on the hypothesis that the rate of transfer of diffusing substance through unit area of a section is proportional to the gradient of concentration measured normal to that section. Mathematically it can be described by Fick's law of diffusion as follows:

$$F = -D \cdot \frac{\partial C}{\partial x} \quad (4.8)$$

F is the rate of transfer per unit area of the section, C is the concentration of the diffusing material, x is the space co-ordinate measured normal to the section and D is called the diffusion coefficient.

Usually the diffusion coefficient may vary but in some cases like diffusion in dilute solutions, D may reasonably be considered constant. If F is measured in g/s per m², C in g/m³ and x in m, then D is measured in m²/s. The negative sign arises because diffusion occurs in the opposite direction to that of increasing concentration [45].

Crank [45] developed the relationship describing the rate of absorption of liquid into a membrane. Considering the diffusion is driven by a concentration gradient and if there is no chemical reaction between the liquid and the membrane which result in mass changes,

then the rate of absorption of the liquid into the membrane is initially linear with $t^{0.5}$, where t is the time of absorption. Crank described the process as follows:

$$\frac{\Delta M(t)}{\Delta M_{\infty}} = 2 \cdot \sqrt{\frac{D \cdot t}{l^2}} \left\{ \sqrt{\frac{1}{\pi}} + 2 \cdot \sum_{n=1}^{\infty} \left[(-1)^n \cdot \text{ierfc} \left(\frac{n \cdot l}{2\sqrt{D \cdot t}} \right) \right] \right\}$$

$$\Delta M(t) = M(t) - M(0)$$

$$\Delta M_{\infty} = M_{\infty} - M(0) \tag{4.9}$$

where $\Delta M(t)$ is the increase in the mass of the membrane (kg) due to the absorption of liquid at time t , $M(t)$ is the mass at time t , $M(0)$ is the initial mass at $t=0$.

ΔM_{∞} is the increase in the saturated mass (kg) at $t=\infty$.

M_{∞} is the saturated mass at $t=\infty$.

D is the diffusion coefficient (m^2/s), l the thickness of membrane (m).

ierfc is a mathematical function, defined as

$$\text{ierfc}(x) = \sqrt{\pi} \exp(x^2) - x \cdot \text{erfc}(x) \tag{4.10}$$

where erfc is the complementary error function. When $x \rightarrow 0$, $\text{ierfc}(x) \rightarrow \pi^{-0.5}$ and when $x \rightarrow \infty$, $\text{ierfc}(x) \rightarrow 0$.

Equation (4.9) is for one-dimensional diffusion, meaning in this case that the specimen is very thin and absorption from the sides of specimens is negligible compare to the flat part. Since the diffusion occurs from both ends of the disc for two-dimensional diffusion, l is replaced by the thickness of the sample disc which is $L=2l$. For early stages of absorption, the second term in equation (4.9) may be neglected and D is very small, leading to an error function approaching zero. Therefore the diffusion coefficient D may be determined from an equation (4.11) as follows:

$$\frac{\Delta M(t)}{\Delta M_{\infty}} = 4 \left(\frac{D}{\pi L^2} \right)^{0.5} t^{0.5} \tag{4.11}$$

Therefore D could be determined from the linear dependence of the graph of $\Delta M(t)/\Delta M_{\infty}$ vs. $t^{0.5}$.

Where $\Delta M(t)/\Delta M_{\infty} = 0.5$ the above relation can lead to calculation of diffusion coefficient D as follows:

$$D = 0.049 [L^2 / t] \quad (4.12)$$

4.9.3 Experimental Method

Specimens of Delrin with a diameter of 19 mm and thickness of 1.3 ± 0.4 mm were used which had a ratio of diameter to thickness as high as 14 and a corresponding ratio of the surface area of the both ends to the side of 7.3. This ensures that the diffusion from both ends of the membrane would be dominating over diffusion from the sides. The samples were initially washed in diluted solution of acetic acid (5%) and dried for 2-3 days to ensure that there was no concentration of water or contaminant in Delrin before immersion. Saline solutions of 0.005, 1, 10 and 100 mS/cm were prepared at 0, 23, 60 and 98 °C. Weight of samples measured initially and after immersion in saline solution intermittently. The increase in the weight of the specimens was measured regularly until saturation in the weights were reached and the coefficients of diffusion were calculated with the help of equation (4.12) when $\Delta M(t)/\Delta M_{\infty} = 0.5$.

Figs. 4.23 and 4.25 show the percentage increase of weight, $\Delta M(t)$, and time of immersion. From equation (4.12), M_{∞} was the weight of the specimen when it reached the maximum saturation level. Figs. 4.24 and 4.26 show the percentage variation of

$\Delta M(t)/\Delta M_{\infty}$ of Delrin as function of the square root of time $t^{0.5}$ for different conductivities of saline solution at 60 and 98 °C. The specimens at 98 °C reached to their saturation level much faster than at 60 °C. Table 4.1 and 4.2 show the calculated values of the diffusion coefficient and the time when $\Delta M(t)/\Delta M_{\infty} = 0.5$ for specimens of Delrin immersed in different saline solution at 60 and 98 °C. These two tables show that the diffusion coefficients are higher at higher temperatures. At the same temperature, 10 and 100 mS/cm solutions had higher diffusion coefficients than lower salinity solutions.

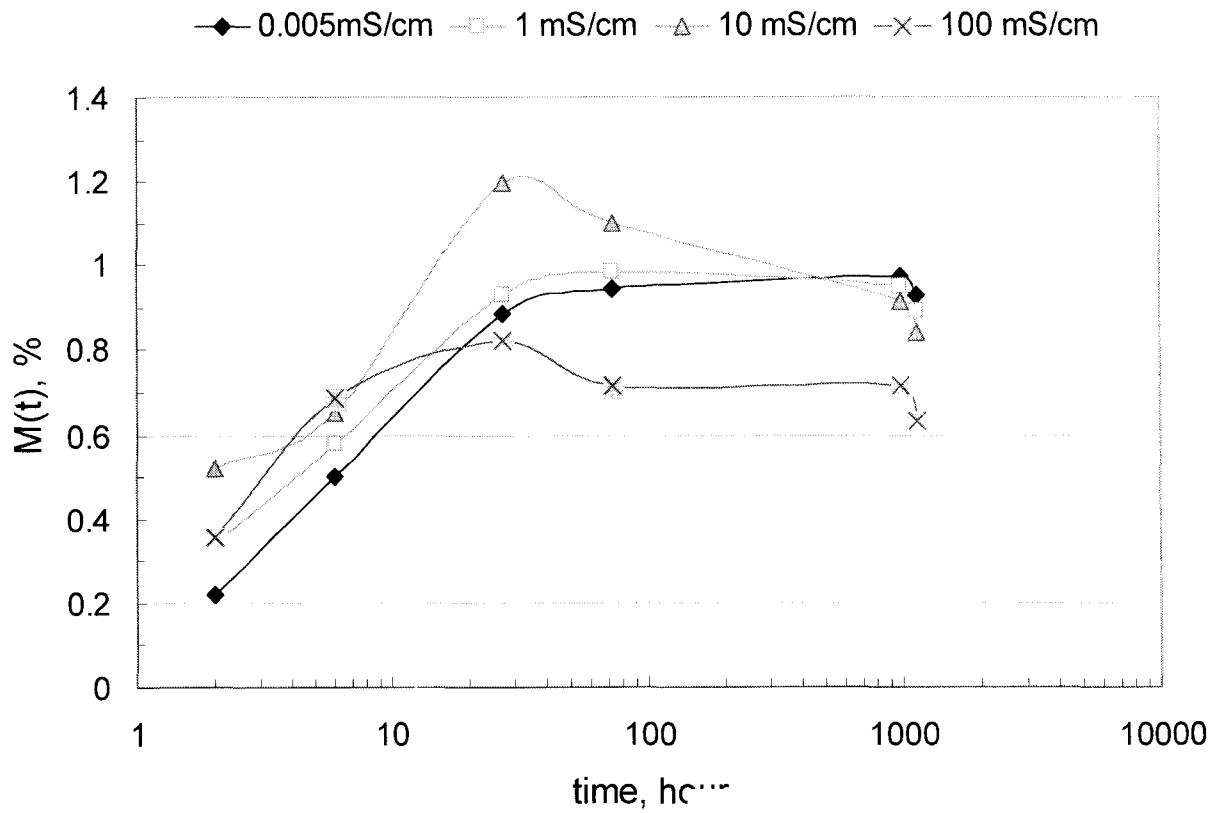


Fig. 4.23: Variation of $M(t)$ of Delrin as a function of time in hours for different conductivities of saline solutions at 60 °C.

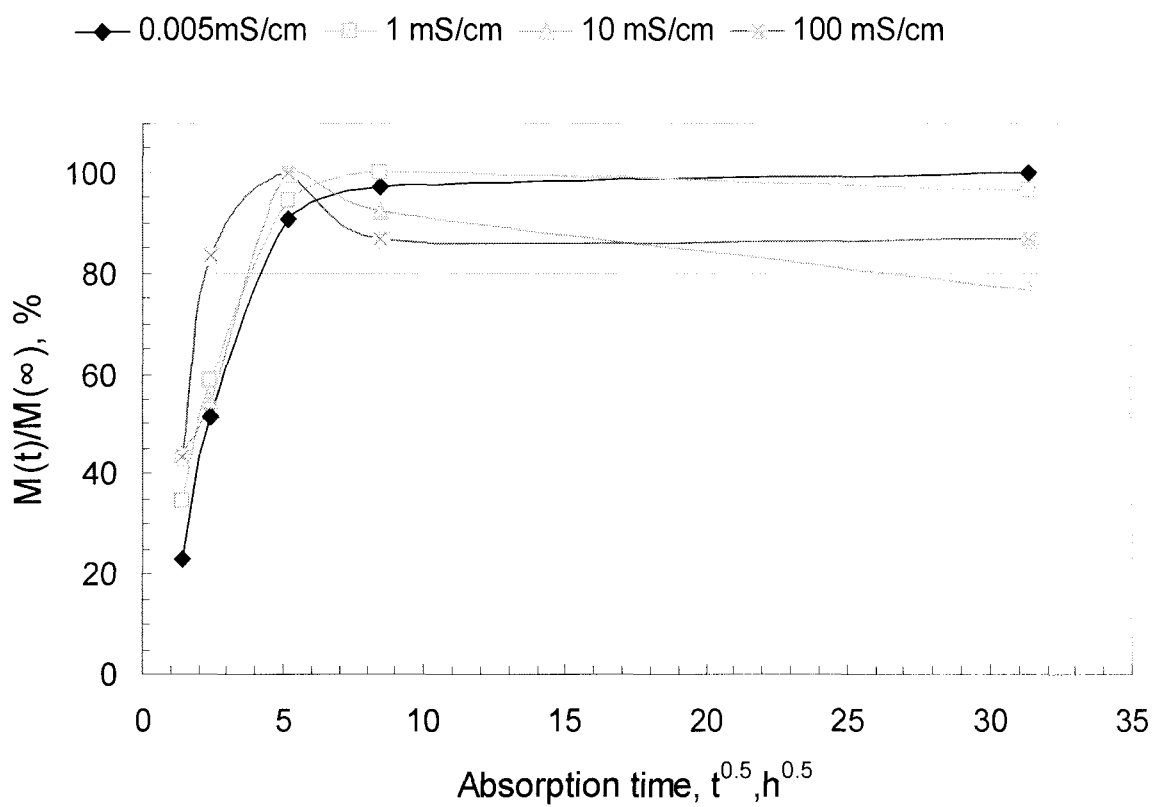


Fig. 4.24: Variation of $M(t)/M_{\infty}$ (%) of Delrin as a function of the square root of time in hours for different conductivities of saline solutions at 60 °C.

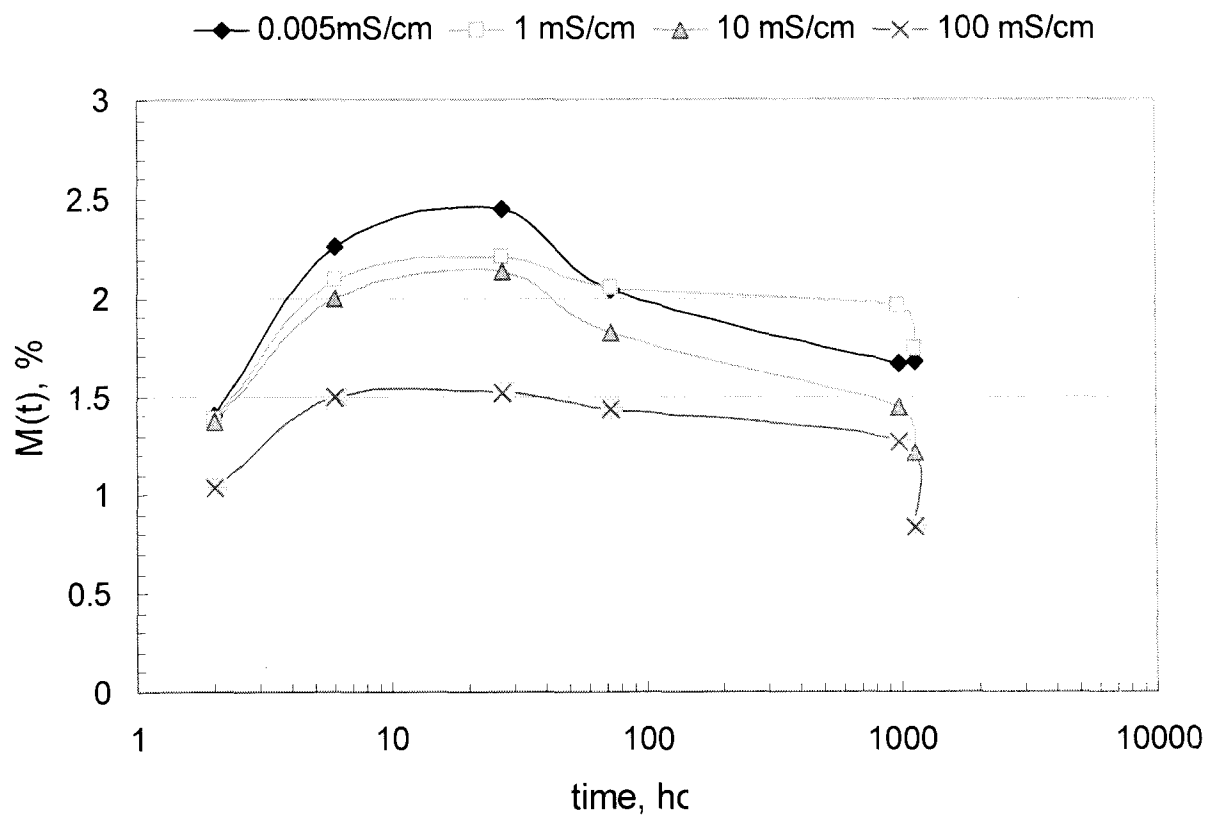


Fig. 4.25: Variation of $M(t)$ of Delrin as a function of time in hours for different conductivities of saline solutions at 98 °C.

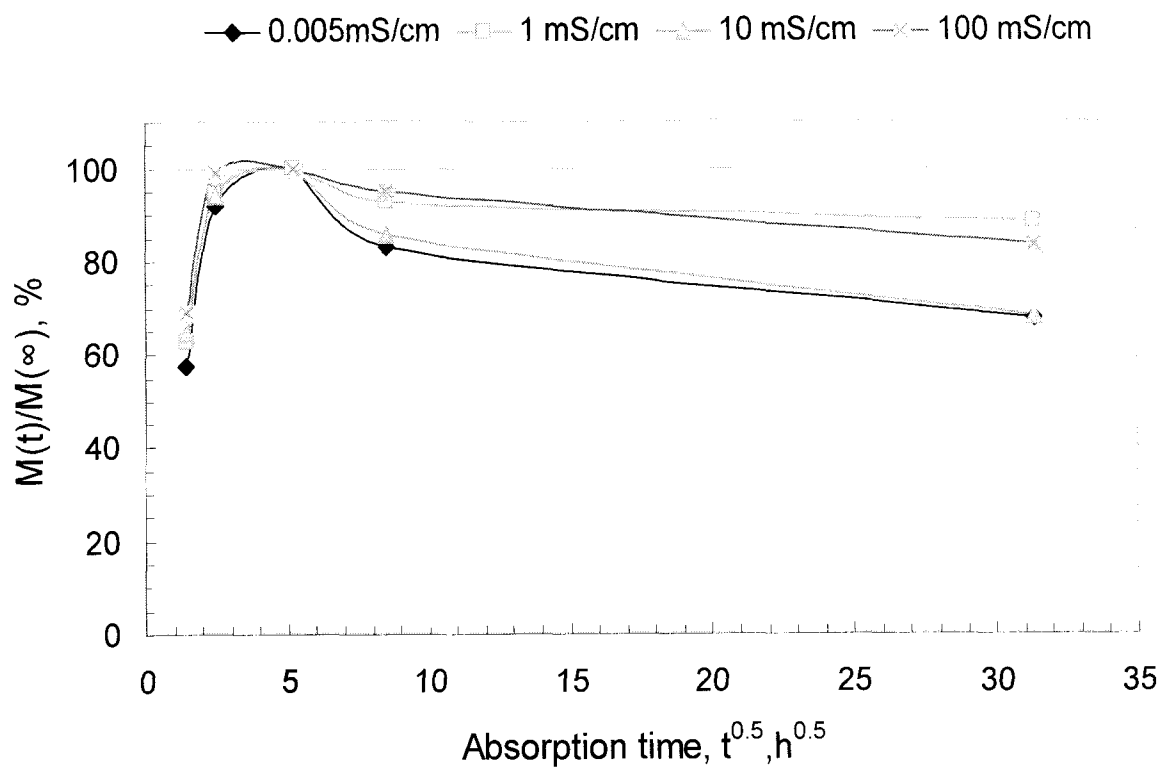


Fig. 4.26: Variation of $M(t)/M_{\infty}(\%)$ of Delrin as a function of the square root of time in hours for different conductivities of saline solutions at 98 °C.

Salinity (mS/cm)	Thickness (mm)	Time t when $\Delta M(t)/\Delta M_{\infty} = 0.5$ (hour)	Diffusion coefficient D (m ² /s)
0.005	1.75	5.74	7.27 E-12
1	1.40	4.31	6.19 E-12
10	1.47	4.02	7.31 E-12
100	0.99	2.52	5.30 E-12

Table 4.1: Diffusion coefficient of Delrin immersed in different salinities at 60 °C

Salinity (mS/cm)	Thickness (mm)	Time t when $\Delta M(t)/\Delta M_{\infty} = 0.5$ (hour)	Diffusion coefficient D (m ² /s)
0.005	1.44	1.65	1.71 E-11
1	1.32	1.47	1.61 E-11
10	1.76	1.42	2.97 E-11
100	1.65	1.30	2.84 E-11

Table 4.2: Diffusion coefficient of Delrin immersed in different salinities at 98 °C

4.9.4 Activation Energy

The percentage increase in the weight of Delrin specimen increased with the increase in temperature and conductivity, up to certain limit, of the saline solution as shown in Figs. 4.23 and 4.25. According to [46] the force that causes diffusion, increases with the increase in temperature of the system. It is logical to expect that because diffusion is driven by concentration gradient due to random motion of molecules which increases with increase in temperature. The dependence of the diffusion coefficient on temperature is given by [42]:

$$D = D_0 \exp\left(\frac{-E_d}{RT}\right) \quad (4.13)$$

where E_d (J/mol) is the activation energy for diffusion which gives a measure of the energy required to loosen a molecule bound by the van der Waals forces, T the absolute temperature (K) and R a universal constant $R= 8.314$ (J/ kmol K) and D_0 is also a constant. Sometimes equation (4.12) is written in the form

$$D = D_0 \exp\left(\frac{-E_d}{kT}\right) \quad (4.14)$$

where $k = 1.38 \times 10^{-23}$ (J/K), the Boltzman constant and the unit for E_d is J[42].

Equation (4.12) can be written as:

$$\ln D = \ln D_0 - \frac{E_d}{RT} \quad (4.15)$$

This equation shows that $\ln D$ and $1/T$ have a linear relationship. Fig. 4.27 shows the Arrhenius plot represents the dependence of the $\ln D$ on the inverse of the absolute

temperature $1/T$. Based on these plots, the activation energy of each salinity calculated and plotted in Fig. 4.28. As it could be observed, the activation energy increased with increasing conductivity of the saline solution. Saline solution of 100 mS/cm has the highest activation energy.

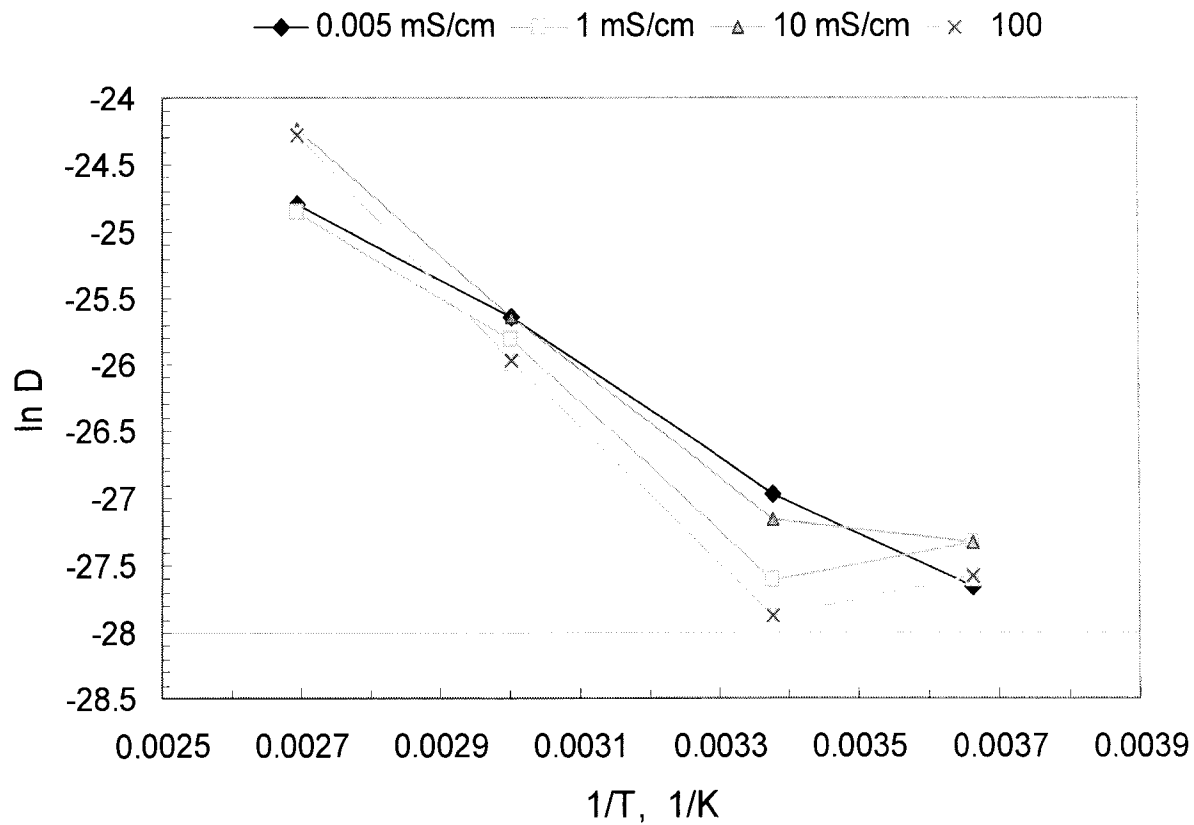


Fig. 4.27: Variation of $\ln D$ of Delrin as a function of $1/T$ for different conductivities of saline solutions.

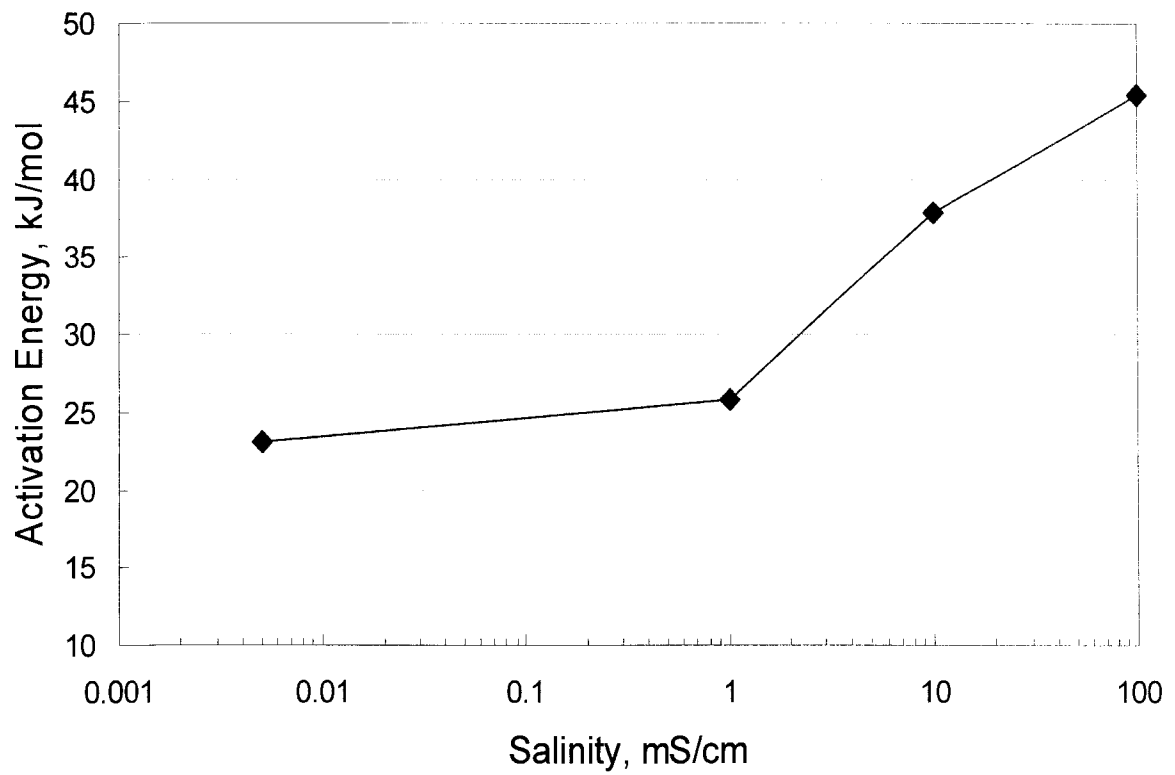


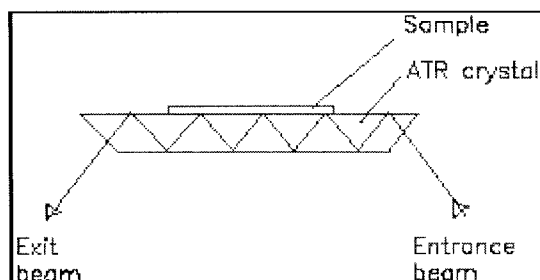
Fig. 4.28: Variation of E_d , activation energy of diffusion of saline solution in Delrin, as a function of conductivity of saline solution.

4.10 Attenuated Total Reflectance FTIR spectroscopy of Delrin

4.10.1 Introduction

In 3.4 the principal of infrared spectroscopy (IR) was generally discussed. Attenuated Total Reflectance (ATR) FTIR is a non-destructive tool for surface analysis of pliable solids such as rubber and plastics. This method works well with samples that are too dense or too thick for standard transmission method.

The ATR instrument consist of two 45° fixed incident angles and a horizontal plate with a KRS5 (orange crystal) for easy sample mounting. The horizontal plate design of ATR accessory accommodates odd shapes as well as liquid, gels and opaque samples. The diagram below shows multiple internal reflection ATR plate and the path of light.



The sample is placed on the horizontal face of the internal reflectance crystal where total internal reflection occurs along the crystal-sample interface. The source of energy entering the crystal is reflected within the crystal, the number of reflections depending upon the crystal length, its thickness and the interface angle. At each reflection, the light beam penetrates the sample a small amount and is absorbed at the characteristic absorption frequencies. Typically, the reflected radiation penetrates the sample to a depth of only few microns. The ATR method requires that the sample of interest be placed in

contact with the ATR crystal which has relatively high reflective index compare to the sample. Some samples need to be pressed against the ATR crystal to obtain good contact. Since the crystals are fairly soft and easily deformed, only limited amount of pressure should be applied to the sample to obtain the necessary contact. KRS-5, zinc selenium and germanium are the most commonly used [52].

4.10.2 ATR FTIR of Delrin and Acetron

Figs. 4.29 to 4.31 show the ATR spectrum of virgin and aged in 0.005 and 10 mS/cm saline solution at 98 °C samples of Delrin. It is clear from these spectra that there is no significant absorption of any chemical groups in the cases of 0.005 and 10 mS/cm. the spectra of the aged specimens are not much different from that of virgin Delrin even after 4600 h of immersion. However, for higher salinity, few peaks have started to develop a decrease in the relative absorption of the reflected infrared spectrum. The chemical group and relative peaks are noted in Fig. 4.29 the spectrum of virgin sample of Delrin. The C-H stretching vibration group decrease on 0.005 and furthermore in 10 mS/cm.

Fig. 4.32- 4.34 show the ATR spectrum of virgin and aged in 0.005 and 10 mS/cm saline solutions at 98 °C samples of Acetron. It is also clear from these spectra that there is no appreciable absorbance of any chemical groups in the case of aged samples.

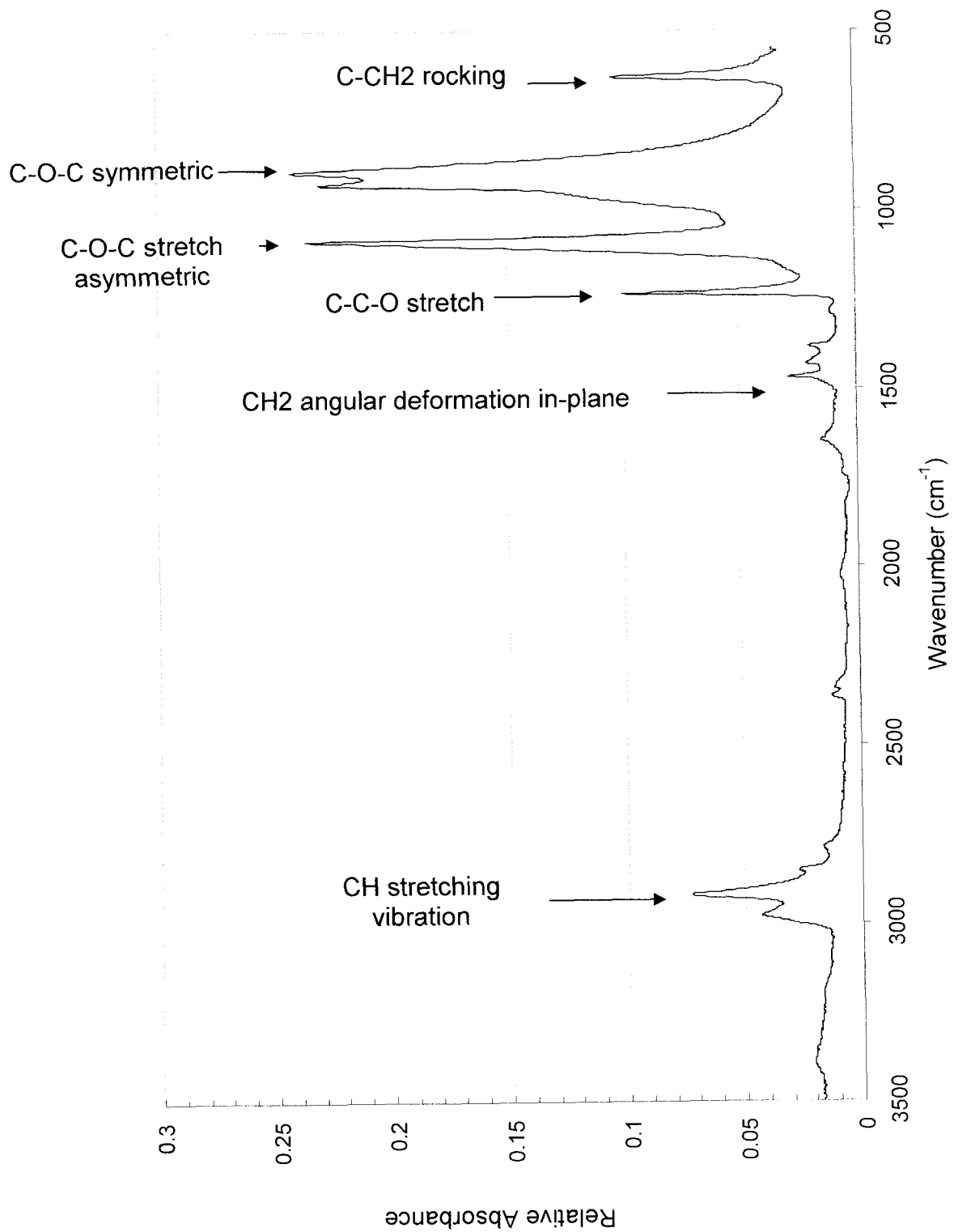


Fig. 4.29: ATR spectrum of virgin sample of Delrin.

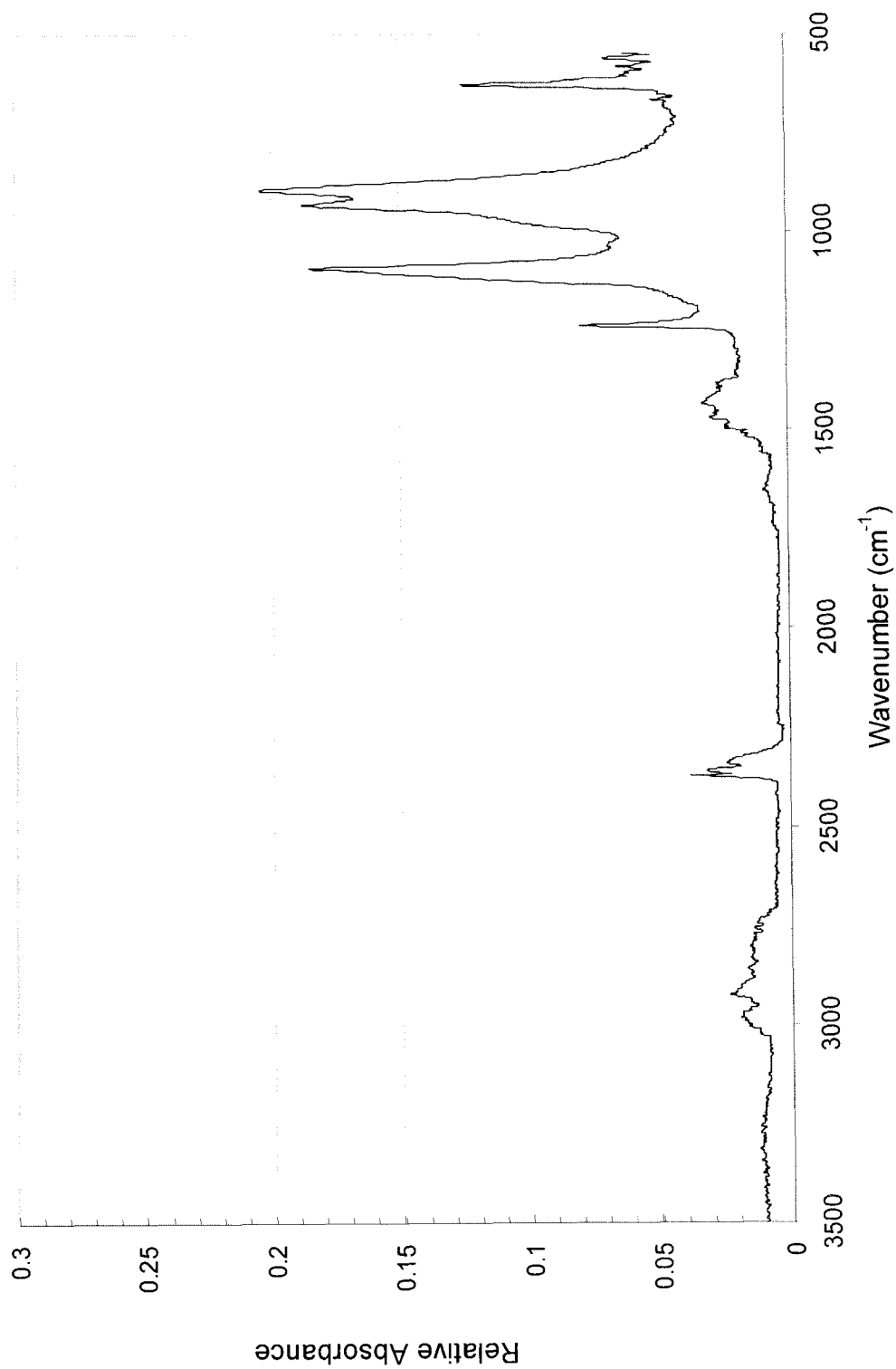


Fig.4.30: ATR spectrum of aged sample of Delrin in 0.005 mS/cm at 98 °C.

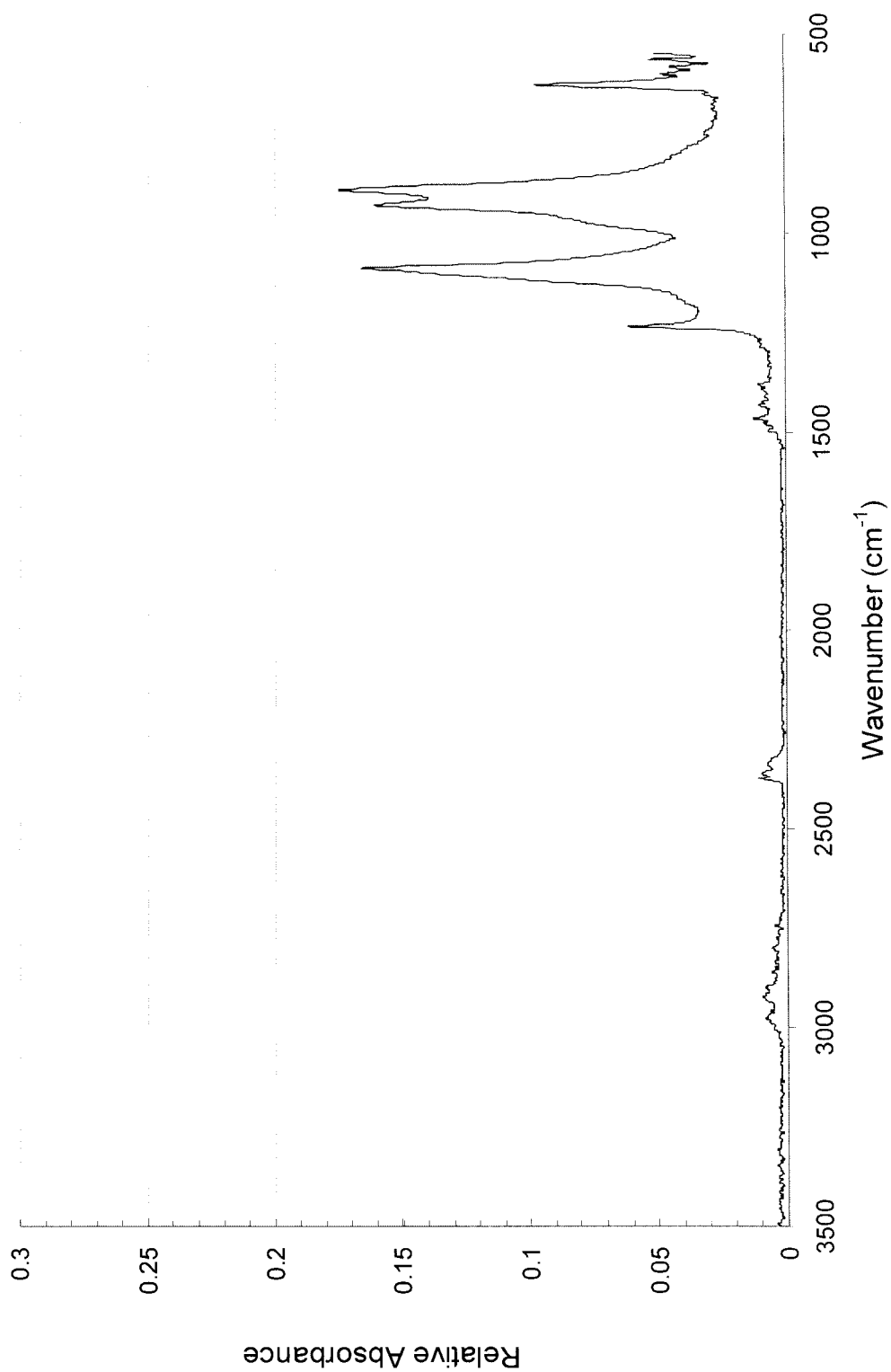


Fig. 4.31: ATR spectrum of aged sample of Delrin in 10 mS/cm at 98 °C

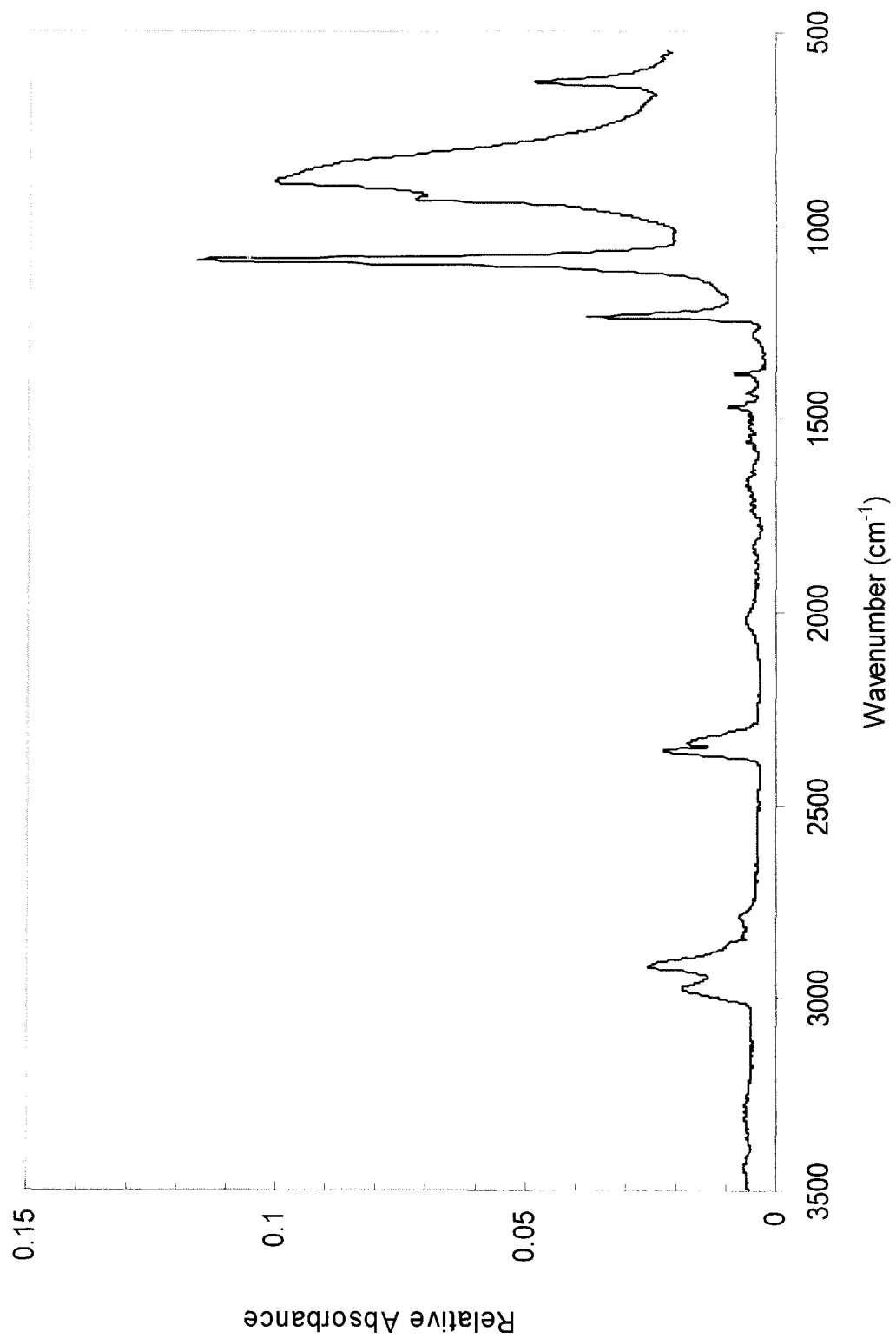


Fig. 4.32: ATR spectrum of virgin ample of Acetron

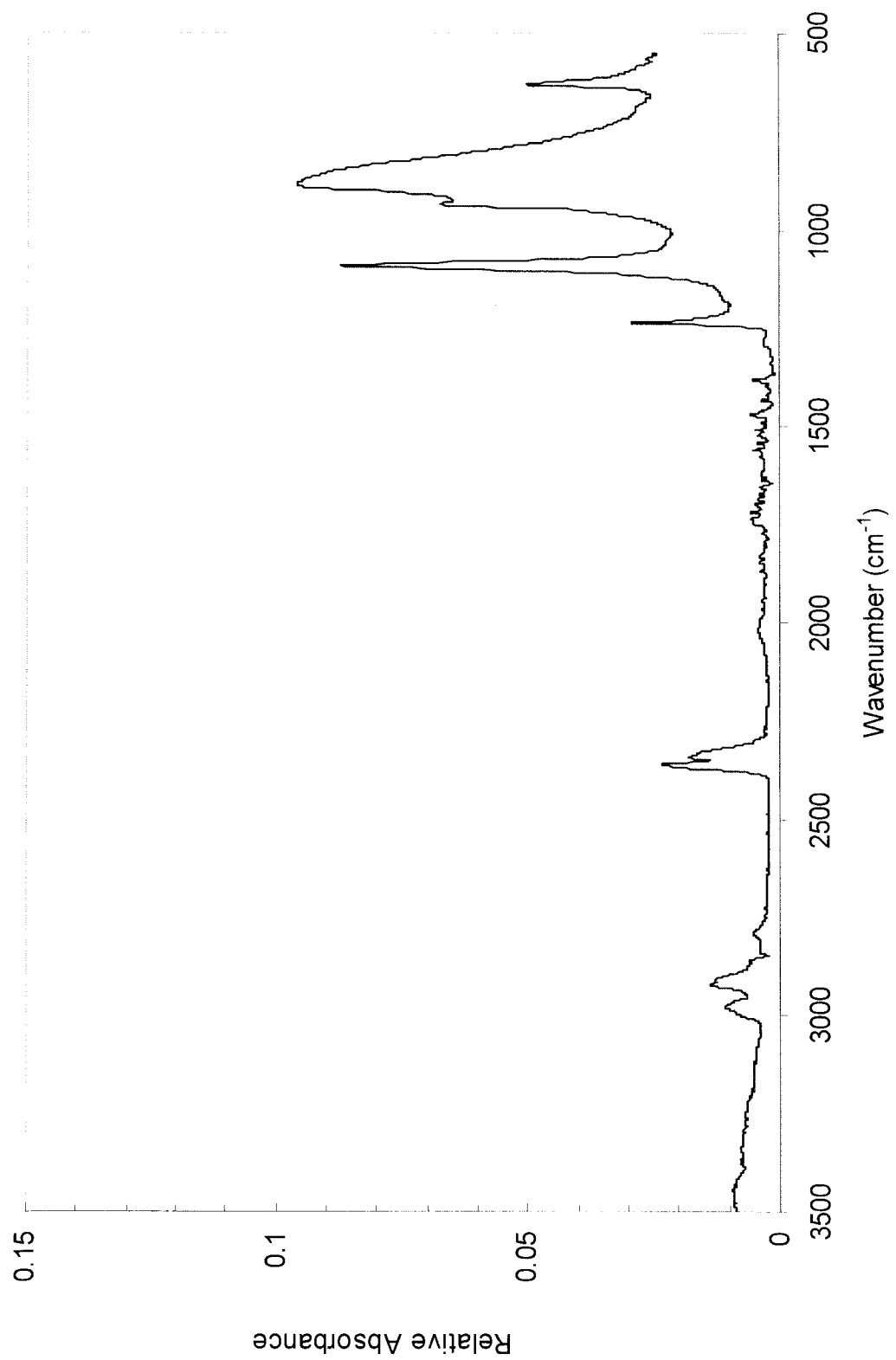


Fig.4.33: ATR spectrum of Acetron aged in 0.005 mS/cm at 98 °C for 768 h

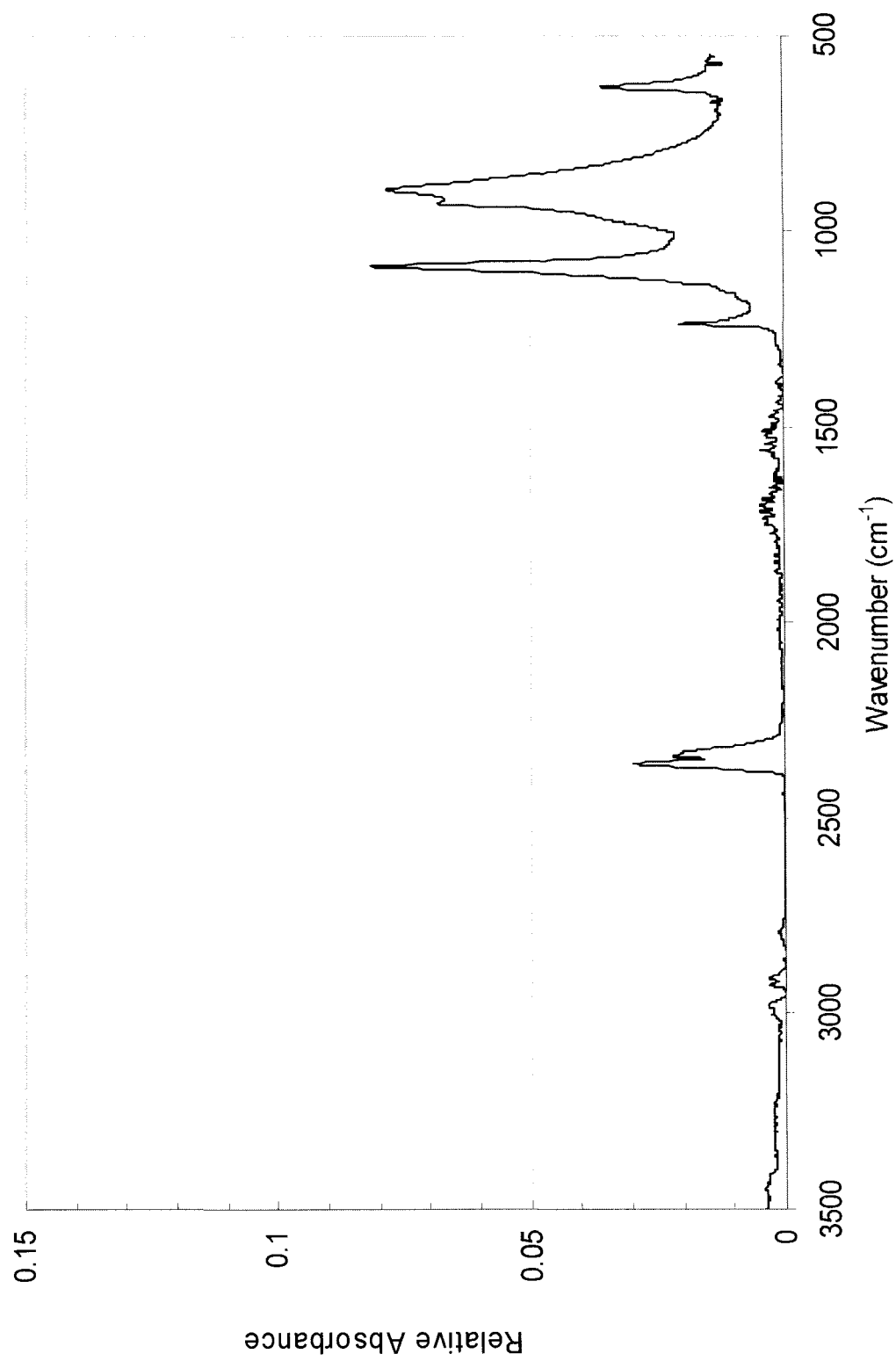


Fig.4.34 ATR spectrum of Acetron aged in 10 mS/cm at 98 °C for 768 h

4.11 Surface Roughness of Delrin

The average surface roughness (ASR) of the virgin specimens of Delrin before immersion was $1.1 \pm 0.3 \mu\text{m}$. Fig. 4.35 shows the variation of ASR as a function of conductivity of the saline solution at different temperatures after immersion of Delrin specimens for 2160 h. The average surface roughness slightly increased after immersion in the saline solution due to the intake of saline solution. For example, the ASR increased from $1.1 \pm 0.3 \mu\text{m}$ before immersion to $2.3 \pm 0.6 \mu\text{m}$, $2.5 \pm 0.5 \mu\text{m}$, $1.9 \pm 0.8 \mu\text{m}$ and $1.4 \pm 0.7 \mu\text{m}$ for 98 ± 2 , 60 ± 2 , 23 ± 3 and 0 ± 1 °C, respectively, after immersion for 2160 h in 10 mS/cm. The increased surface roughness was partially responsible for the decrease in the contact angle and therefore the loss of hydrophobicity of Delrin.

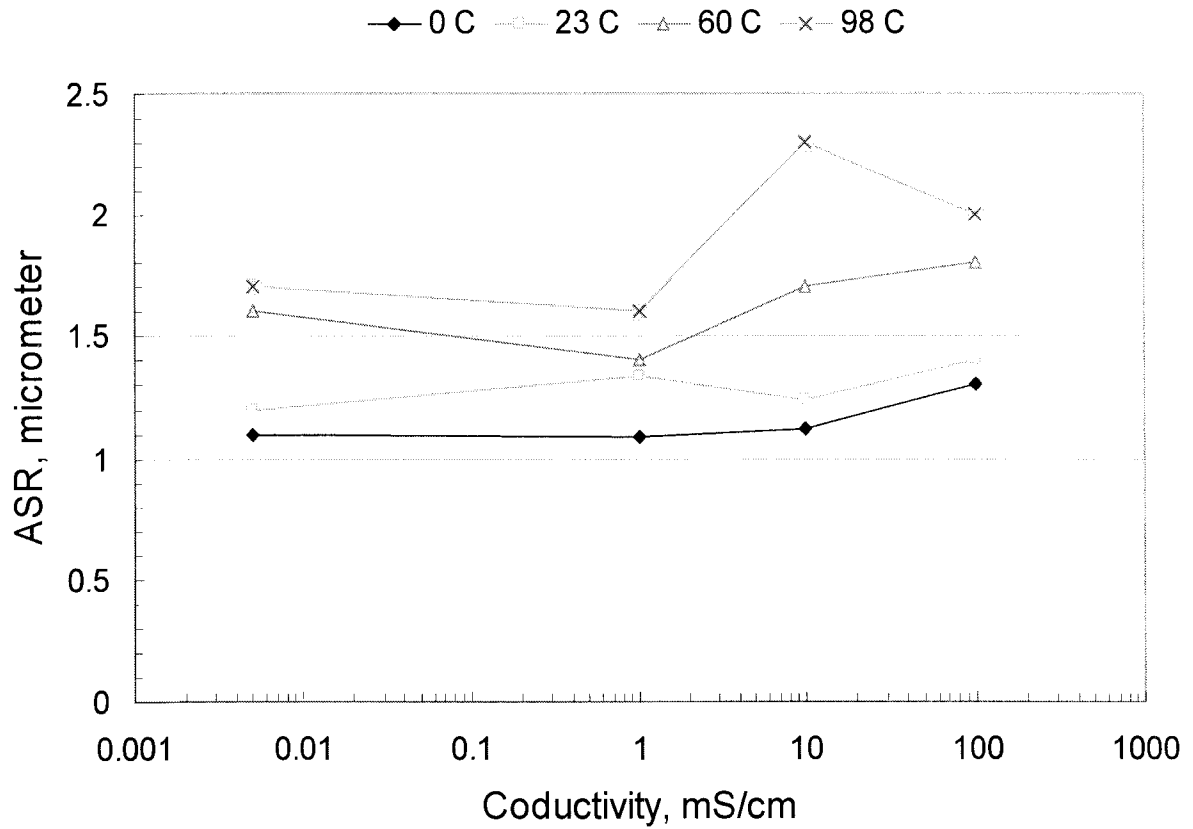


Fig. 4.35: Variation of average surface roughness (ASR) of Delrin after immersion in saline solutions of different conductivities for 2160 h at different temperatures.

Chapter 5

5. Effect of Water Salinity, Temperature and Time of Immersion on ac and dc Flashover Voltage of Delrin

5.1 Solid Insulators and Breakdown Phenomena

5.1.1 Introduction

Dielectric materials are evaluated by their ability to withstand electrical stress and their failure under such stress is considered a breakdown. Depending on the environment and mode of use of the dielectric material, the dielectric strength will vary widely [47]. Even where the conditions of applications and electrical field distribution are mostly the same, however, breakdown is still found to occur over a wide range of applied stresses [20]. Experimental evidence has made it clear that, in practice, the failure of a solid polymeric material is a complicated process, which often involves combinations of several breakdown mechanisms described in the literature [49]. Important types of breakdown are as follows:

5.1.2 Intrinsic Breakdown

The material under examination in intrinsic breakdown is pure and homogenous. Temperature and other environmental elements are carefully controlled and the sample is so stressed that there are no external discharges [20]. As applied voltage is increased a small current begins to flow. As the voltage continues to increase this current remains constant until a certain critical voltage is reached. At this critical point the current suddenly increases rapidly to a high value; breakdown is said to take place at this point

and the critical voltage is the breakdown voltage. In the case of the intrinsic breakdown the current rises to the maximum value allowed by the power supply in approximately 10^{-8} s. It is therefore described that the breakdown is electronic in nature. Based on this assumption that the random motion of electrons is increased, and at the time of electrical breakdown they gain energy from the electrical field faster than they lose it to the material, Frolich [20] proposed a model of intrinsic breakdown. Practically, except for the plastic materials such as polyethylene, there has been no experimental proof to show whether an observed breakdown is intrinsic or not, and therefore, conceptually, it remains an ideal mechanism identified as the highest value obtained after all secondary effects have been eliminated [49].

5.1.3 Thermal Breakdown

Thermal breakdown takes place when the heat input cannot be balanced by the heat loss from the insulation either in macroscopic scale or, more usually, in a small area. As power is dissipated by the insulation, heating occurs which usually causes an exponential increase in the electrical conductivity as more carriers become available for conduction. Alternatively, the increased segmental motion may increase the mobility for intrinsic ionic conduction. If the electrical stress is sustained, the current density increases in the area of elevated temperature. This results in further increase of the local temperature through Joule heating and hence the conductivity, and therefore ‘thermal runaway’ may occur. In general this leads to a highly localized filamentary breakdown path; however under appropriate conditions, breakdown may occur on a broad front [51].

5.1.4 Discharge Breakdown

Polymeric materials usually contain voids which are difficult to eliminate [50]. In partial discharge breakdown, sparks occur within voids in the insulation causing degradation of the void walls and progressive deterioration of the dielectric.

5.1.5 Free Volume Breakdown

Free volume breakdown carriers are accelerated through spaces within low-density amorphous regions; the energy thereby gained is lost through collisions [20].

5.1.6 Electromechanical Breakdown

Electrostatic forces maintain the major effect on stressing dielectrics. At fields approaching breakdown, such mechanical pressure can reach magnitudes of the order of several tens of kilograms per square centimeter and will cause deformation of compliant materials such as polymers. According to the principal of minimum potential energy the mechanical stress P_c acting on the conductor surfaces is equal to the energy density stored in the field [53]. Thus

$$P_c = \frac{1}{2} \epsilon \cdot E^2 \quad (5.1)$$

where E is the field strength and ϵ is the permittivity of the dielectric. On this basis, Stark and Garton [20, 54], have proposed that an electrically stressed material may fail by mechanical collapse. In the case of a plane slab of material with electrodes which will follow any motion allowed by the dielectric, for equilibrium, the electrostatic force is balanced by the elastic reaction so that for large strains

$$\frac{1}{2} \cdot \left[\epsilon \epsilon_o \left(\frac{V}{d} \right)^2 \right] = Y \cdot \ln \left(\frac{d_o}{d} \right) \quad (5.2)$$

where V is the voltage applied across a specimen of undistorted thickness, d_o , and Young's modulus, Y . Both sides of equation (5.2) have units of mechanical stress. Differentiation of $d^2 \ln(d_o/d)$ with respect to d , to find the critical values of d , readily shows that thickness, d , under stress condition cannot have a stable value greater than $d_o \exp(-1/2)$. Consequently, the critical value of stress will be given by

$$E_c = \frac{V_c}{d} \quad (5.3)$$

and at $d = d_o \exp(-1/2)$ from equation (5.2)

$$E_c = \left(\frac{Y}{\epsilon \epsilon_o} \right)^{1/2} \quad (5.4)$$

which must be multiplied by $\exp(-1/2) \approx 0.6$, if the undistorted thickness, d_o , is used in computing the stress. This hypothesis assumes that breakdown has not occurred by another process prior to the establishment of the critical stress and is also confined to substances which can deform sufficiently without fracture.

5.1.7 Flashover Voltage

Flashover is a breakdown of the air or gas very close to the solid surface or dissolved in liquid insulation. Flashover in solids is a surface phenomenon and can be controlled by these factors:

1. Adjusting the creepage distance
2. Insulator surface design.
3. Removing air or gas (other than electronegative types) from critical areas by varnish, impregnation, potting, oil filling, or embodiment of electrodes.

4. Changing the gas to electronegative type (such as SF₆) so those electrons may be trapped before they form a corona cloud.
5. Using semi-conducting components or surface treatment materials to grade the stress below the corona inception voltage.
6. Using stress rings to alter the electric field in the vicinity of the gas-insulation-electrode area.
7. Avoiding the use of high-dielectric constant materials adjacent to air.

Flashover voltage is affected by humidity, type of voltage, spacing, and dielectric constant of the solid insulator, contamination, and uniformity of the field. Moisture as a surface contaminant promotes surface leakage, tracking, flashover, and dielectric breakdown by bridging weak spots.

5.2 Flashover of Delrin under stress of water salinity and temperature

5.2.1 Introduction

During exposure to a saline solution the surface of a polymeric insulating material acquires gradual changes, which affect its flashover voltage. The surface of Delrin is usually hydrophobic due to its low surface energy [20], but under the continuous stress of salinity and higher temperatures, surface energies temporarily increase and therefore the surface become hydrophilic. In this state small electric current start to flow across the surface. As the applied voltage increases the current also increases until flashover occurs across the surface. In this study the effect of immersion of Delrin in a saline solution at different temperatures and for different durations on the surface flashover voltage is reported.

5.2.2 Experimental Procedure

Cylindrical rods of Delrin of 19 mm in diameter and 9.3 ± 0.3 mm in length were immersed in saline solution of 0.005, 1, 10 and 100 mS/cm at temperatures of 0, 23, 60 and 98 °C for up to 90 days. The specimens were removed from the solution at different times and placed between 152 mm diameter of stainless steel electrodes and either dc or ac flashover voltages were determined. A new specimen was used for each experimental reading.

The experimental procedure for the measurement of the contact angle is the same as described in Chapter 4, the contact angle was determined at 23 ± 3 °C and at relative humidity of $55\pm 15\%$. After removal of the specimens from the saline solutions at

different temperatures, they were allowed to dry and reach room temperature before the contact angle was measured. The contact angle was determined within 30 s after placing a droplet of water on the specimen. The contact angle was measured at 6 to 8 different locations on each specimen. After these measurements, the flashover voltage was measured in 2 minute intervals until a saturated value of the flashover voltage was reached.

5.2.3 Results and discussion

5.2.3.1 dc Flashover Voltage

Fig. 5.1 shows the arrangement used to measure the dc flashover voltage. The high voltage power supply of “Spellman, model SL150” with a maximum output of 150 kV was used during the experiment. Fig. 5.2 shows the dc flashover voltage against the number of shots. It can be observed that the flashover voltage rapidly increased until a saturated value was reached. Figs. 5.3 to 5.6 show the dc flashover voltage of Delrin versus time of immersion in different saline solutions at a temperature range of 0 to 98 °C. Fig. 5.3 shows the variation of dc flashover of Delrin immersed in distilled water with times of immersion at 0, 23, 60 and 98 °C. The flashover voltage at higher temperatures fluctuated and decreased. Fig. 5.4 and 5.5 shows the flashover of Delrin immersed in saline solutions of 1, 10 and 100 mS/cm at 0, 23, 60 and 98 °C. The flashover voltage decreased with increasing temperature in all salinities.

To compare the effect of salinity on the dc flashover voltage at a certain temperature, Fig. 5.7 shows the variation of the flashover and time of immersion at 60 °C in saline

solutions of 0.005, 1, 10 and 100 mS/cm. As Fig. 5.7 shows the salinity of 10 mS/cm had the highest decrease in the dc flashover voltage. The value of the dc flashover before immersion was 26 kV and after immersion in 10 mS/cm for 90 days at 0, 23, 60 and 98 °C dropped to 18.1, 16.5, 13.1 and 11.5 kV, respectively.

Fig. 5.8 shows the dc flashover voltage versus temperature after 90 days of aging of Delrin specimen. It can be observed from Fig. 5.8 that the flashover voltage decreased with increasing temperature and increasing time of immersion.

The mid salinity solutions had the same effect on the decrease of the contact angle. In chapter 4 the effect of salinity and temperature on the contact angle of Delrin has been studied. Fig. 5.9 shows the variation of the dc flashover and the contact angle of Delrin immersed in 10 mS/cm at 98 °C. It can be observed that the flashover voltage decreases with the decreasing contact angle.

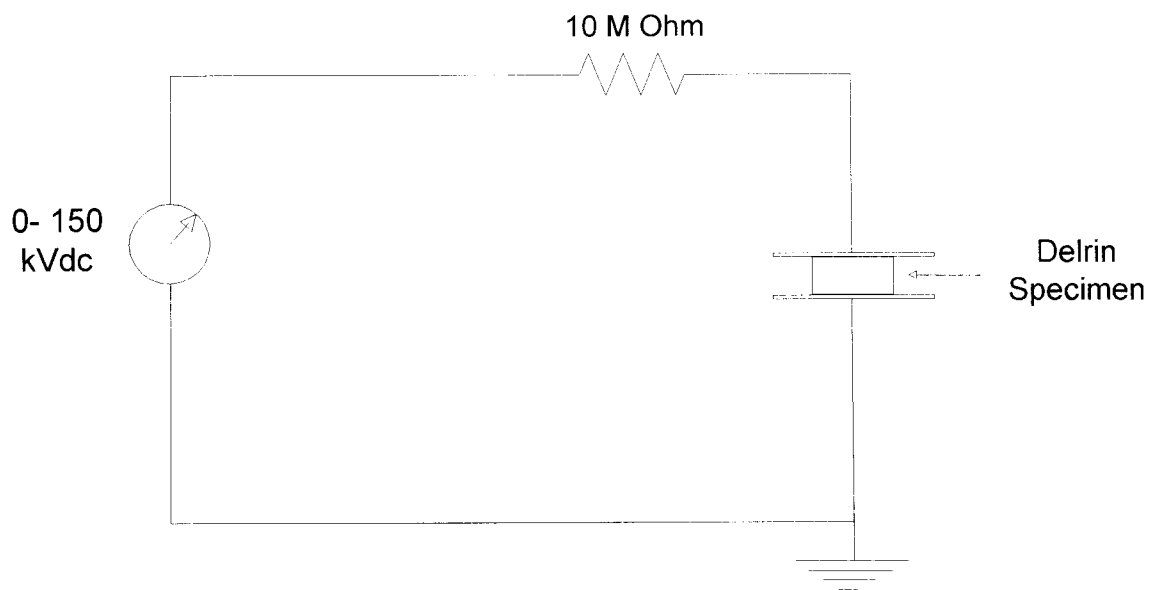


Fig. 5.1: Arrangement to measure the dc flashover voltage

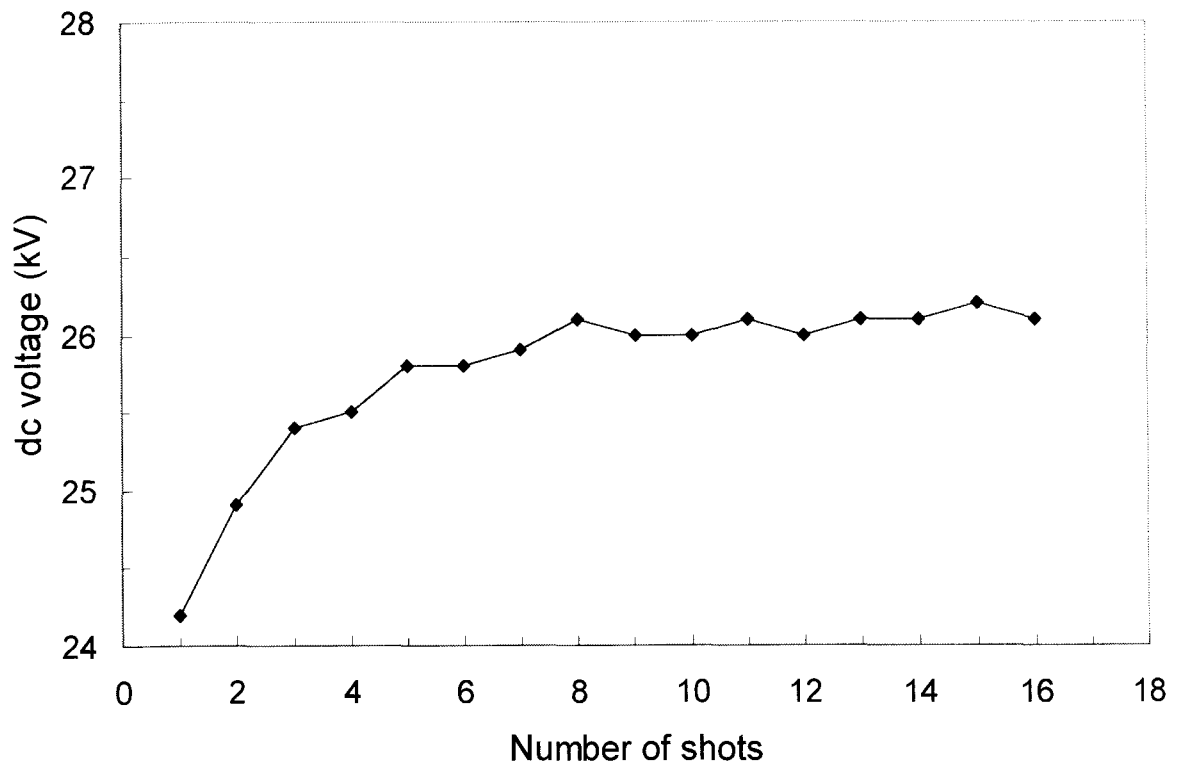


Fig. 5.2: dc flashover voltage of Delrin versus number of shots at 23 ± 3 °C before immersion in a saline solution.

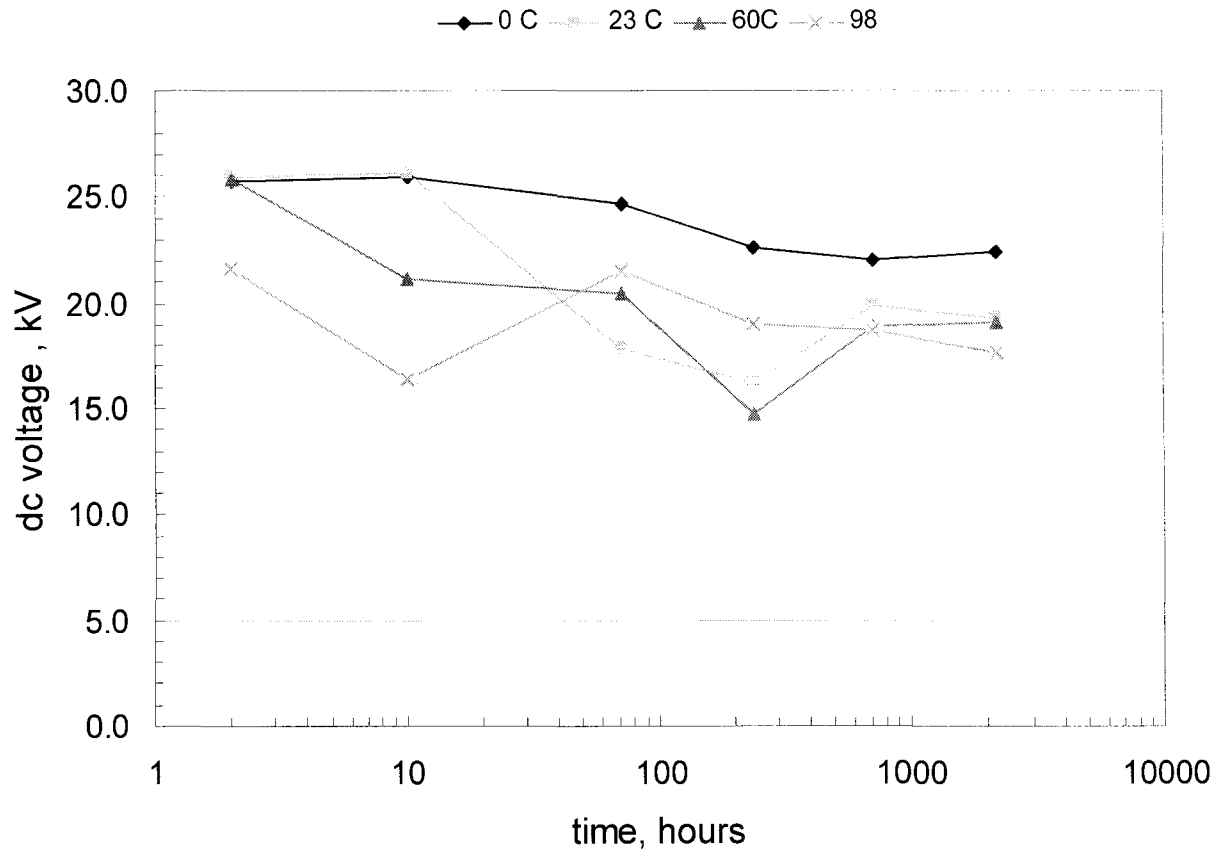


Fig. 5.3: dc flashover voltage of Delrin versus time of immersion in distilled water at 0, 23, 60 and 98 °C.

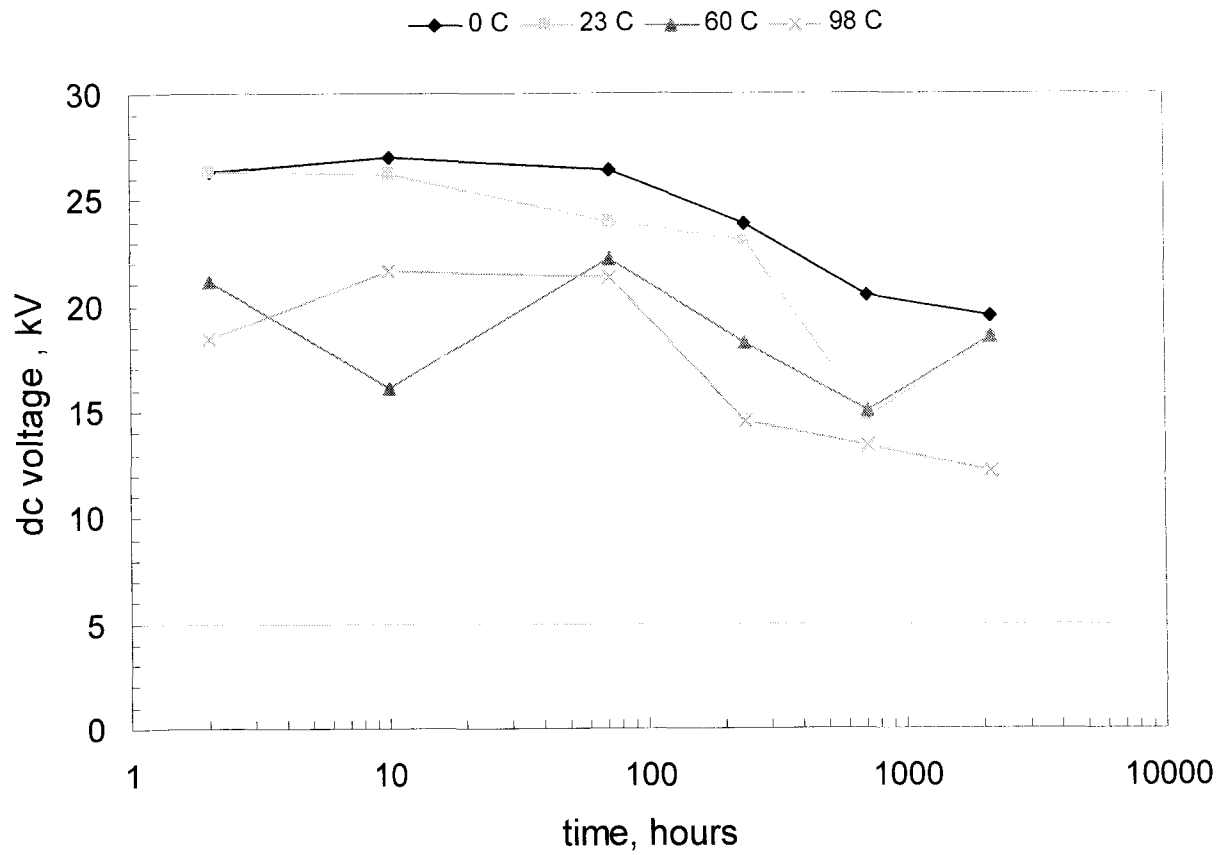


Fig. 5.4: dc flashover voltage of Delrin versus time of immersion in saline solution of 1 mS/cm at 0, 23, 60 and 98 °C.

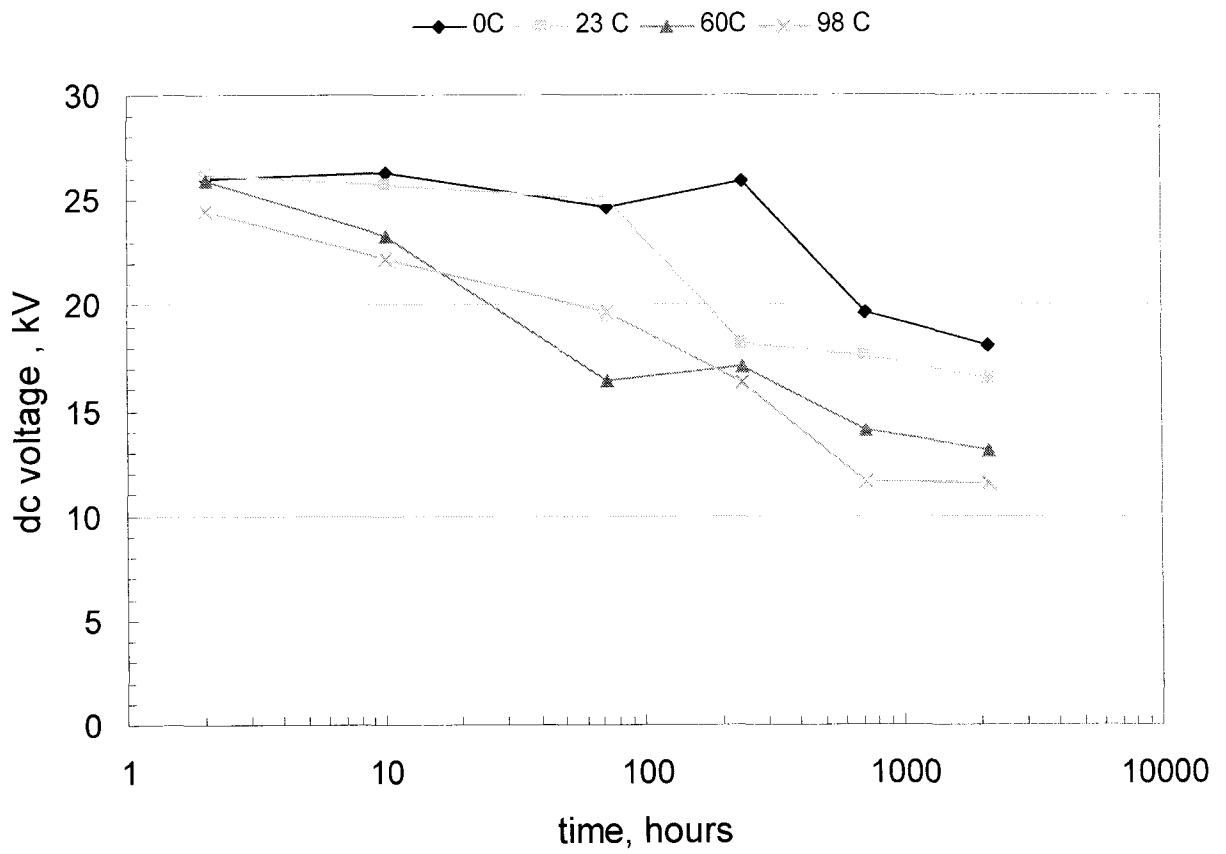


Fig. 5.5: dc flashover voltage of Delrin versus time of immersion in saline solution of 10 mS/cm at 0, 23, 60 and 98 °C.

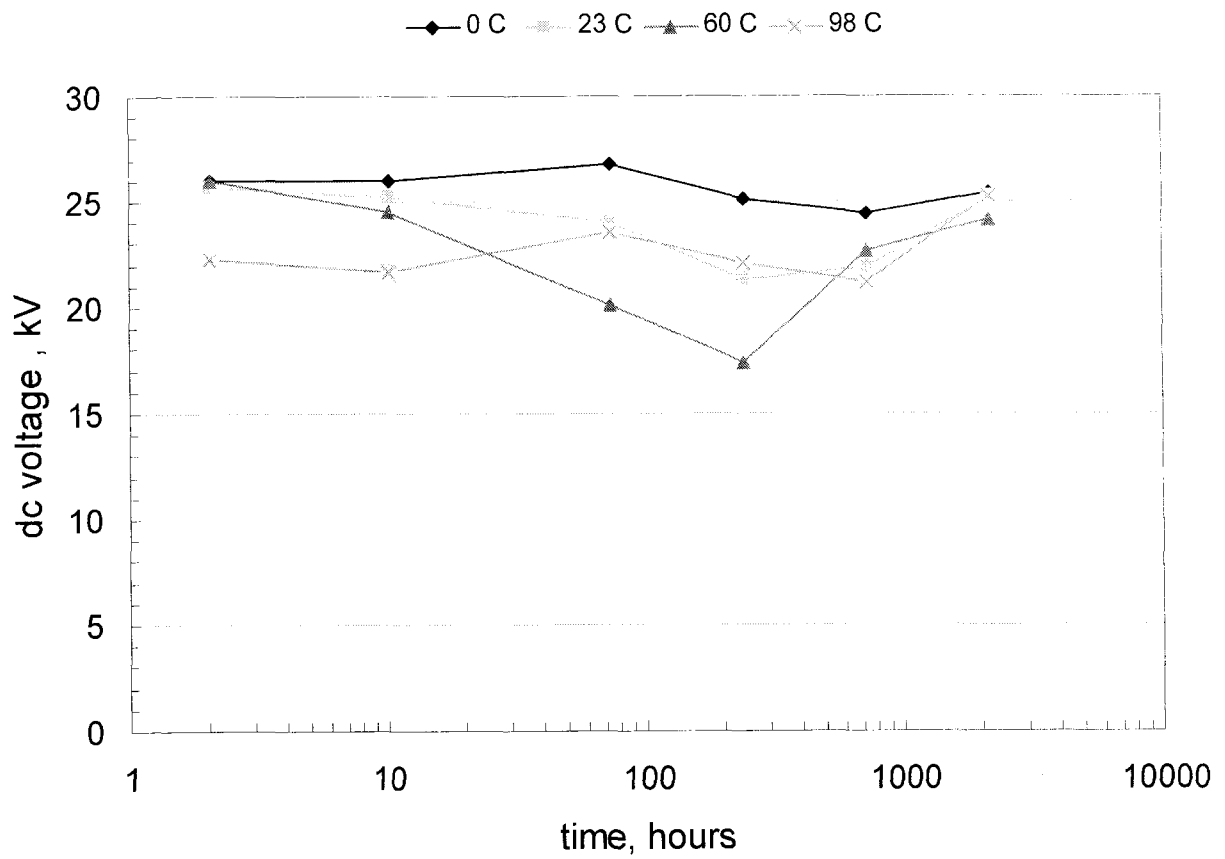


Fig. 5.6: dc flashover voltage of Delrin versus time of immersion in saline solution of 100 mS/cm at 0, 23, 60 and 98 °C.

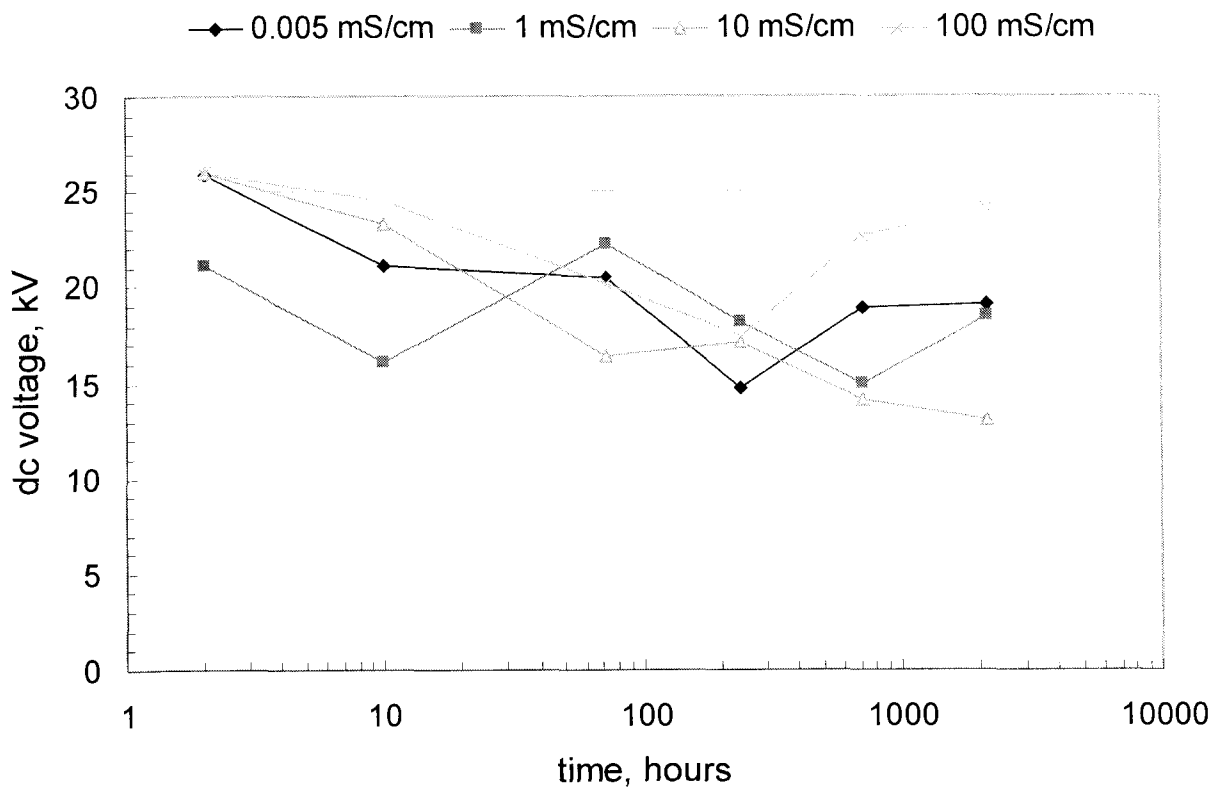


Fig. 5.7: dc flashover voltage of Delrin versus time of immersion in different saline solution at 60 °C.

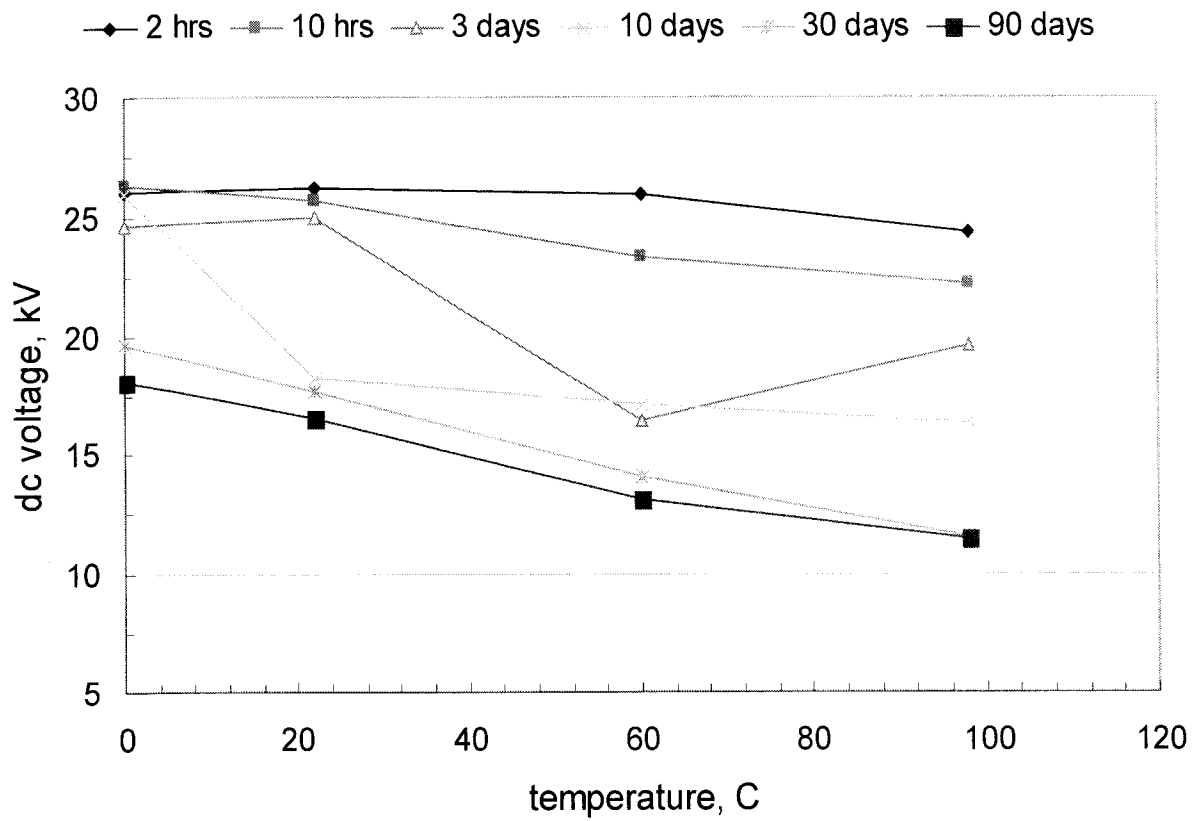


Fig. 5.8: dc flashover voltage of Delrin versus temperature of saline solution of 10 mS/cm.

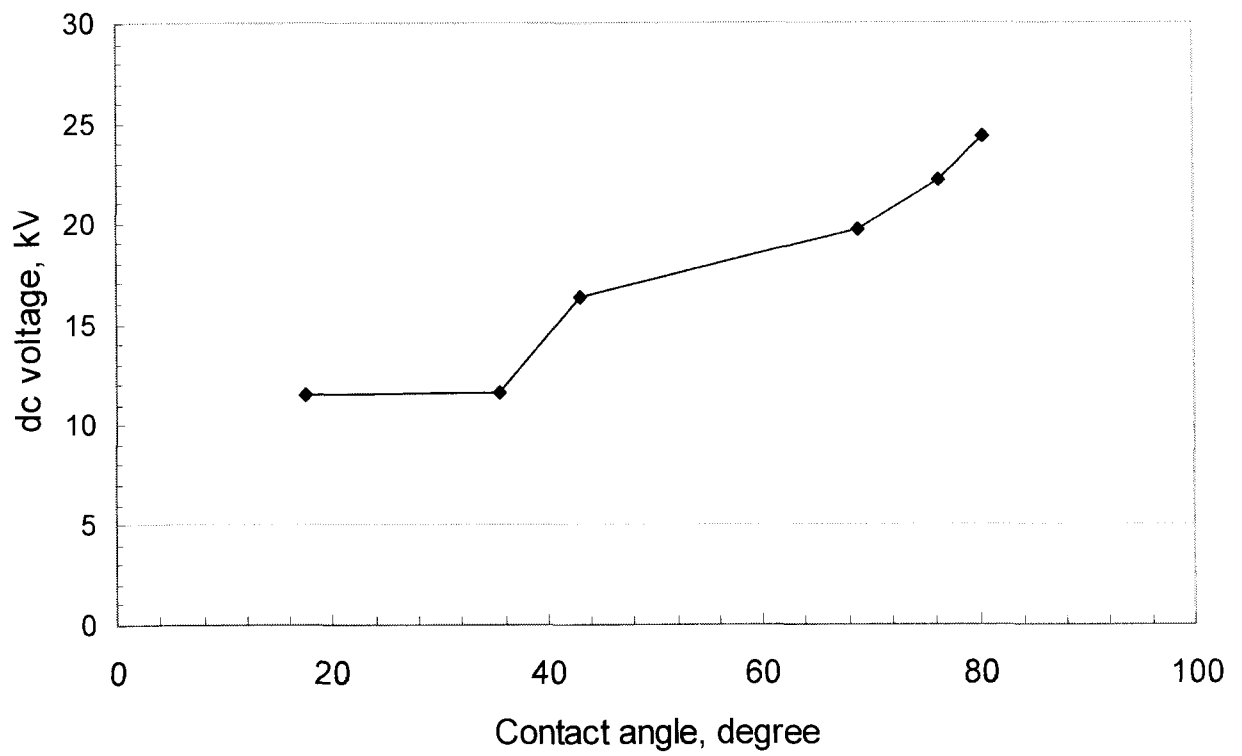


Fig. 5.9: dc flashover voltage of Delrin versus the contact angle in 10mS/cm saline solution at 98 °C.

5.2.3.2 ac Flashover Voltage

The ac flashover was also measured in Delrin specimens aged at 0, 23, 60 and 98 °C and in saline solution of 0.005, 1, 10 and 100 mS/cm. Fig. 5.10 shows the arrangement which has been used to measure the ac flashover voltage. Fig. 5.11 shows the ac flashover voltage against the number of shots. It can be observed that the flashover voltage increased rapidly until a saturated value was reached.

Figs. 5.12 to 5.15 show the ac flashover voltage after 90 days of aging in distilled water, 1, 10 and 100 mS/cm solution at different temperatures. It could be observed that the ac flashover did not decrease as much as dc flashover voltage. In saline solution of 1, 10 and 100 mS/cm the ac flashover retained a steady value during the aging process. Although in distilled water as can be seen in Fig. 5.12, there was a slight decrease of ac flashover from 26kV to 25kV.

These results show that Delrin has stable dielectric resistance against alternative electrical fields. Despite aging under the stress of heat and salinity, the ac flashover remained at a steady range. This could prove another advantage of Delrin as a high voltage insulator in addition to the other superb mechanical and electrical characteristics of this polymer.

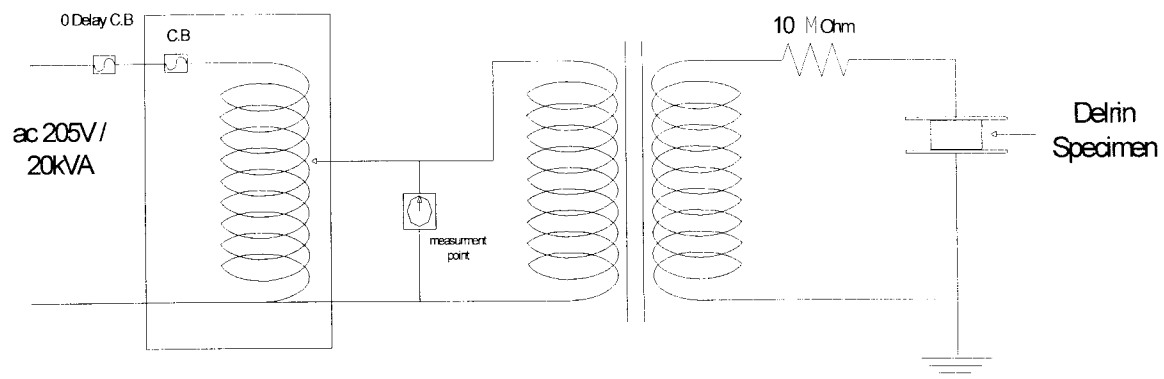


Fig. 5.10: Arrangement to measure the ac flashover voltage

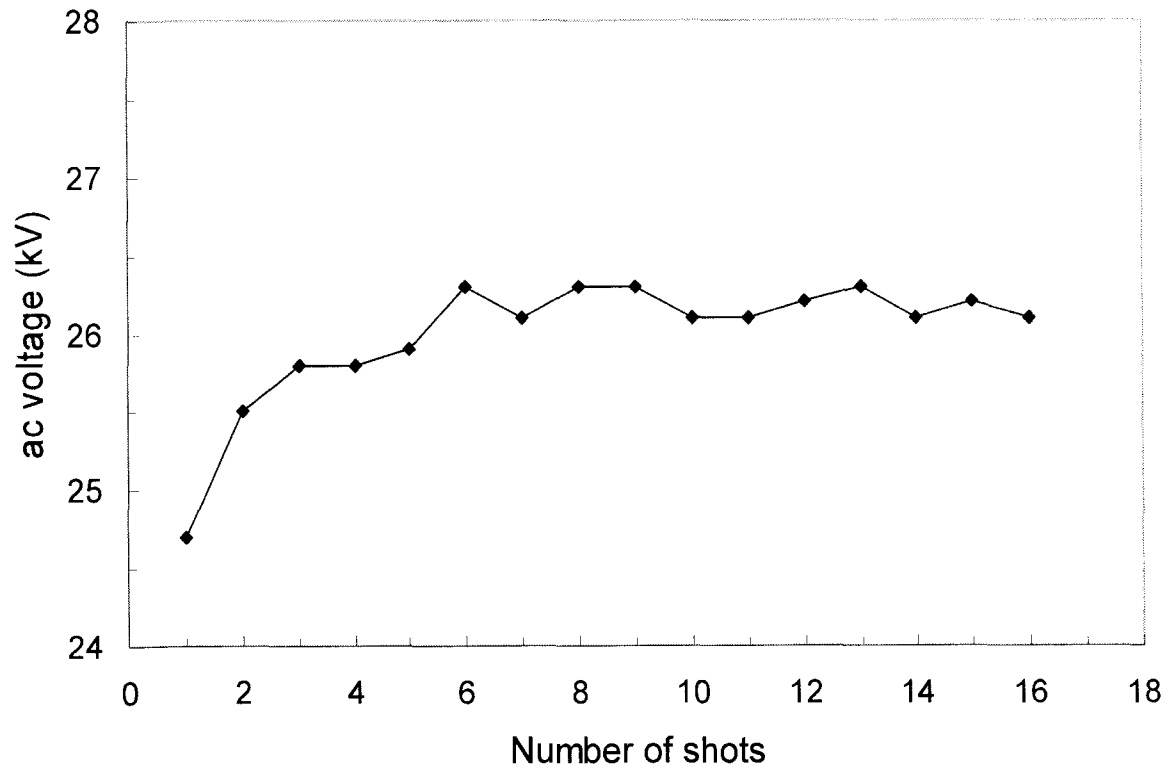


Fig. 5.11: ac flashover voltage of Delrin versus number of shots at 23 ± 3 °C before immersion in a saline solution.

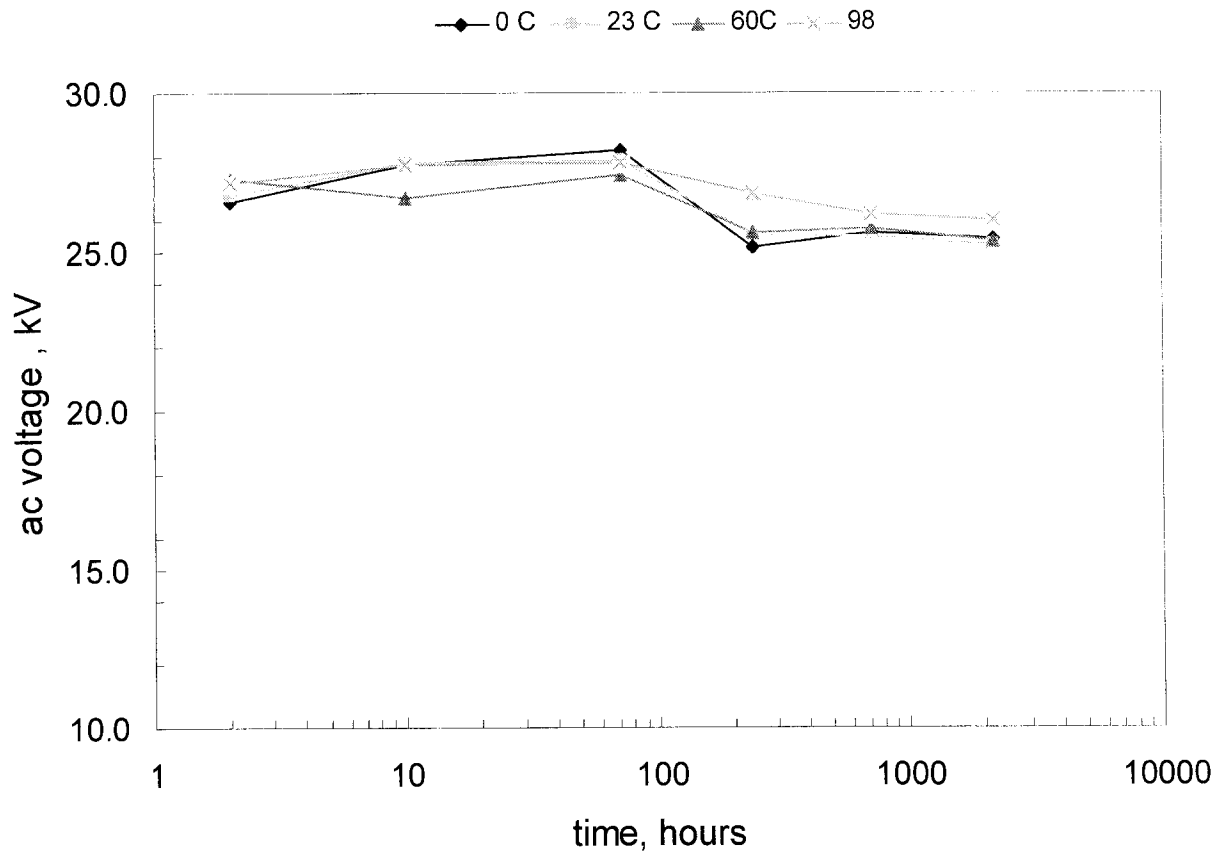


Fig. 5.12: ac flashover voltage of Delrin versus time of immersion in distilled water at 0, 23, 60 and 98 °C.

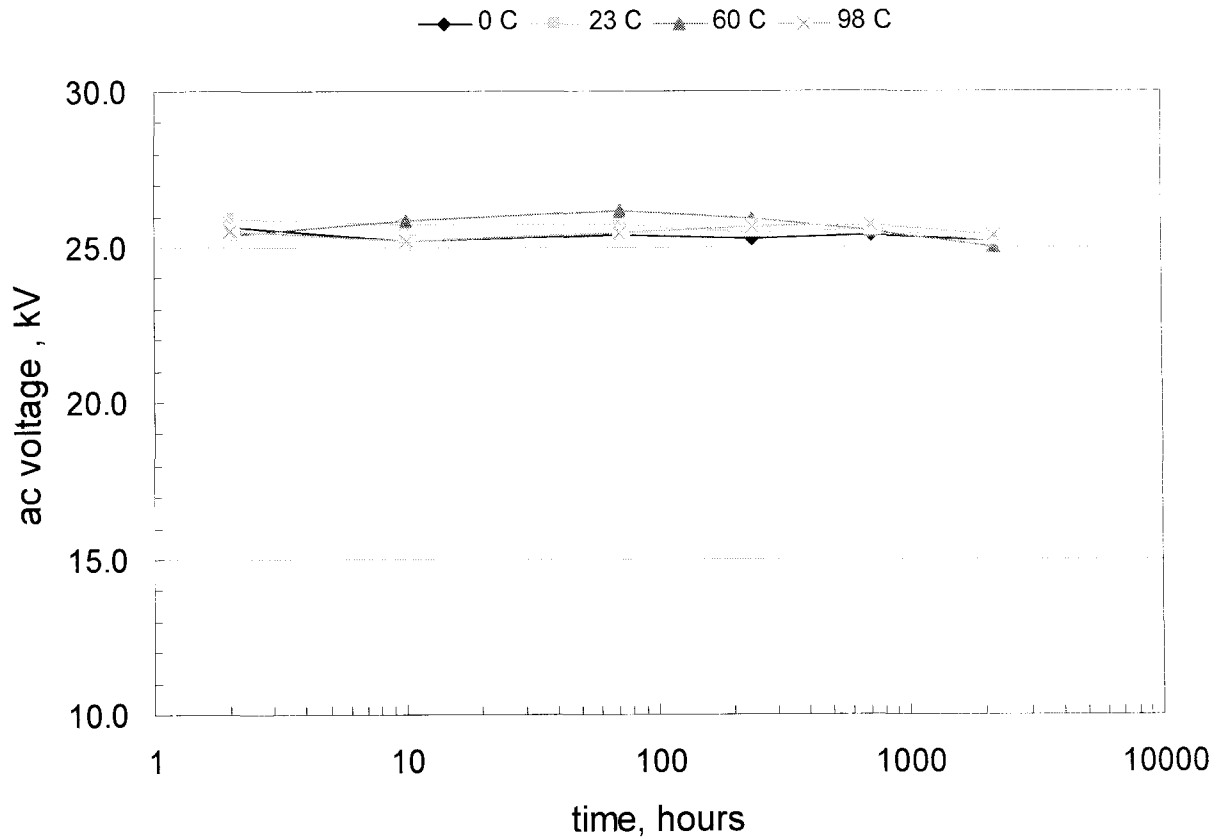


Fig. 5.13: ac flashover voltage of Delrin versus time of immersion in saline solution of 1 mS/cm at 0, 23, 60 and 98 °C.

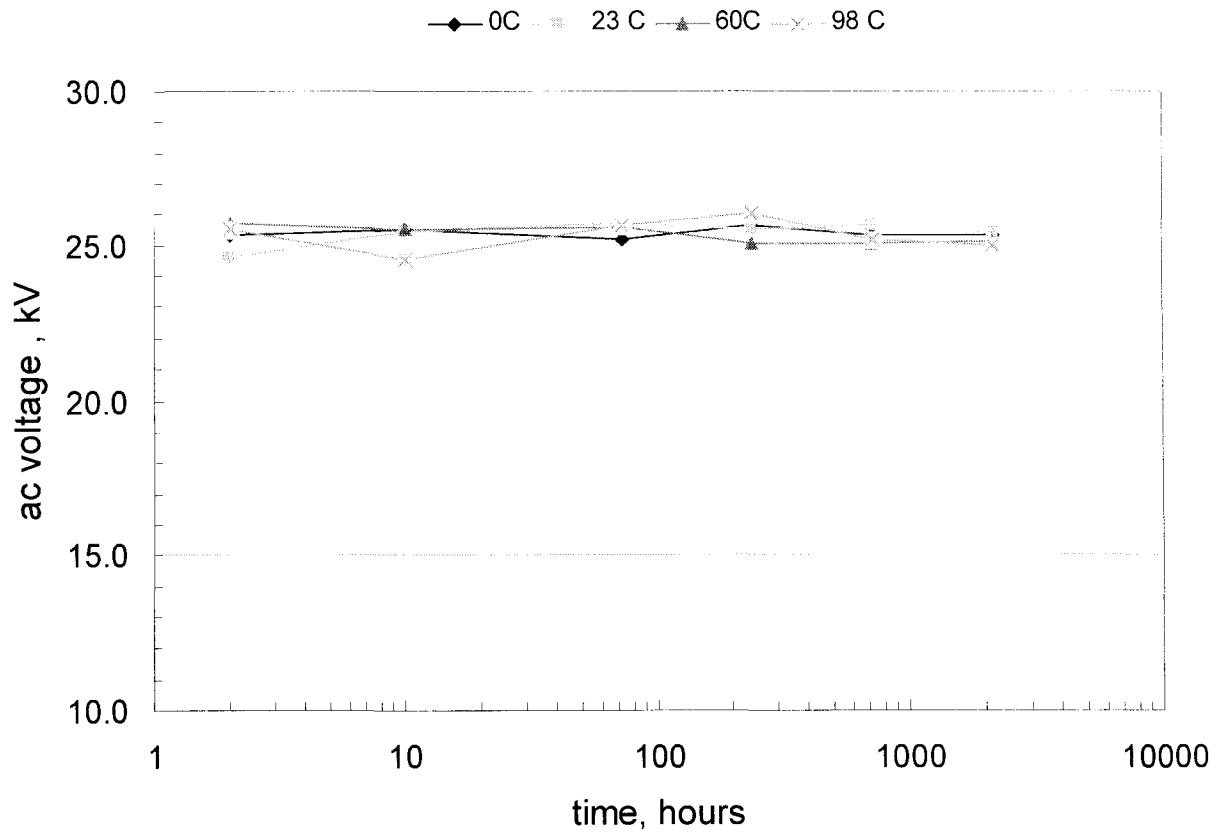


Fig. 5.14: ac flashover voltage of Delrin versus time of immersion in saline solution of 10 mS/cm at 0, 23, 60 and 98 °C.

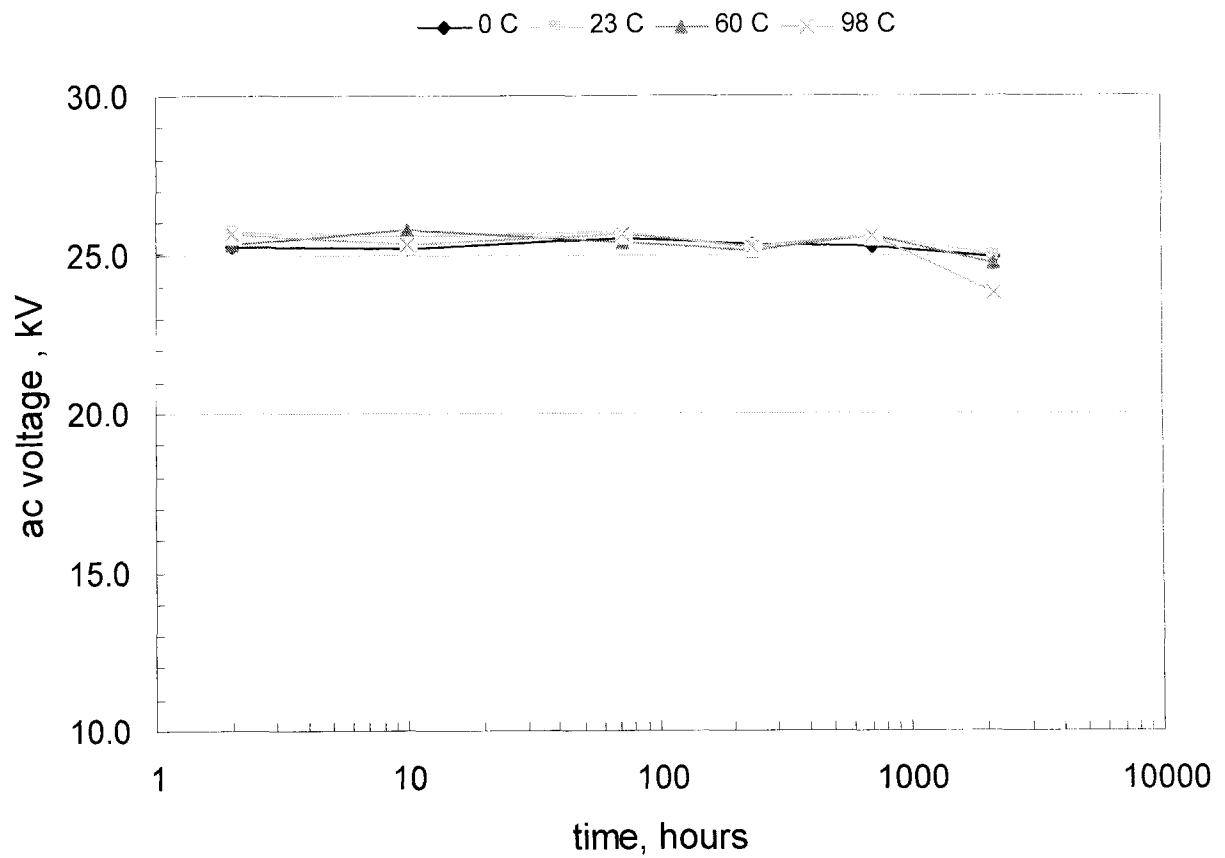


Fig. 5.15: ac flashover voltage of Delrin versus time of immersion in saline solution of 100 mS/cm at 0, 23, 60 and 98 °C.

Chapter 6

6. Recovery of Hydrophobicity in Delrin

6.1 Introduction

In Chapter 4 the reduction of the contact angle of a droplet of water on the surface of Delrin after immersion in different saline solutions and air at different temperatures has been studied. The weight of Delrin and Acetron increased due to the absorption of saline solution on the surface of the specimens, thereby resulting in the observed decrease in the contact angle and therefore loss of hydrophobicity in Delrin. The loss of hydrophobicity could also occur due to oxidation of the polymer surface but this was not the case here. Extended loss of hydrophobicity of an insulation material could result in leakage current and gradual development of dry band arcing. Such discharges produce heat and carbonization of the polymer surface. Carbonization may result in tracking and permanent damage to the insulation [17]. In this chapter, the recovery of hydrophobicity of Delrin after its loss due to immersion in saline solutions for 4600 h is reported and discussed.

6.2 Experimental Method

Cylindrical rods of Delrin measuring 19 mm in diameter were cut to 9.3 ± 0.3 mm length were first immersed in saline solutions of varying conductivity from 0.005 to 100 mS/cm at 0, 23, 60 and 98 °C for 4600 h. Specimens of Delrin were also aged in air at the above temperatures. The contact angle of a sessile droplet of distilled water (0.005 mS/cm), having a volume of 4-5 μ l, on the surface of Delrin was measured on a horizontal surface

with a goniometer [19]. The side surface of each cylindrical specimen was used to avoid the inconsistency in the cut surface. The contact angle decreased from the original value of $82 \pm 2^\circ$ to low values after 4600 h of immersion in saline solutions. The decrease in the contact angle was larger with higher temperatures of saline solutions. Mid salinity solutions of 1-10 mS/cm had the most decrease in the contact angle of Delrin. After removal of the specimens from the saline solutions they were left in air at $23 \pm 3^\circ\text{C}$ and $55 \pm 15\%$ relative humidity for an additional time of up to 4800 h. The recovery of the contact angle and the percentage reduction in the weight due to drying of Delrin specimens were determined. The changes in the weight of the specimen were correlated to the contact angle and hence to the recovery of the hydrophobicity in Delrin. The specimens of Delrin were also subjected to RF discharges for varying duration of time from 10, 15 and 20 minutes. The contact angle decreased sharply from its original value of $82 \pm 2^\circ$ to 74° , 72° and 69° , respectively then after 120 h the contact angle recovered its initial value. The changes that took place in the surface hydrophobicity of Delrin during the recovery process are discussed in the following sections.

6.3 Recovery of the Contact Angle

Figs. 6.1 to 6.4 show the recovery of the contact angle of Delrin as a function of time in air at $23 \pm 3^\circ\text{C}$, for the specimens which were aged in different saline solutions of varying conductivity from 0.005 to 100 mS/cm at $0 \pm 1^\circ\text{C}$, $23 \pm 3^\circ\text{C}$, $60 \pm 2^\circ\text{C}$ and $98 \pm 2^\circ\text{C}$. The Initial values of the contact angle shown in Figs. 6.1 to 6.4 were measured immediately after removal of the Delrin specimens from the saline solutions. The time of recovery lasted up

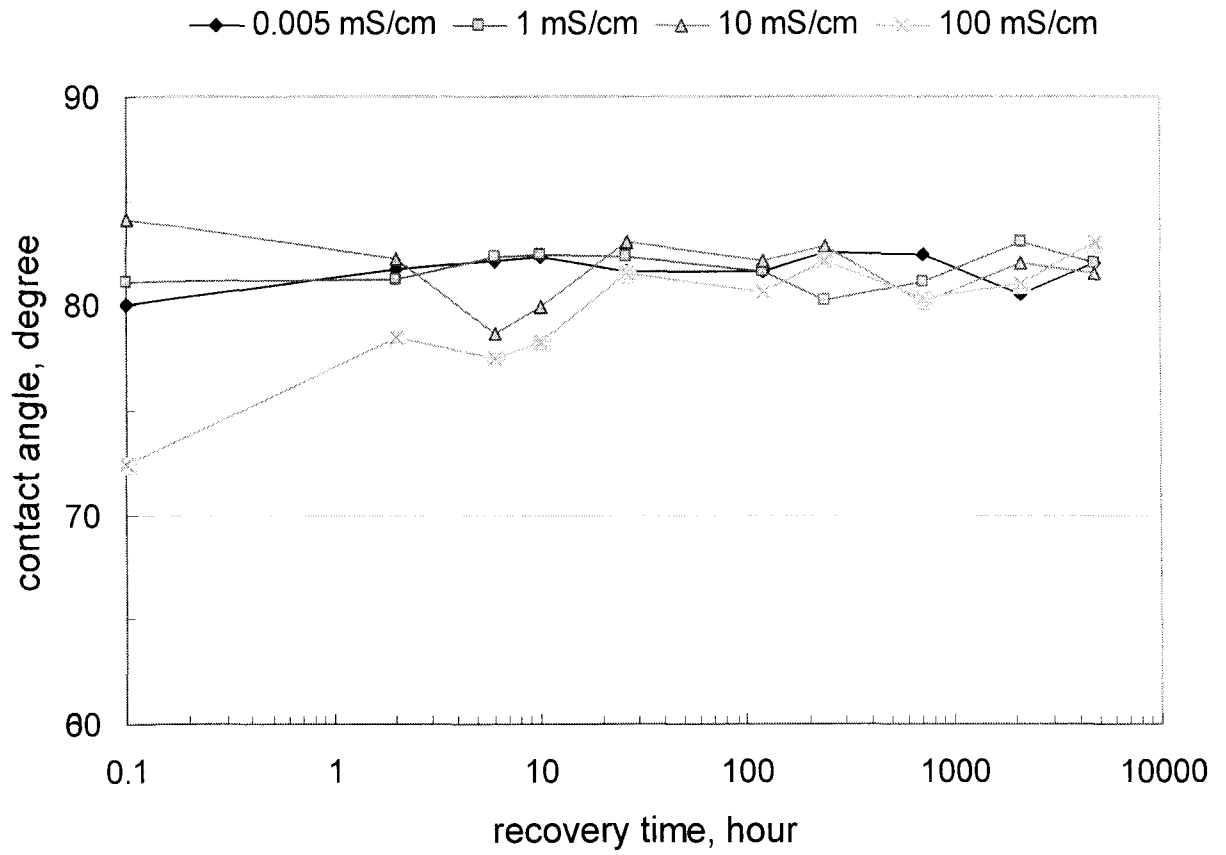


Fig. 6.1: Recovery of the contact angle on Delrin in air at 23 ± 3 °C after immersion in different saline solutions for 4600 h at 0 ± 1 °C

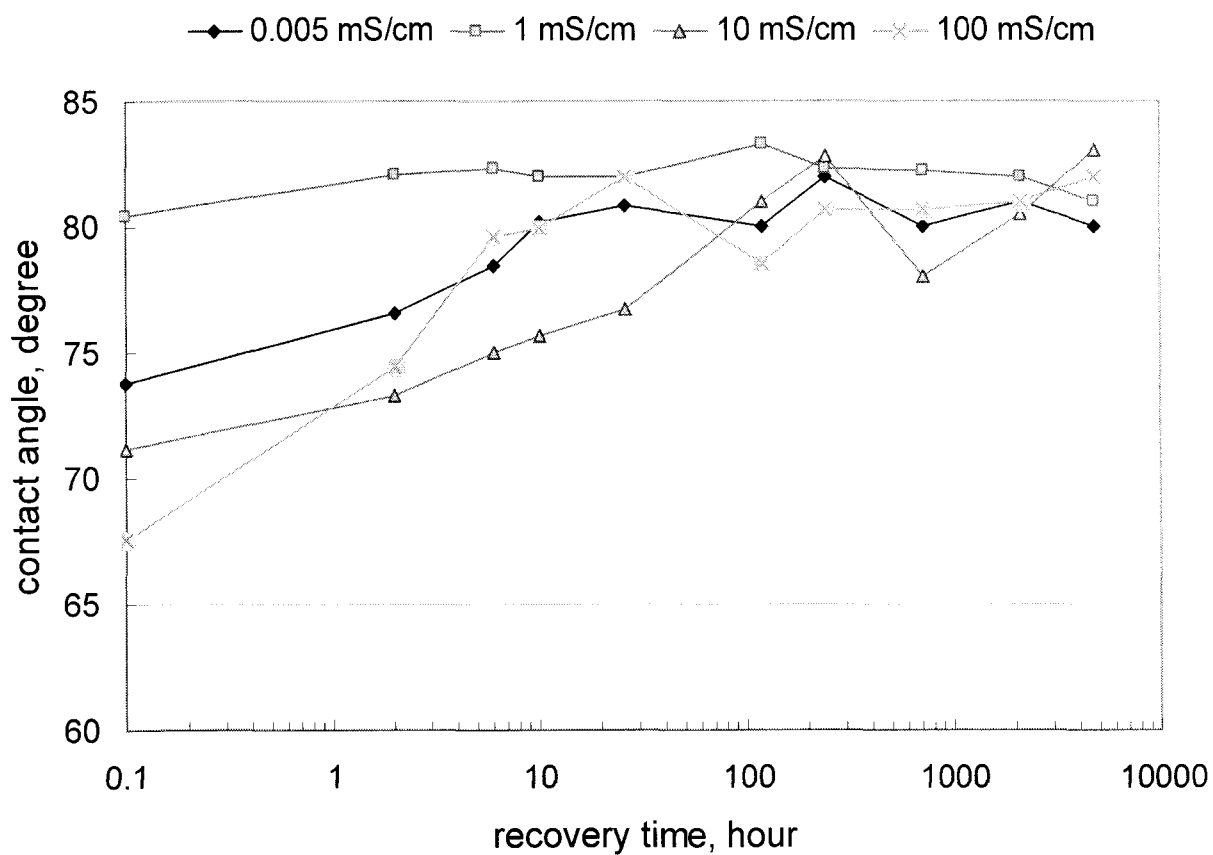


Fig. 6.2: Recovery of the contact angle on Delrin in air at 23 ± 3 °C after immersion in different saline solutions for 4600 h at 23 ± 3 °C

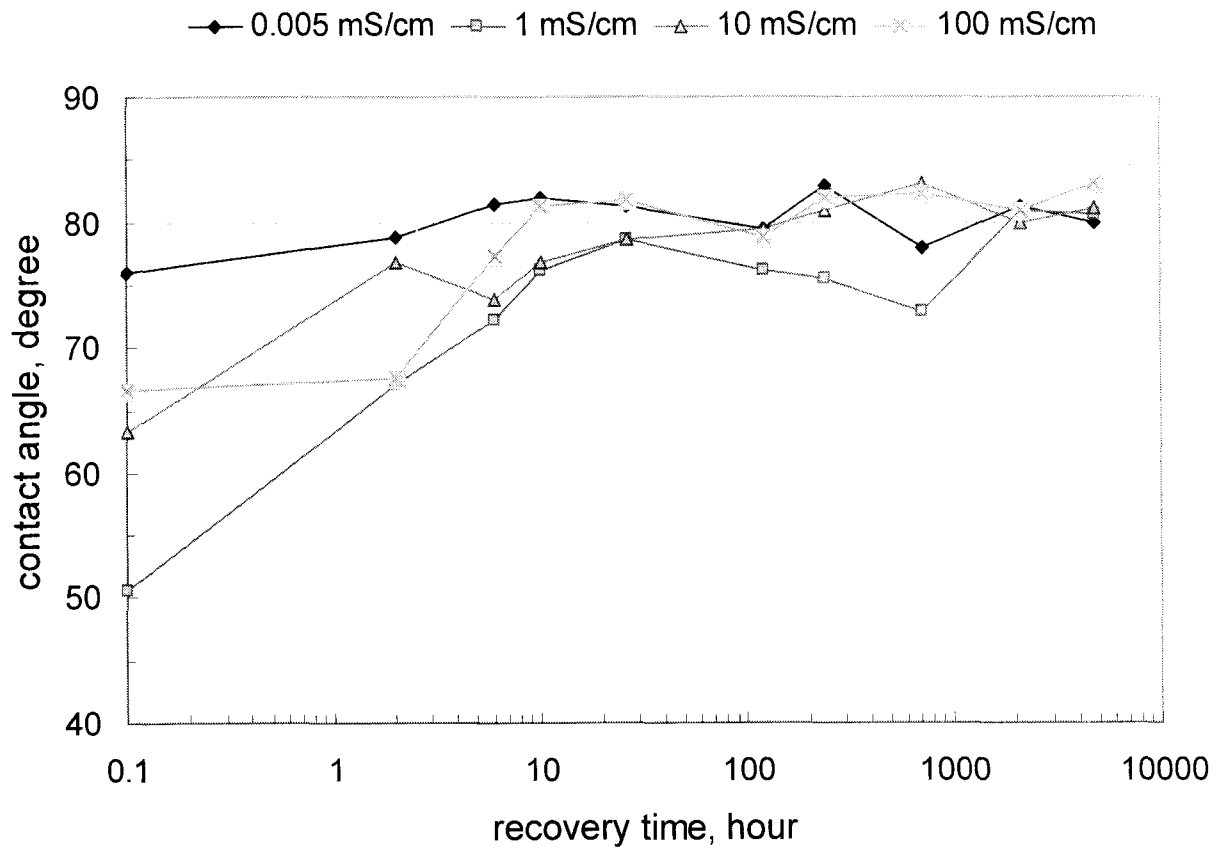


Fig. 6.3: Recovery of the contact angle on Delrin in air at 23 ± 3 °C after immersion in different saline solutions for 4600 h at 60 ± 3 °C

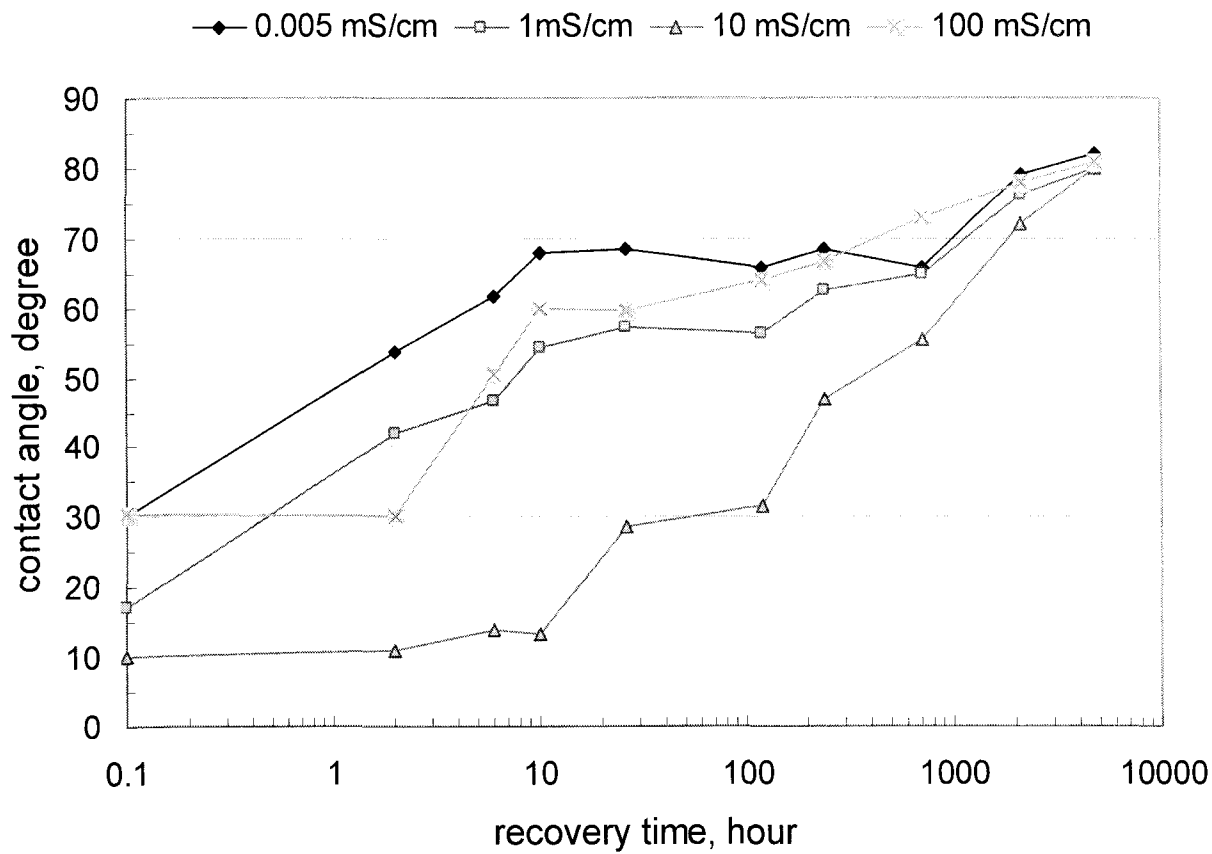


Fig. 6.4: Recovery of the contact angle on Delrin in air at 23 ± 3 °C after immersion in different saline solutions for 4600 h at 98 ± 3 °C

to 4800 h for all the specimens. The contact angle of Delrin specimens that were aged in air at varying temperatures of 0 °C to 98 °C was also measured during recovery as a function of time at 23±3 °C. The slight changes of the contact angle were recovered after 2 h of recovering in air within the above condition.

It may be observed from Fig. 6.1 that the contact angle of Delrin aged at 0±1 °C did not have a considerable decrease and after removal from stress conditions of different salinity solutions the contact angle recovered quickly to its initial value of 82°.

Fig. 6.2 shows the recovery of the contact angle for Delrin specimens aged at 23±3 °C. It may be observed that the contact angle recovered steadily for the conductivity levels of 0.005, 1, 10 and 100 mS/cm from 74, 80, 71 and 68° to the initial value of the contact angle, 82° after 240 h.

Fig. 6.3 shows the recovery of the contact angle for Delrin specimens aged at 60±2 °C in different saline solutions. The contact angle had a more significant decrease compare to 0 and 23 °C. The contact angle recovered from 76, 50, 63 and 66° to the initial value of the contact angle 82° after 2400 h.

It may also be observed from Figs. 6.1 to 6.3 that the rate of recovery of the contact angle was larger, the lower the temperatures of saline solution. This may be due to less absorption of the saline solutions at low temperatures during immersion which subsequently released and evaporated from the surface of Delrin during the recovery.

Fig. 6.4 shows the recovery of the contact angle at room temperature in air for the Delrin specimens aged at 98 ± 2 °C. The recovery of the contact angle took place steadily for all conductivity levels. The recovery rates were slower for 1 and especially for 10mS/cm. This is thought to be due to slower rates of releasing of saline solutions for these specimens.

Fig. 6.5 shows the contact angle as a function of conductivity of the solution on Delrin after 720 h of recovery in air at 23 ± 3 °C and subsequent to aging at different temperatures. It may be observed from Fig. 6.5 that mid salinity solutions of 10mS/cm had a slower contact angle recovery rate. Also, at a fixed conductivity level, the contact angle decreased with increase in temperature. This is thought to be due to enhanced uptake of the saline solutions at high temperatures.

6.4 Reduction of the Weight during Recovery

The percentage (%) decrease in the weight of Delrin specimens during the recovery after aging, in different saline solutions and temperatures was also measured.

Fig. 6.6 shows the percentage decrease in the weight of the Delrin specimens after 4800 h of recovery in air at 23 ± 3 °C and $55 \pm 15\%$ relative humidity levels and as a function of the conductivity of saline solution for different temperatures. These specimens were previously immersed in different saline solutions at different temperatures for 4600 h. It may be observed from Fig. 6.6 that the percentage reduction in weight at a fixed aging temperature increased in mid salinity of 10 mS/cm. At a fixed conductivity level, the

percentage reduction in weight increased with increasing temperature. This is because at a fixed conductivity of the saline solution, the uptake of the saline solution was observed to be higher with higher temperatures. Therefore, the loss of water during the recovery in air is also expected to be higher. A comparison of Figs. 6.5 and 6.6 suggests that the level of the recovered contact angle strongly depends on the amount of water lost from the specimens during the recovery in air.

6.5 Recovery of the contact angle after Exposure to RF Discharges

The specimens of Delrin were subjected to RF discharges for three different durations of 10, 15 and 20 minutes. The contact angle decreased from 82 to 74°, 72° and 69° respectively after the application of RF discharge. These specimens were left in air at 23 ± 3 °C and $52\pm 4\%$ relative humidity level. Fig. 6.7 shows the recovery trend of the contact angle after applying RF discharge to the Delrin specimens. It may be observed from Fig. 6.7 that the contact angle recovered its initial value of 82 for all specimens after 120 h. The shorter the period of the RF discharge application, the faster the recovery rate.

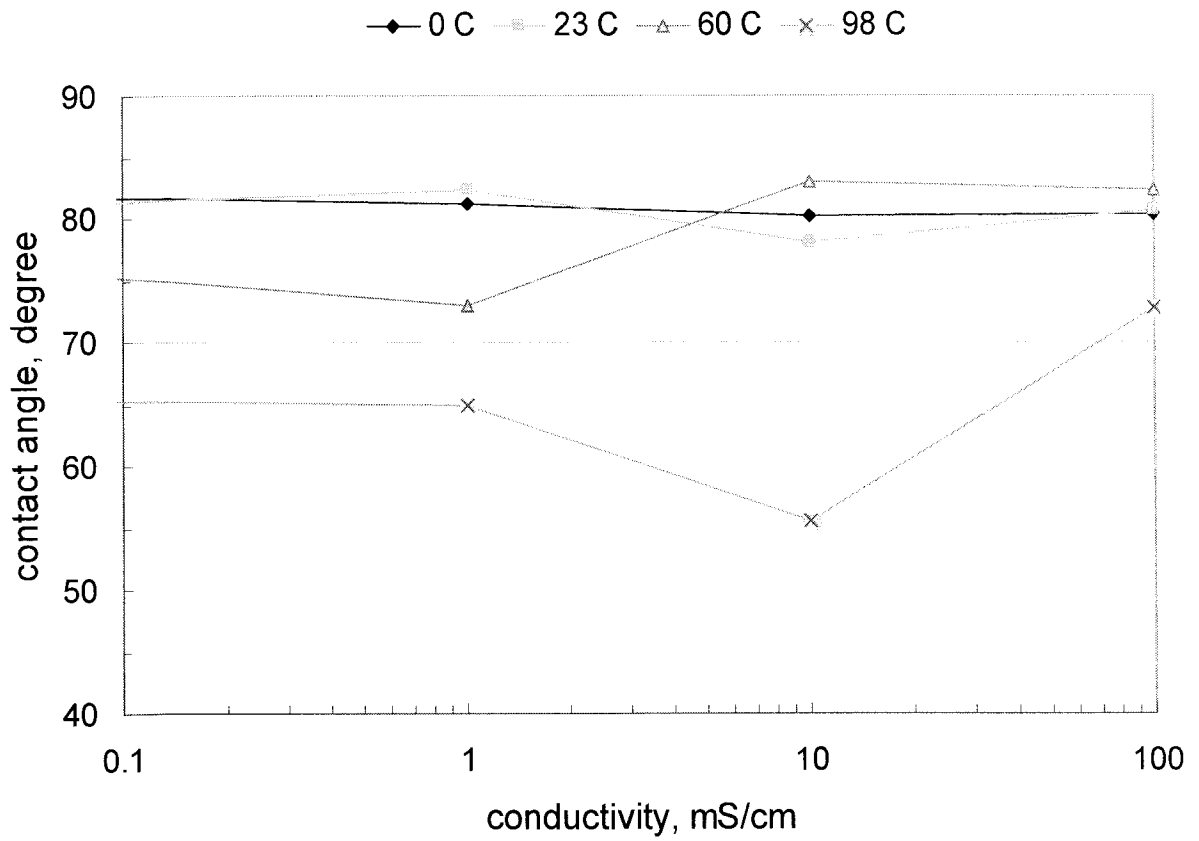


Fig. 6.5: Contact angle on Delrin after 720 h recovery in air at 23 ± 3 °C as a function of the conductivity level of saline solutions at different temperatures.

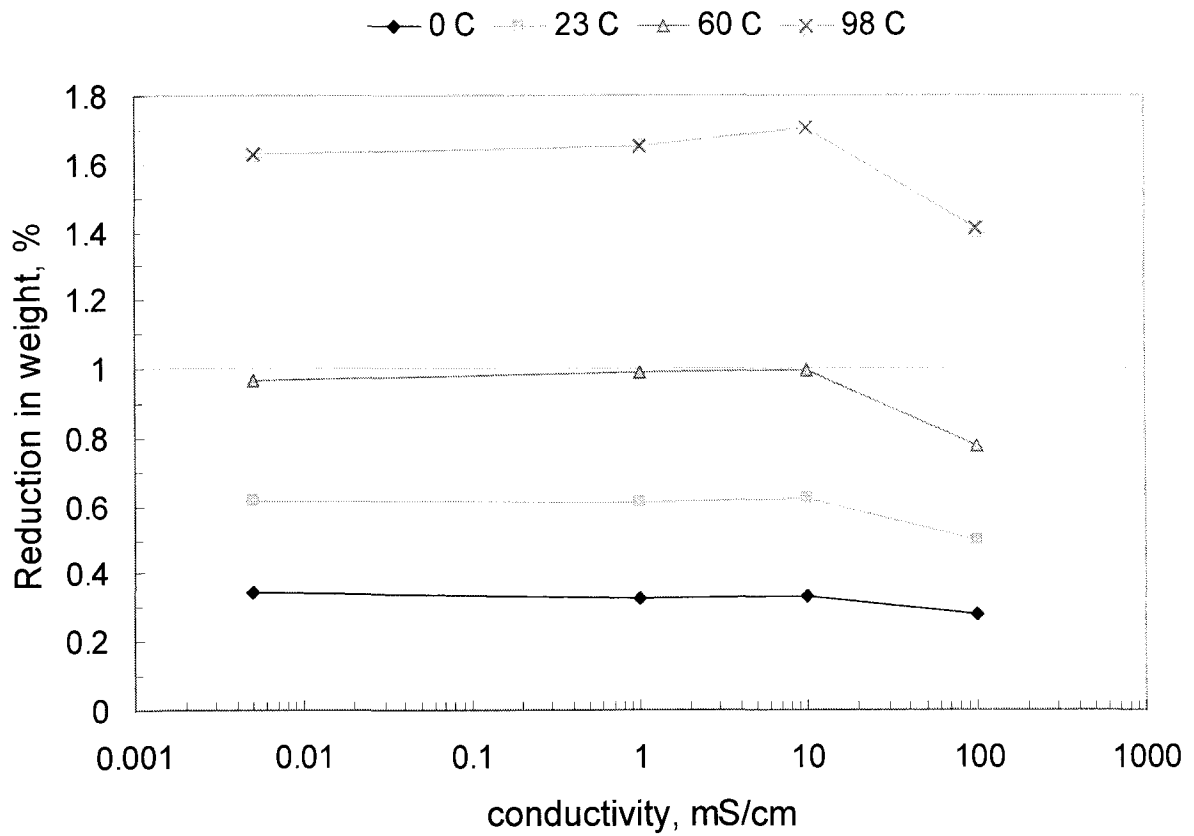


Fig. 6.6: Reduction in weight (%) of Delrin after recovery in air at 23 ± 3 °C for 4800 h as a function of the conductivity level of saline solutions at different temperatures.

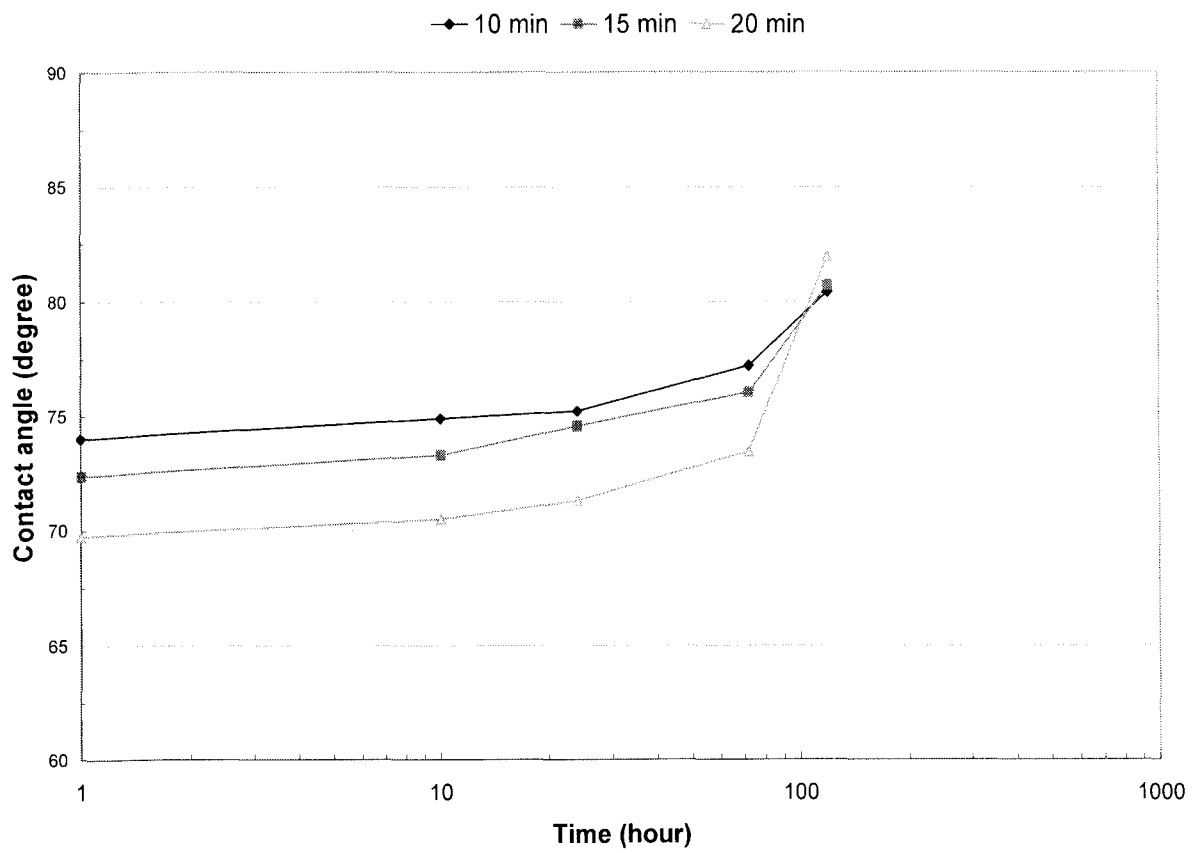


Fig. 6.7: Recovery of the contact angle of Delrin after applying RF discharge for durations of 10, 15 and 20 minutes.

6.6 Recovery of the Surface Free Energy

The surface free energies of Delrin and its components were calculated from the measurement of the contact angle of two liquids with known surface energies, water and methyl iodine. The dispersion and polar components were calculated with a MATLAB program (Appendix A). Figs. 6.8 to 6.11 show the recovery trend of the dispersion component γ_{SD} (J/m^2), the polar component γ_{SH} (J/m^2) and finally the surface free energy of the solid γ_S (J/m^2) vs. recovery time (hours) after immersion in 10 mS/cm saline solution for 4600 h at 0, 23, 60 and 98 °C. As can be seen in these graphs, the change in the value of the surface energy of the solid is due to the change in the polar component of the surface energy γ_{SH} . Fig. 6.11 shows the recovery of the surface free energies of Delrin aged in 10 mS/cm at 98 °C and the decrease in γ_S is more significant than other cases. γ_S decreased from 0.075 J/m^2 to 0.04 J/m^2 during the recovery period. As can be observed in Figs. 6.8 to 6.10, the aged samples recovered to the saturated value of the surface energy of 0.04 J/m^2 much sooner than those in Fig. 6.11 and this is due to the extreme loss of hydrophobicity and subsequent increase of surface energies during aging in 10 mS/cm at 98 °C.

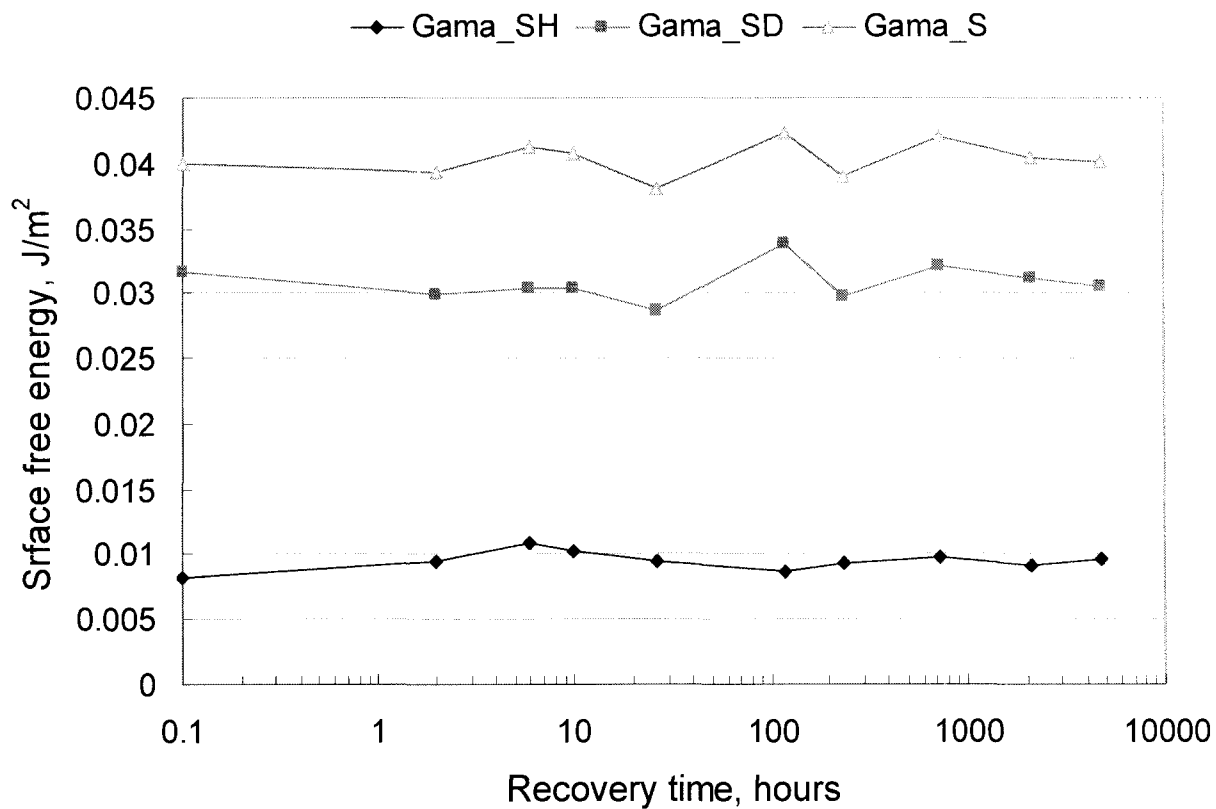


Fig. 6.8: Surface free energy, γ_S (J/m^2) and its polar component, γ_{SH} (J/m^2) and dispersion component, γ_{SD} (J/m^2) during recovery in air at 22 ± 3 °C after aging in 10 mS/cm saline solution at 0 ± 2 °C

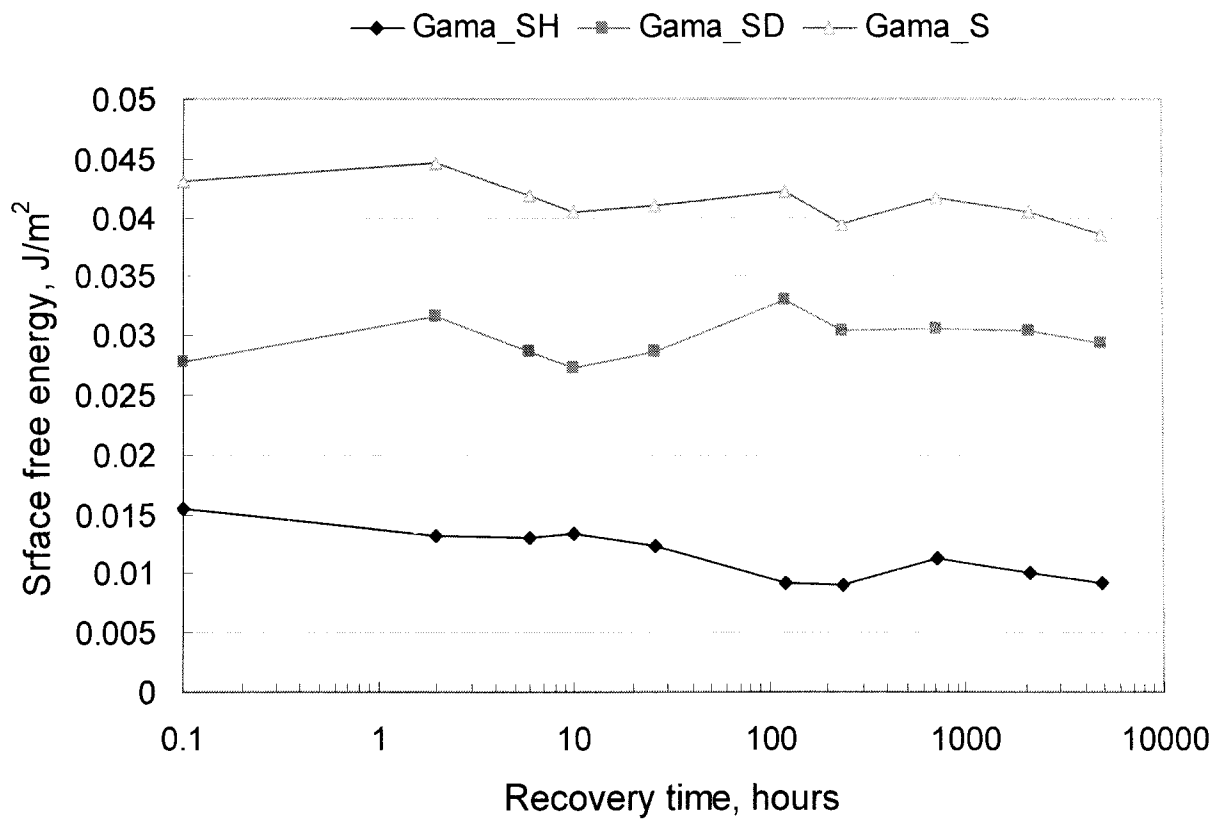


Fig. 6.9: Surface free energy, γ_s (J/m²) and its polar component, γ_{SH} (J/m²) and dispersion component, γ_{SD} (J/m²) during recovery in air at 22±3 °C after aging in 10 mS/cm saline solution at 22±3 °C

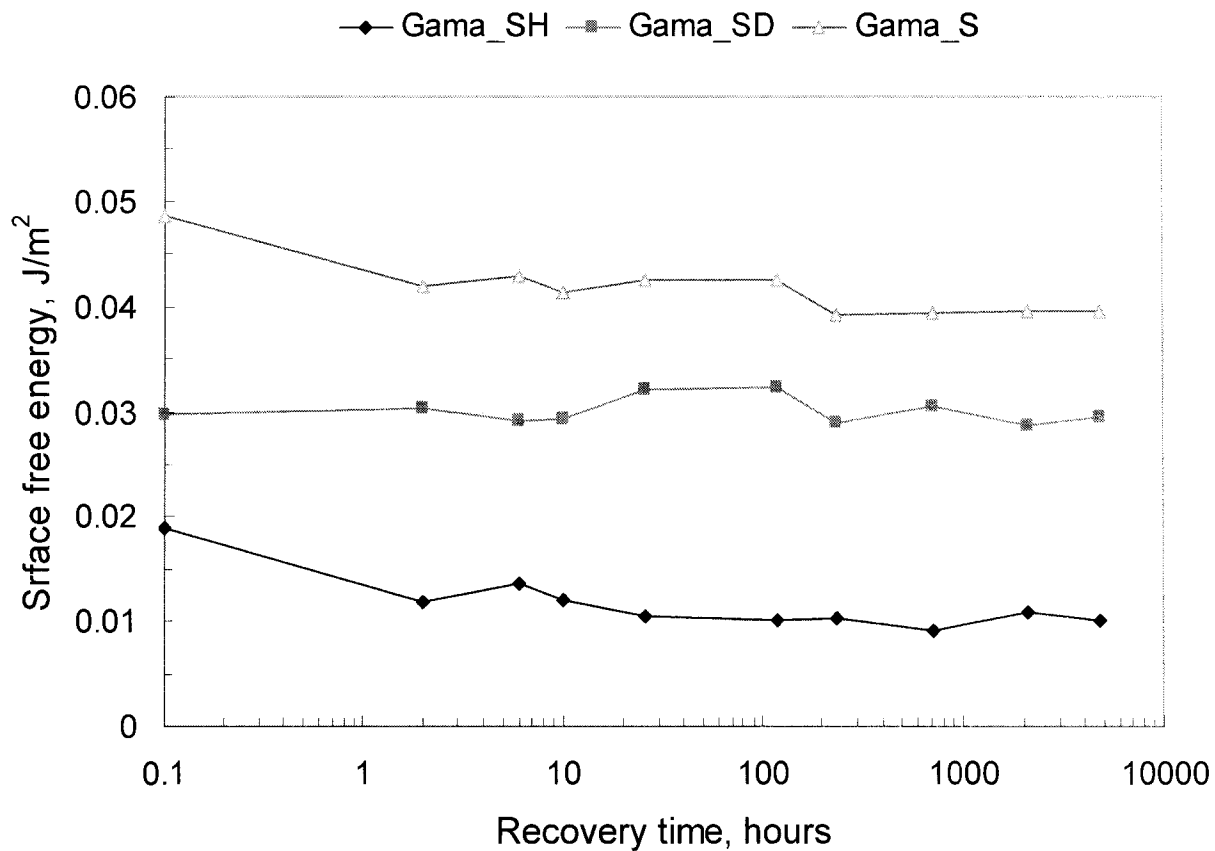


Fig. 6.10: Surface free energy, γ_S (J/m^2) and its polar component, γ_{SH} (J/m^2) and dispersion component, γ_{SD} (J/m^2) during recovery in air at 22 ± 3 °C after aging in 10 mS/cm saline solution at 60 ± 2 °C

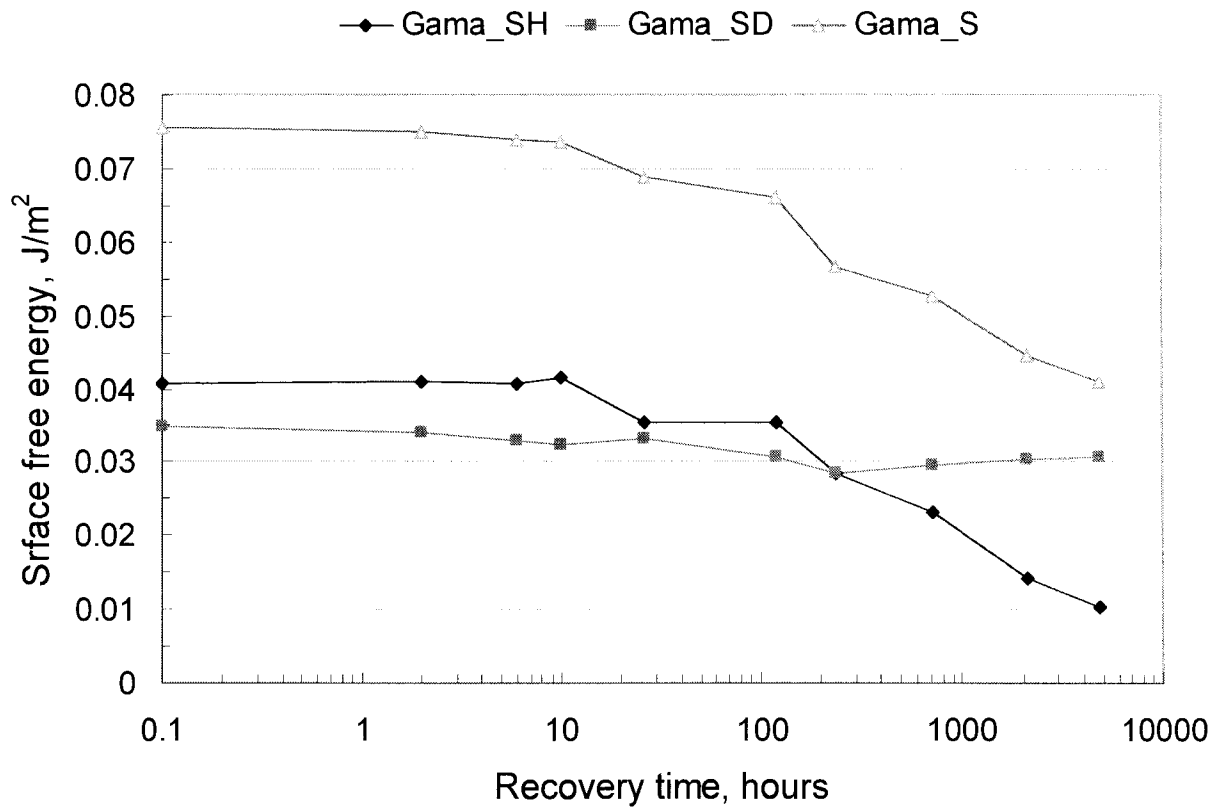


Fig. 6.11: Surface free energy, γ_S (J/m²) and its polar component, γ_{SH} (J/m²) and dispersion component, γ_{SD} (J/m²) during recovery in air at 22 ± 3 °C after aging in 10 mS/cm saline solution at 98 ± 2 °C

Chapter7

7. Conclusion & Suggestions

7.1 Conclusion

7.1.1 Loss of Hydrophobicity:

In the aging process of Delrin, the loss of hydrophobicity depends on the duration of immersion, the salinity of solution and the temperature of the saline solution. With increasing temperature and time of immersion the hydrophobicity of Delrin decreases until there is a complete loss of hydrophobicity to such an extent that the formation of a droplet on the surface is almost impossible. Increasing salinity of the solution up to a certain level contributes to loss of hydrophobicity. The most significant decrease of the contact angle was in 10 mS/cm solution at 98 °C which was less than 20°. The loss of hydrophobicity was due to the increased uptake of water and weakening of C-O bonds. The loss of hydrophobicity due to oxidation of Delrin could not be observed by ATR spectra. The microphotographs taken by Scanning Electron Microscopy have shown more details of surface after immersion in different salinities at 98 °C after 4600 h. The contact angle decreased with increasing surface roughness. The surface free energies of Delrin increased with the decreasing contact angle.

7.1.2 Effect of water salinity, temperature and duration of immersion on dc and ac flashover voltage:

This study shows that the dc flashover voltage of Delrin follows the same trend of decrease as that of the contact angle. Increasing temperature, longer duration of

immersion and increasing the salinity up to certain level causes the dc flashover voltage to decrease. Despite the above stress condition, the ac flashover voltage did not change and maintained a steady value of 25-26 kV.

7.1.3 Recovery of Hydrophobicity:

After the removal of Delrin from the stress conditions the recovery of the hydrophobicity began. In all cases the contact angle of Delrin recovered to its initial value of 82° but the period of recovery was different for different salinities and temperatures. The higher the temperature, the longer the period of recovery. The mid-salinity solution of 10 mS/cm had the longest recovery period since the contact angle had the largest decrease. In this case, the contact angle recovered from 11° to its initial value within 4800 h. In summary the recovery was longer the greater the loss of hydrophobicity.

The recovery of the contact angle after the application of RF discharge was also studied. The longer the period of RF application, the larger is the decrease in the contact angle. Therefore, the recovery is slower when the RF application period is longer. After 120 h the contact angle completely recovered to its initial value for all the durations used of RF application.

7.2 Suggestions for Future Research

The hydrophobicity and dc/ac flashover voltage of Delrin have been studied at various temperatures and conductivity levels. However, there are many aspects of hydrophobic

behavior of acetal, such as Delrin that require further investigation. Therefore, a few suggestions are made here for future research.

1. Ultra Violet radiation is one of the major causes of surface degradation of polymeric materials in outdoor applications. Delrin as an acetal resin is sensitive to UV radiation. To strengthen Delrin against UV radiation different fillings and additives have been used which might effect the dielectric strength or hydrophobic behavior of Delrin as a high voltage insulating material. Therefore, the study of the hydrophobicity of Delrin and Delrin with UV protective additives under stress of UV radiation is recommended for future research.

2. Delrin has metal-like mechanical characteristics and has a very high wear resistance. The copolymer of Acetal resin, Acetron has more chemical resistance than Delrin. In the case of surface degradation under stress of salinity, high temperature or UV radiation, based on the mechanical characteristics, Delrin or Acetron could be used as the core of high voltage insulators. The possibility of using any high hydrophobic material like silicone rubber as coating for Delrin or Acetron as a high voltage insulator should also be considered.

3. Injection molding and extrusion are the most common methods for the processing of Delrin. The quality of the surface of Delrin is partially dependent on the quality of these processes. Studying injection molding and extrusion and their effects on the surface properties of Delrin should also be considered for future research.

4. Oxidation of polymer insulation under the influence of ac field in service conditions has been cited as a reason for the initiation and growth of water trees by many authors [19]. Water treeing causes accelerated aging in underground cables, and is also considered to be a reason for the loss of hydrophobicity of the polymer surface due to the formation of hydrophilic compounds such as ketones, aldehydes and carboxylates (C=O). Despite the loss of hydrophobicity, no oxidation was found in Delrin, although proof of this behavior is still required.

References

- [1] J. S. T. Looms, "Insulators for high Voltages", Peter Peregrinus Ltd., London, UK, 1988.
- [2] S. Wu, "Polymer Interface and Adhesion", Marcel Dekker Inc., 1992.
- [3] S. H. Kim, "Electrical Performance and Surface Analysis of RTV Silicone Rubber Coatings for HV Outdoor Insulators", Ph. D Dissertation, University of Windsor, Windsor Ontario, Canada, 1992.
- [4] H. Z. Syed and R. Hackam "Effects of Water Salinity, Electrical Stress and Temperature On the AC and DC Flashover Voltages of Polytetraflouroethylene" Proc. IEEE Electrical Insulation Conference & Electrical Manufacturing & Coil Winding Conference, Cincinnati, October 16-18, 2001, pp.23-27
- [5] Dupont Design Guide-Module III, Delrin Acetal resin
- [6] Quadrant Engineering Plastic Products Data Sheet, Acetron GP and Delrin Quadrant EPP, 2120 Fairmont Ave. P. O. Box 14235 , Reading , PA 19612-4235
- [7] E. A. Showaib and M. G. Wyzgoski, "Effect of stabilizer on fatigue resistance of a PolyOxyMethylene (Acetal) copolymer", Journal of Materials science, No. 37 pp.1895-1905, 2002.
- [8] T. Tokoro and R. Hackam, "Effects of Water Salinity, Electrical Stress and Temperature On the Hyrdophobicity of Nylon", Conference on Electrical Insulation and Dielectric Phenomena, Virginia Beach, VA, pp 290-293, 1995.
- [9] T. Tokoro and R. Hackam, "Recovery of hydrophobicity of Nylon aged by Heat and Saline Water", IEEE International Symp. On Electrical insulation, pp.283-286, 1996.

- [10] S. H. Kim, E. A. Cherney and R. Hackam, "Hydrophobicity Behaviour of Insulators Coated with RTV Silicone Rubber", IEEE Transactions on Electrical Insulation, Vol. 27, No. 3, pp.610-622, June 1992.
- [11] S. M. Gubanski and A. E. Vlastos, "Wettability of Naturally Aged Silicone and EPDM Composite Insulators", IEEE Transactions on Power Delivery, Vol. 5, No. 3, pp.1527-1535, 1990.
- [12] S. Wu, "Polymer Interface and Adhesion", Marcel Dekker Inc., 1992.
- [13] K.L. Mittal, "Contact Angle, Wettability and Adhesion", VSP BV, P.O Box346, 3700 AH Zeist, The Netherlands, 1993.
- [14] J. Israelachvili, "Intermolecular & Surface Forces" 2nd Edition, Academic Press Ltd., London, UK,1992.
- [15] S. H. Kim, E. A. Cherney and R. Hackam, "Hydrophobicity Behavior of Insulators Coated with RTV Silicone Rubber", IEEE International Conference on Properties and Applications of Dielectric Materials, pp.972-976, 1991.
- [16] M. Ishii and M. Komatsubara, "Hydrophobicity of Organic Insulating Materials", IEEE Conference on Electrical Insulation and Dielectric Phenomena, pp.134-139, 1998.
- [17] H. Deng and R. Hackam, "Hydrophobic Property of XLPE Filled with Calcium Carbonate", IEEE Transactions on Dielectrics and Electrical Insulation, Vol. 3, No. 4, pp.577-586, August 1996
- [18] R. S. Gorur, J. W. Chang and O.G. Amburgey, "Surface Hydrophobicity of Polymers Used for Outdoor Insulation", IEEE Transactions on Power Delivery, Vol. 5, No. 4, pp.1923-1931, November 1990.

- [19] M. Ashraf Khan "Surface Properties of High Density Polyethylene and Cross-linked Polyethylene", M.A.Sc Thesis, University of Windsor, Windsor, Ontario, Canada, 1998.
- [20] H.Z. Syed, "Aging characteristics of Polytetrafluoroethylene (PTFE)", M.A.Sc Thesis, University of Windsor, Windsor, Ontario, Canada, 2002.
- [21] S. H. Kim, "Electrical Performance and Surface Analysis of RTV Silicone Rubber Coatings for HV Outdoor Insulators", Ph. D Dissertation, University of Windsor, Windsor Ontario, Canada 1992.
- [22] H. Deng, "Electrical Performance and of RTV Silicone Rubber Coatings for HV Outdoor Insulators", M.A.Sc Thesis, University of Windsor, Windsor, Ontario, Canada, 1995.
- [23] U. Kalteborn, J. Kindersberger, R Barsch and H. Jahn, "On the Electrical Performance of Polymeric Insulating Materials in a Rotating-Wheel-Dip-Test", IEEE Conference on Electrical Insulation and Dielectric Phenomena, pp.398-401, 1997.
- [24] H. J. Kloes and D. Koenig, "Thin Solid Silicone Layers on the Surface of Model Insulators made of Resin and their Influence on the Wet Surface Performance under High Electrical Stress", IEEE Conference on Electrical Insulation and Dielectric Phenomena, pp 121-124, 1997.
- [25] A. W. Adamson and A. P. Gast, "Physical Chemistry of Surfaces", John Wiley & Sons, Inc., pp 362-366 and 589, 6th edition , 1997.

- [26] R. S. Gorur, "Research into Polymeric Materials for High Voltage Outdoor Insulators", Ph. D. Dissertation, University of Windsor, Windsor, Ontario, Canada, 1986.
- [27] P. J. Goddew, "Electron Microscopy and Analysis", Wykeham Publications (London) Ltd., 1975.
- [28] E. F. Steenis and F. H. Kreuger, "Water Treeing in Polyethylene Cables", IEEE Transactions on Electrical Insulation, vol. 25, no.5, 1990, pp.989-1028.
- [29] R. Patsch, "Electrical and Water Treeing- A Chairman's View", IEEE Transactions on Electrical Insulation, Vol. 27, No. 3, pp.532-542, June 1992.
- [30] J. Ross and J. Smith, "Composition and Growth of Water Trees in XLPE", IEEE Transactions on Electrical Insulation, Vol. 27, No. 3, pp.519-531, June 1992.
- [31] N. L. Alpert, William E. Keiser and Herman A. Szymanski, "IR – Theory and Practice of Infrared Spectroscopy", Plenum Press, New York , 1970.
- [32] J. E. Stewart, "Infrared Spectroscopy-Experimental Methods and Techniques", Marcel Dekker Inc., New York, pp.302-457, 1970.
- [33] T. Zhao and R. Allen Bernstorff, "Aging Tests of Polymeric Housing Materials for Non-Ceramic Insulators", IEEE Electrical Insulation Magazine, Vol. 14, No. 2, pp.26-33, March/April, 1998.
- [34] R. Zbinden, "Infrared Spectroscopy of High Polymers", Academic Press Inc., 1964.
- [35] R. A. Smith, F. E. Jones and R. P. Chasmer, "The Detection and Measurement of Infrared Radiation", Oxford University Press, Amen House, London, UK, 1958.

- [36] W. Brugel, "An Introduction to Infrared Spectroscopy", Methuen and Company, 1962.
- [37] P. R. Griffiths and J. A. de Haseth, "Fourier Transform Infrared Spectroscopy", John Wiley and Sons, 1986.
- [38] F. Sheinman, "An Introduction to Spectroscopic Methods for Identification of Organic Compounds", Pergamon Press Ltd., 1970.
- [39] John R. Ferraro and Louis J. Basile, "Fourier Transform Infrared Spectroscopy, Vol-II", Academic Press Inc., 1979.
- [40] C. Hall, "Polymer Materials", Macmillan, 1980.
- [41] F.M Clark, "Insulating Materials for Design and Engineering Practice", John Wiley and Sons, Inc., pp.466-505, 1962.
- [42] T. Tokoro and R. Hackam, "Loss and Recovery of Hydrophobicity, Surface Energies, Diffusion Coefficients and Activation Energy of Nylon", IEEE Transaction on Dielectrics and Electrical Insulation, Vol. 6, No.5, pp.754-761 October 1999.
- [43] T. Tokoro and R. Hackam, "Loss and Recovery of Hydrophobicity, Surface Energy of HTV Silicone Rubber", IEEE Transaction on Dielectrics and Electrical Insulation, Vol. 8, No. 6, pp.1088-1097, December 2001.
- [44] S. Pelissou and H. J. Wintle, "Water Content of XLPE Cable Insulation", IEEE International Symposium on Electrical Insulation, pp.165-168, 1992.
- [45] J. Crank, "The Mathematics of Diffusion", Oxford University Press, Ely House, London, UK, 1957.

- [46] H. Zhang and R. Hackam, "Surface Resistance of PVC in the Presence of Salt-Fog", IEEE Conference on Electrical Insulation and Dielectric Phenomena, pp.137-141, 1997.
- [47] J.C. Anderson, "Dielectrics", Reinhold Publishing Corporation, New York (1964).
- [48] R. Saums., "Materials for Electrical Insulating and Dielectric Functions", Hayden Book Company, 1978.
- [49] L. A. Dissado and J. C. Fothergill, "Electrical degradation and Breakdown in Polymers", IEE Materials and Devices Series 9, 1992.
- [50] E. Kuffel, W. S. Zaengl and J. Kuffel, "High Voltage Engineering Fundamentals", Second Edition, Newnes, 2000.
- [51] N. Klein, L. Marton, "Advanced Electronics & Electron Physics" Vol. 26 Academic Press, New York, 1969.
- [52] H. Phan, "Analysis of Polymers using Attenuated Total Reflectance FTIR Spectroscopy" MIDAC Corporation, application notes, AP-108.
- [53] K. C. Kao, "Some electromechanical effects on dielectrics" pp.629-632 British Journal of Applied Physics, Vol. 12, November 1961
- [54] K. H. Stark and C. G. Garton, "Nature" 176, p.1225, 1955

Appendix A

Calculation of surface energy component

Known parameters [42]:

$$\gamma_{L(\text{water})} = 72.8 \times 10^{-3} \text{ J/m}^2$$

$$\gamma_{LD(\text{water})} = 22.1 \times 10^{-3} \text{ J/m}^2$$

$$\gamma_{LH(\text{water})} = 50.7 \times 10^{-3} \text{ J/m}^2$$

$$\gamma_{L(\text{methylene iodide})} = 50.8 \times 10^{-3} \text{ J/m}^2$$

$$\gamma_{LD(\text{methylene iodide})} = 44.1 \times 10^{-3} \text{ J/m}^2$$

$$\gamma_{LH(\text{methylene iodide})} = 6.7 \times 10^{-3} \text{ J/m}^2$$

$$\theta_W = 82^\circ$$

$$\theta_M = 45^\circ$$

$$\cos\theta(\text{water}) = 0.139$$

$$\cos\theta(\text{methylene iodide}) = 0.707$$

A MATLAB code has been written to calculate γ_{SD} and γ_{SH} . The results are as follows:

```
%how to calculate the surface energy of Delrin
%GamaL (water)= 72.8 x 10-3 J/m2
%GamaL (methylene iodide )= 50.8 x 10-3 J/m2
%GamaLD(water)= 22.1 x 10-3 J/m2
%GamaLD(methylene iodide)= 44.1 x 10-3 J/m2
%GamaLH(water) = 50.7 x 10-3 J/m2
%GamaLH(methylene iodide) = 6.7 x 10-3 J/m2
%
%tetaW(contact angle for water)= 82o
%tetaM(contact angle for water)= 45o
%Cos(tetaW) (for water)= 0.139
%Cos(tetaM) (for methylene iodide)= 0.707
%Water parameters:
tetaDeg1 = 82
teta1 = tetaDeg1*pi/ 180
GamaL1 = 72.8e-3
GamaLD1 = 22.1e-3
GamaLH1 = 50.7e-3
%Methyl Iodin parameters:
tetaDeg2 = 45
teta2 = tetaDeg2*pi/ 180
GamaL2 = 50.8e-3
GamaLD2 = 44.1e-3
GamaLH2 = 6.7e-3
%calculating parameters for equations involve surface energy
c1 =GamaL1*(1+ cos(teta1))
c2 =GamaL2*(1+ cos(teta2))
A1 = 4*(GamaLD1 + GamaLH1) - c1
```

```

B1 = 4*GamaLD1*GamaLH1 - (c1*GamaLH1)
C1 = 4*GamaLD1*GamaLH1 - (c1*GamaLD1)
D1 = c1*GamaLD1*GamaLH1
A2 = 4*(GamaLD2 + GamaLH2) - c2
B2 = 4*GamaLD2*GamaLH2 - (c2*GamaLH2)
C2 = 4*GamaLD2*GamaLH2 - (c2*GamaLD2)
D2 = c2*GamaLD2*GamaLH2
%defining the polynominal coefficient to calculate x1(GammaSD) and
%y1(GamaSH) and then GamaL=GamaSD+GamaSH
p1 = (A1*B2 - A2*B1)
p2 = A2*D1 + B2*C1 - (C2*B1 + D2*A1)
p3 = C2*D1 - D2*C1
P1 = [p1 p2 p3]
x1 = roots(P1)
hx1 = D1 - B1*x1
hx2 = C1 + A1*x1
y1 = hx1./hx2
GamaL = x1 + y1

```

Appendix B

List of different grades of Delrin prepared by DuPont
(<http://plastics.dupont.com>)

Extrusion Resins

<u>Delrin® 150 NC010 (IS</u>	High Viscosity Extrusion Acetal
------------------------------	---------------------------------

General Purpose Resins

<u>Delrin® 100P NC010 (ASTM)</u>	High Viscosity Acetal
<u>Delrin® 100P NC010 (ISO)</u>	High Viscosity Acetal
<u>Delrin® 111P NC010 (ASTM)</u>	High Viscosity Acetal, Enhanced Crystallization
<u>Delrin® 111P NC010 (ISO)</u>	High Viscosity Acetal, Enhanced Crystallization
<u>Delrin® 1260 NC010 (ISO)</u>	Low Viscosity Acetal Copolymer
<u>Delrin® 311DP NC010 (ISO)</u>	Medium-high Viscosity Acetal, Enhanced Dimensional Stability and Productivity
<u>Delrin® 460 NC010 (IS</u>	Medium Viscosity Acetal Copolymer
<u>Delrin® 500P NC010 (ASTM)</u>	Medium Viscosity Acetal
<u>Delrin® 500P NC010 (ISO)</u>	Medium Viscosity Acetal
<u>Delrin® 511P NC010 (ASTM)</u>	Medium Viscosity Acetal, Enhanced Crystallization
<u>Delrin® 511P NC010 (ISO)</u>	Medium Viscosity Acetal, Enhanced Crystallization
<u>Delrin® 900P NC010 (ASTM)</u>	Low Viscosity Acetal
<u>Delrin® 900P NC010 (ISO)</u>	Low Viscosity Acetal
<u>Delrin® 911P NC010 (ASTM)</u>	Low Viscosity Acetal, Enhanced Crystallization
<u>Delrin® 911P NC010 (ISO)</u>	Low Viscosity Acetal, Enhanced Crystallization

Low Warp Resins

<u>Delrin® DBR180 NC0C (ISO)</u>	Medium-high Viscosity Acetal Bridge Resin
<u>Delrin® DBR80 NC00C (ISO)</u>	High Viscosity Modified Acetal Resin

Low Wear and Friction Resins

<u>Delrin® 100AL NC010 (ISO)</u>	Lubricated, Moderate Flow Acetal
<u>Delrin® 100KM NC000 (ISO)</u>	Acetal Resin with Outstanding Abrasion Resistance
<u>Delrin® 500AF (ASTM)</u>	20% Teflon® PTFE Fiber in Acetal
<u>Delrin® 500AF (ISO)</u>	20% Teflon® PTFE Fiber in Acetal
<u>Delrin® 500AL NC010 (ASTM)</u>	Lubricated, Moderate Flow Acetal
<u>Delrin® 500AL NC010 (ISO)</u>	Lubricated, Moderate Flow Acetal
<u>Delrin® 500CL NC010 (ASTM)</u>	Chemically Lubricated, Medium Flow Acetal
<u>Delrin® 500CL NC010 (ISO)</u>	Chemically Lubricated, Medium Flow Acetal
<u>Delrin® 500TL NC010 (ASTM)</u>	1.5% Teflon® PTFE Micropowder in Acetal
<u>Delrin® 500TL NC010 (ISO)</u>	1.5% Teflon® PTFE Micropowder in Acetal
<u>Delrin® 511S2 NC010</u>	Medium Viscosity Acetal with 2% Silicone Oil
<u>Delrin® 520MP NC010 (ASTM)</u>	20% Teflon® PTFE Micropowder in Acetal
<u>Delrin® 520MP NC010 (ISO)</u>	20% Teflon® PTFE Micropowder in Acetal
<u>Delrin® 911AL NC010 (ISO)</u>	Lubricated Acetal Resin For Dimensionally Stable Parts
<u>Delrin® 911AL NC010 (ISO)</u>	Lubricated Acetal Resin For Dimensionally Stable Parts
<u>Delrin® DE20055 NC0 (ISO)</u>	Lubricated Medium Viscosity Acetal With Teflon® PTFE Micropowder

Toughened Resins

<u>Delrin® 100ST NC010 (ASTM)</u>	Super Tough Acetal
<u>Delrin® 100ST NC010 (ISO)</u>	Super Tough Acetal
<u>Delrin® 100T NC010</u>	Toughened Acetal
<u>Delrin® 300AT BK000 (ISO)</u>	Antistatic, Toughened Acetal
<u>Delrin® 300AT BK000 (ISO)</u>	Antistatic, Toughened Acetal
<u>Delrin® 500MT NC010 (ASTM)</u>	Moderately Toughened, Medium Viscosity Acetal
<u>Delrin® 500MT NC010 (ISO)</u>	Moderately Toughened, Medium Viscosity Acetal
<u>Delrin® 500T NC010 (ASTM)</u>	Toughened Acetal
<u>Delrin® 500T NC010 (ISO)</u>	Toughened Acetal

UV Resistant/Weatherable Resins

<u>Delrin® 127UV BK601 (ASTM)</u>	UV Stabilized Black Acetal, High Viscosity
<u>Delrin® 127UV NC010 (ASTM)</u>	UV Stabilized Acetal, High Viscosity
<u>Delrin® 127UV NC010 (ISO)</u>	UV Stabilized Acetal, High Viscosity
<u>Delrin® 527UV BK601 (ASTM)</u>	UV Stabilized Black Acetal, Medium Viscosity
<u>Delrin® 527UV NC010 (ASTM)</u>	UV Stabilized Acetal, Medium Viscosity
<u>Delrin® 527UV NC010 (ISO)</u>	UV Stabilized Acetal, Medium Viscosity
<u>Delrin® 927UV NC010 (ISO)</u>	UV Stabilized Acetal, Low Viscosity

Unreinforced Resins

<u>Delrin® 100AL NC010 (ISO)</u>	Lubricated, Moderate Flow Acetal
<u>Delrin® 100P NC010 (ASTM)</u>	High Viscosity Acetal
<u>Delrin® 100P NC010 (ISO)</u>	High Viscosity Acetal
<u>Delrin® 100ST NC010 (ASTM)</u>	Super Tough Acetal
<u>Delrin® 100ST NC010 (ISO)</u>	Super Tough Acetal
<u>Delrin® 100T NC010</u>	Toughened Acetal
<u>Delrin® 111P NC010 (ASTM)</u>	High Viscosity Acetal, Enhanced Crystallization
<u>Delrin® 111P NC010 (ISO)</u>	High Viscosity Acetal, Enhanced Crystallization
<u>Delrin® 1260 NC010 (ISO)</u>	Low Viscosity Acetal Copolymer
<u>Delrin® 127UV BK601 (ASTM)</u>	UV Stabilized Black Acetal, High Viscosity
<u>Delrin® 127UV NC010 (ASTM)</u>	UV Stabilized Acetal, High Viscosity
<u>Delrin® 127UV NC010 (ISO)</u>	UV Stabilized Acetal, High Viscosity
<u>Delrin® 142CM NC010 (ISO)</u>	High Viscosity Acetal for 2 Component Molding
<u>Delrin® 150 NC010 (IS)</u>	High Viscosity Extrusion Acetal
<u>Delrin® 311DP NC010 (ISO)</u>	Medium-high Viscosity Acetal, Enhanced Dimensional Stability and Productivity
<u>Delrin® 460 NC010 (IS)</u>	Medium Viscosity Acetal Copolymer
<u>Delrin® 500AL NC010 (ASTM)</u>	Lubricated, Moderate Flow Acetal

<u>Delrin® 500AL NC010 (ISO)</u>	Lubricated, Moderate Flow Acetal
<u>Delrin® 500CL NC010 (ASTM)</u>	Chemically Lubricated, Medium Flow Acetal
<u>Delrin® 500CL NC010 (ISO)</u>	Chemically Lubricated, Medium Flow Acetal
<u>Delrin® 500MT NC010 (ASTM)</u>	Moderately Toughened, Medium Viscosity Acetal
<u>Delrin® 500MT NC010 (ISO)</u>	Moderately Toughened, Medium Viscosity Acetal
<u>Delrin® 500P NC010 (ASTM)</u>	Medium Viscosity Acetal
<u>Delrin® 500P NC010 (ISO)</u>	Medium Viscosity Acetal
<u>Delrin® 500T NC010 (ASTM)</u>	Toughened Acetal
<u>Delrin® 500T NC010 (ISO)</u>	Toughened Acetal
<u>Delrin® 500TL NC010 (ASTM)</u>	1.5% Teflon® PTFE Micropowder in Acetal
<u>Delrin® 500TL NC010 (ISO)</u>	1.5% Teflon® PTFE Micropowder in Acetal
<u>Delrin® 511P NC010 (ASTM)</u>	Medium Viscosity Acetal, Enhanced Crystallization
<u>Delrin® 511P NC010 (ISO)</u>	Medium Viscosity Acetal, Enhanced Crystallization
<u>Delrin® 527UV BK601 (ASTM)</u>	UV Stabilized Black Acetal, Medium Viscosity
<u>Delrin® 527UV NC010 (ASTM)</u>	UV Stabilized Acetal, Medium Viscosity
<u>Delrin® 527UV NC010 (ISO)</u>	UV Stabilized Acetal, Medium Viscosity
<u>Delrin® 542CM NC01C (ISO)</u>	Medium Viscosity Acetal for 2 Component Molding
<u>Delrin® 900P NC010 (ASTM)</u>	Low Viscosity Acetal
<u>Delrin® 900P NC010 (ISO)</u>	Low Viscosity Acetal
<u>Delrin® 911AL NC010 (ISO)</u>	Lubricated Acetal Resin For Dimensionally Stable Parts
<u>Delrin® 911AL NC010 (ISO)</u>	Lubricated Acetal Resin For Dimensionally Stable Parts
<u>Delrin® 911P NC010 (ASTM)</u>	Low Viscosity Acetal, Enhanced Crystallization
<u>Delrin® 911P NC010 (ISO)</u>	Low Viscosity Acetal, Enhanced Crystallization
<u>Delrin® 927UV NC010 (ISO)</u>	UV Stabilized Acetal, Low Viscosity
<u>Delrin® DBR180 NC0C (ISO)</u>	Medium-high Viscosity Acetal Bridge Resin

<u>Delrin® DBR80 NC00C (ISO)</u>	High Viscosity Modified Acetal Resin
<u>Delrin® DE20055 NC0 (ISO)</u>	Lubricated Medium Viscosity Acetal With Teflon® PTFE Micropowder

Glass Reinforced Resins

<u>Delrin® 525GR NC00C (ASTM)</u>	25% Glass Reinforced Acetal
<u>Delrin® 525GR NC00C (ISO)</u>	25% Glass Reinforced Acetal

Glass or Mineral Filled Resins

<u>Delrin® 570 NC000 (IS)</u>	20% Glass Fiber Filled Acetal
<u>Delrin® 930MF NC000 (ISO)</u>	Mineral Filled Acetal

Static Dissipative Resins

<u>Delrin® 300AS BK000 (ISO)</u>	Antistatic Stiffened Carbon Fiber Filled Acetal
<u>Delrin® 300AT BK000 (ISO)</u>	Antistatic, Toughened Acetal
<u>Delrin® DE10010 NC0</u>	Stainless Steel Filled Acetal

Aesthetic Resins

<u>Delrin® 142CM NC01C (ISO)</u>	High Viscosity Acetal for 2 Component Molding
<u>Delrin® 500LM BKL00</u>	Medium Viscosity Acetal for Laser Marking
<u>Delrin® 542CM NC01C (ISO)</u>	Medium Viscosity Acetal for 2 Component Molding
<u>Delrin® DS100 NC000 (ISO)</u>	Paintable, High Viscosity Acetal
<u>Delrin® DS500 NC000 (ISO)</u>	Paintable, Medium Viscosity Acetal
<u>Delrin® DS500M NC00C (ISO)</u>	Medium Viscosity Acetal Resin for Metal Plating
<u>Delrin® DS900 NC000 (ISO)</u>	Paintable, Low Viscosity Acetal
<u>Delrin® DS900M NC00C (ISO)</u>	Low Viscosity Acetal Resin for Metal Plating

VITA AUCTORIS

Name: Hadi Tajalli

Place of Birth: Mashhad, Iran

Year of Birth: 1970

Education: Hekmat High School, Mashhad, Iran
1983-1987

University of Tehran, Tehran, Iran
1987-1992 B.Sc.

University of Windsor, Windsor, Ontario
2002-2005 M.A.Sc.